



Thesis

Master of Computer Engineering

***Indoor Positioning System for Mobile Devices using
Radio Frequency and Perfect Sequences***

*(Sistema de localização automática de dispositivos móveis com recurso à
sequências perfeitas de rádio frequência)*

Josip Bagarić

Leiria, September 2016



Thesis

Master of Computer Engineering

***Indoor Positioning System for Mobile Devices using
Radio Frequency and Perfect Sequences***

*(Sistema de localização automática de dispositivos móveis com recurso à
sequências perfeitas de rádio frequência)*

Josip Bagarić

Master's thesis carried out under the guidance of Dr. João da Silva Pereira, professor of the
School of Technology and Management of the Polytechnic Institute of Leiria.

Leiria, September 2016

Dedication

This thesis was made possible by the continuous support of my friends and family. I would like to dedicate this thesis to my parents Milan and Jadranka Bagarić, who support my every action.

Acknowledgements

First and foremost, I would like to express my gratitude to my mentor Prof. João da Silva Pereira for his continuous support, guidance, knowledge and patience with me while working on this thesis. Without his help, the completion of this thesis would not be possible.

Secondly, I would like to thank Instituto Politécnico de Leiria, Escola Superior de Tecnologia e Gestão for providing me with the space and resources to work on and finish the thesis.

Lastly, thank you goes to Instituto de Telecomunicações for funding the research used in this thesis.

Summary

Keywords: indoor, positioning, system, radio, frequency, perfect, sequences, opdg, zigbee, golay, chu, modulation, raspberry pi, accf, standing, wave, cancellation, transmitters.

Abstract

Recent advancements in the area of nanotechnology have brought us into a new age of pervasive computing devices. These computing devices grow ever smaller and are being used in ways which were unimaginable before. Recent interest in developing a precise indoor positioning system, as opposed to existing outdoor systems, has given way to much research heading into the area. The use of these small computing devices offers many conveniences for usage in indoor positioning systems. This thesis will deal with using small computing devices Raspberry Pi's to enable and improve position estimation of mobile devices within closed spaces. The newly patented Orthogonal Perfect DFT Golay coding sequences will be used inside this scenario, and their positioning properties will be tested. After that, testing and comparisons with other coding sequences will be done.

List of Figures

Figure 1: Transition to distributed systems	25
Figure 2: Mobile computing system.....	26
Figure 3: Smart home.....	27
Figure 4: Wifarer [27]	36
Figure 5: IndoorAtlas [29].....	37
Figure 6: Pozyx system elements	38
Figure 7: ByteLight business model.....	39
Figure 8: Carrefour smartphone app - uses Phillips' IPS	40
Figure 9: Autocorrelation vs. Cross-correlation [39]	45
Figure 10: Normalized absolute periodic autocorrelation - ZigBee pseudorandom noise (PN) codes, with a resolution of 16 bits.....	51
Figure 11: Normalized absolute periodic autocorrelation – OPDG codes, with a resolution of 16 bits.....	52
Figure 12: Normalized absolute periodic autocorrelation - OPDG codes with the code length of 128, with a resolution of 16 bits	52
Figure 13: Standing wave cancellation	54
Figure 14: Standing Wave Cancellation - Mechanism.....	55
Figure 15: Indoor Positioning System - Network Topology.....	56
Figure 16: The Raspberry Pi	57
Figure 17: Si4703 FM Tuner.....	58
Figure 18: FM receiver module.....	59
Figure 19: Si4703 to Raspberry Pi connection.....	60
Figure 20: FM Transmitter	61
Figure 21: IPS - simplified scenario.....	62
Figure 22: Transmitter software flowchart.....	63

Figure 23: Receiver software flowchart	64
Figure 24: TCP Communication - Transmitter to Receiver.....	65
Figure 25: ACCF Ratio calculation.....	65
Figure 26: FM Transmitter - Antenna connection	68
Figure 27: Linear scenario.....	73
Figure 28: Test scenario 1 - Results	74
Figure 29: Test scenario 2 - Results	75
Figure 30: Test scenario 3 - Results	76
Figure 31: Test scenario 4	77
Figure 32: Test scenario 4 - Results	79
Figure 33: Test scenario 5	79
Figure 34: ACCF measurements - ZigBee vs. OPDG	81
Figure 35: Test results – Golay, Chu, ZigBee and OPDG	82
Figure 36: Triangulation process.....	83
Figure 37: Theoretical four mechanism IPS	90

List of Tables

Table 1: Test Scenario 1 - Parameters.....	74
Table 2: Test scenario 2 - Parameters	75
Table 3: Test scenario 3 - Parameters	76
Table 4: Average indoor location estimation error between two transmitters - Golay, Chu, ZigBee and OPDG	83
Table 5: Influence radii of transmitters	84
Table 6: Average indoor location estimation error in a scenario with four transmitters – Golay, Chu, ZigBee and OPDG.....	85

List of Equations

Equation 1: Discrete Fourier Transform (DFT)	45
Equation 2: Inverse Discrete Fourier Transform (IDFT)	45
Equation 3: Periodic cross-correlation between two different sequences.....	45
Equation 4: Periodic cross-correlation between two different sequences (alternate)	46
Equation 5: Generic algorithm for Golay sequence generation	47
Equation 6: Polyphase perfect sequences.....	48
Equation 7: IDFT to DFT.....	48
Equation 8: Recursive algorithm.....	48
Equation 9: Recursive decoding method.....	49
Equation 10: Vector A.....	49
Equation 11: Decoding process - First method	49
Equation 12: Decoding process - Second method.....	49
Equation 13: Autocorrelation Crest Factor (ACCF)	51

List of Acronyms

ACCF	Autocorrelation Crest Factor
AN	Antinode
AOA	Angle-of-arrival
BLE	Bluetooth Low Energy
CDMA	Code-Division Multiple Access
CEO	Chief Executive Officer
COTS	Commercial off-the-shelf
DFT	Discrete Fourier Transform
DOP	Dilution Of Precision
DPDT	Double Pole Double Throw
DS-CDMA	Direct-Sequence Code-Division Multiple Access
DVD	Digital Versatile Disc
FM	Frequency Modulation
GPIO	General-Purpose Input/Output
GPS	Global Positioning System
HF	High Frequency
IDFT	Inverse Discrete Fourier Transform
IM/DD	Intensity Modulation and Direct Detection
IPS	Indoor Positioning System
LED	Light-emitting Diode
LOS	Line-of-sight
MPI	Multipath Interference
N	Node
NFC	Near-Field Communication

NLOS	Non-line-of-sight
OPDG	Orthogonal Perfect DFT Golay
PC	Personal Computer
PN	Pseudorandom Noise
RFID	Radio Frequency Identification
RSS	Received Signal Strength
SCP	Secure Copy Protocol
SFTP	Secure File Transfer Protocol
TCP	Transmission Control Protocol
TDM	Time-Division Multiplexing
TDM-CDMA	Time-Division Multiplexing and Code-Division Multiple Access
TDOA	Time-difference-of-arrival
TOA	Time-of-arrival
USB	Universal Serial Bus
UWB	Ultra-wideband
VLC	Visible Light Communication
WAV	Waveform Audio File Format
WPS	Wi-Fi Positioning System

Index

Dedication	v
Acknowledgements	vii
Summary	ix
Abstract	xi
List of Figures	xiii
List of Tables.....	xv
List of Equations	xvii
List of Acronyms.....	xix
Index	xxi
Introduction	25
Bibliography review	31
1.1. State of the art.....	31
1.1.1. Research	33
1.1.2. Commercial	36
Methodology	41
1.2. Received Signal Strength and Triangulation	43
1.3. Autocorrelation and Cross-correlation	44
1.4. Orthogonal Perfect DFT Golay coding sequences	47
1.5. Autocorrelation Crest Factor (ACCF)	51

1.6.	Standing Wave Cancellation	53
1.7.	Indoor Positioning System.....	56
1.7.1.	Raspberry Pi	57
1.7.2.	FM Receiver Module	58
1.7.3.	Control Software	61
	Setting up.....	67
1.8.	Transmitters	68
1.8.1.	Hardware	68
1.8.2.	Software	68
1.9.	Receiver	70
1.9.1.	Hardware	70
1.9.2.	Software	70
	Tests	73
1.10.	Linear scenario tests.....	73
1.10.1.	Test scenario 1	74
1.10.2.	Test scenario 2	75
1.10.3.	Test scenario 3	76
1.11.	Two-dimensional scenario tests	77
1.11.1.	Test scenario 4 - TDM.....	77
1.11.2.	Test scenario 5 – Simultaneous emitting.....	79
	Results	81
	Conclusion.....	87
	Future work	89
	Bibliography.....	91

Appendices and attachments	97
Appendix I – Scientific Paper	98
Appendix 2 – Scientific Paper.....	119
Appendix 3 – Patent	129

Introduction

Looking at the world in which we live in, there is no denial that technology makes a big part of our everyday lives. Wherever we go, whatever we do, technology follows us and helps us on the way. Computers (big and small) make a big part of this technology. Computing has been constantly evolving since the arrival of the first personal computers (PC's) [1]. To this day, computing has gone through a number of revolutions to get to the point in which it is now.

The first revolution in computing happened with the emergence of distributed systems [2]. Distributed systems imply a collection of (static) computers, which are interconnected and work to achieve a certain purpose, as can be seen in Figure 1. These systems transformed the way we work. By implementing distributed systems of computers into the workplace, classrooms and other places, many of the tasks done before started being automated, thus making them easier to do by introducing fault-tolerance. Distributed systems also provided us with remote access to information, remote communication between computers, distributed security and high availability.

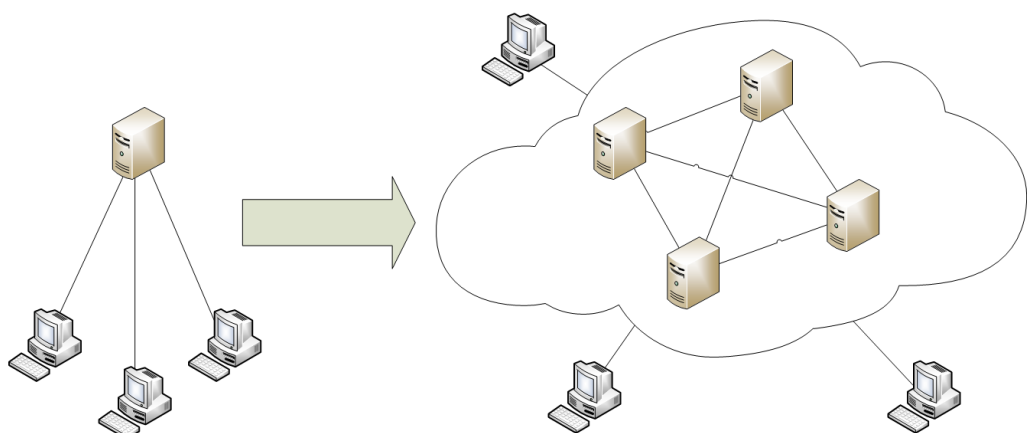


Figure 1: Transition to distributed systems

The second revolution in computing arrived in the form of mobile computing [3]. Mobile computing was built on the current distributed systems, and brought many improvements that transformed the computing space. It allowed for networking and information access on the go, which is the main feature in today's workspaces and homes (Figure 2). It also allowed for location sensitivity, application adaptiveness and energy awareness in computing systems. These improvements have transformed (and are still transforming) the way we work, live, play and learn.

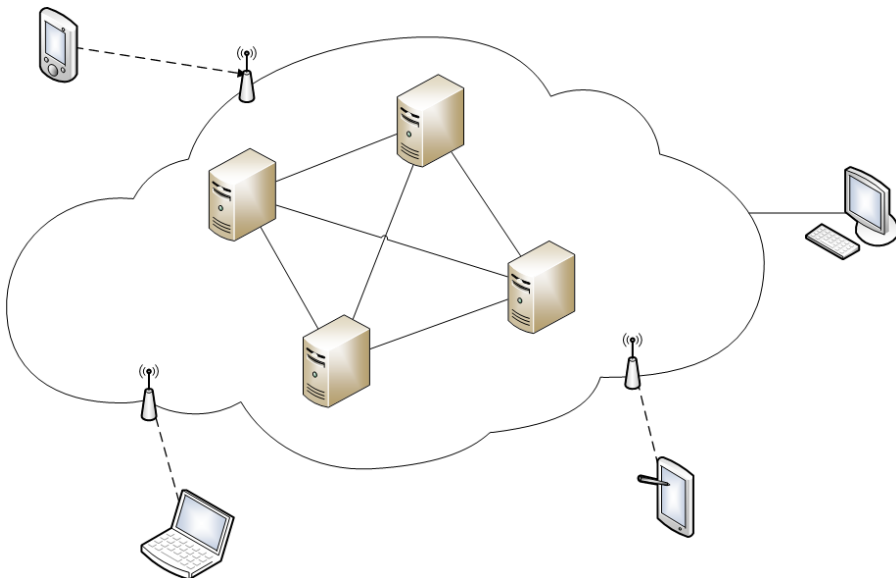


Figure 2: Mobile computing system

While the mobile computing trend has taken a major swing in our lives, there is another trend in computing slowly approaching. A new revolution in computing is called pervasive computing, sometimes called ubiquitous computing [4]. This trend in computing takes computing to a whole other level.

Pervasive computing has different goals in mind when compared to the distributed systems and mobile computing. The main goal of pervasive computing is to remove technology from the eyes of the user, while still enhancing the user's life. The main distinction between pervasive systems and other systems is the fact that it is context-aware.

An example of pervasive computing are smart spaces (smart houses, smart streets). These spaces help the user with his everyday chores at home and elsewhere, while not providing him the details of how they do it. They take input from our environment, and adjust certain parameters of our environment dynamically and autonomously. One example of such action would be adjusting the air conditioning temperature inside closed spaces depending on the temperature outside the space, so that it never exceeds the difference of 7 degrees Celsius and never drops under the standard room temperature. This makes the user unaware of how the actual system works. It just works, and the user always expects the optimal temperature without his intervention.

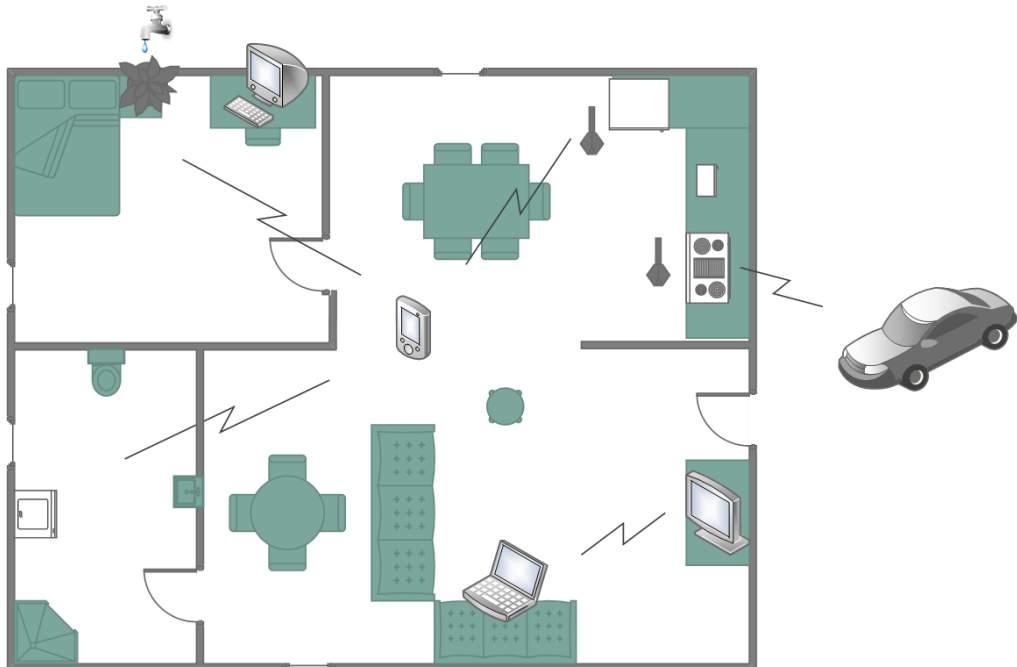


Figure 3: Smart home

In Figure 3 you can see an example of how a smart home would function. A smart home serves as a great example of a pervasive system. After being woken up by an alarm clock (depending on your online calendar) your breakfast starts getting ready and your coffee is being prepared as you get out of bed. After getting out of bed you sit at the table and eat your breakfast and drink your coffee. The water in your shower starts to warm up, and your washing machine sends you a notification to your phone that the laundry you left to wash during the night is finished. After taking a shower, you get dressed and start walking towards the car. As you exit the house, your refrigerator

sends you a message, telling you that your milk has expired and that you should buy more when returning home. As you approach the car, the car unlocks itself. Sensing that the temperature outside is low, the car starts the engine a few minutes earlier to warm it up, to avoid the possibility of you being late for work. You sit in your car and the car autonomously drives you to work, taking the most optimal road with the least traffic.

Besides the example above, pervasive computing encompasses a huge number of different computing devices, serving many purposes, and has a huge potential in improving life standard, automating mundane tasks, improving business analytics, improving traffic safety, and many other areas. That is one of the reasons why lots of research and development has been going on in this area in recent years.

Here, we will focus on a specific part of pervasive systems, called the Indoor Positioning System (IPS).

Indoor positioning systems are able to estimate the location of entities inside closed spaces. Many types of positioning systems depend, to varying degrees, on line-of-sight (LOS) between transmitters and receivers, as does the conventional well-known Global Positioning System (GPS). These systems allow for accurate outdoor location estimation approximately around 3 meters (best case scenario), dependent on the GPS system, propagation errors, signal multipath, receiver clock errors, GPS satellite orbit errors, number of satellites in LOS, satellite position geometry and the variation in atmospheric conditions. These are computed in terms of GPS dilution of precision (DOP).

Indoor, underground and heavy woods environments (among others) are not suitable for GPS as only minimal and/or partial LOS can be achieved causing lack of coverage and insufficient accuracy in estimation. Additionally, for a positioning system to be usable indoors, the error of estimation has to be lowered from meters to centimeters, as the estimation error in meters would often fail to estimate the correct location of an entity or object.

This thesis will deal with researching into the topic of indoor positioning systems [5]. The methodology of implementing an IPS will be explained. All of the related technologies and methods will be explained in detail, and the purpose of these will be shown. After that, a model of the IPS will be created and shown. Testing scenarios will be set up, tests performed and results displayed.

This work was based on my research published in the following publications:

- M. Ferreira, J. Bagarić, Jose M. Lanza-Gutierrez, S. Priem-Mendes, J. S. Pereira, Juan A. Gomez-Pulido, *On the Use of Perfect Sequences and Genetic Algorithms for Estimating the Indoor Location of Wireless Sensors*, International Journal of Distributed Sensor Networks, April 22, 2015 [6]
- J. Bagarić, M. Ferreira, J. S. Pereira, S. Priem-Mendes, *Estimating Indoor Location Using Wireless Communication Between Sensors*, ConfTele 2015, Conference on Telecommunications - Aveiro, Portugal, September 18, 2015 [7]
- J. Bagarić, J. S. Pereira, S. Priem-Mendes, *Standing Wave Cancellation – Wireless Transmitter, Receiver, System and Respective Method*, Submitted patent, Portuguese Patent #109137 [8]

Bibliography review

1.1. State of the art

With the current pace of technological advancements, the need of an NLOS positioning system grows ever larger. The omnipresence of small and powerful computer and processing units has given way to practical uses of NLOS positioning systems, mainly focusing on indoor scenarios. Taking into consideration the well-known example of the GPS [9], we can display the amount of factors that are being taken into consideration in order to estimate the location of the receiver. Some of these factors include propagation errors, which occur when the signal propagates through the troposphere, and signal multipath, which occurs when the signal is reflected from different entities, resulting in a delay due to the extra time it takes to get to the receiver. Other factors include mismatches in clock between satellites and the receivers, deviations in the satellite orbit, number of satellites visible, etc. While the errors in indoor positioning systems are also influenced by some of these factors, there are also a number of additional factors that have to be taken into account when building an IPS.

Indoor position of a receiver can be calculated in a multitude of ways. A popular method of calculating the indoor position is to use some of the wireless technologies available today. Many of the systems try to use existing (or new) **Wi-Fi** access points to create a Wi-Fi Positioning System (WPS) by measuring the received signal strength (RSS) for each of the available access points, and then calculating the position accordingly. The problem with WPS is its lack of precision due to the possible signal fluctuations that may occur, increasing errors and inaccuracies.

Another way to calculate the position would be to use compass chips to determine **magnetic positioning**. By sensing and recording the local magnetic variations caused by the iron in the buildings, a compass (e.g. inside a regular smartphone) would be able to map the indoor location

with the accuracy of 1-2 meters. While the error margin of this method is considered to be low, it still does not yield results that are accurate enough to be useful in purposes where centimeters make a difference.

Bluetooth [10] is another example using wireless communication, however it is known to be an indoor proximity solution, not an indoor positioning solution. It is mostly used for geo-fencing and micro-fencing.

Radio frequency identification (RFID) [11] can also be used for indoor positioning but, despite its cost-effectiveness, it does not support any metrics. Visible light communication (VLC) also grants some positioning properties, where indoor lighting can be used as a transmitter of information, and a smartphone camera can be used to detect changes in light to determine its location based on the source that emits it. This method can yield accuracies up to decimeters, but suffers of sporadic detection points. Tango Google Project is one of such VCL examples.

Ultra-wideband (UWB) [12] can also be a viable solution for positioning purposes, as it provides location accuracy up to 10 cm. UWB uses brief bursts of radio energy, akin to some radars, and then measures the time it takes for the signal to reach the other receivers. This avoids the multipath problems due to the brevity of the radio wave. While this gives accurate results, the problem is that UWB waves get blocked very easily, around 40 percent of the time.

Using **ultrasound** for indoor positioning has also received quite a bit of attention, due to the high accuracy of its slow-moving waves. Ultrasound can be used to track and identify the location of objects using inexpensive tags embedded into devices which provide ultrasound sensors with their location. The shortcoming of this technology is its short range, which makes it impractical in many situations, despite its high accuracy and robustness when compared to radio technologies, where the waves can pass through the walls more easily than ultrasounds.

1.1.1. Research

In this section we investigate the different approaches that are currently being researched.

1.1.1.1. Ultrasonic positioning systems

A number of ongoing researches have been dealing with ultrasound as a media for indoor positioning.

Indoor Positioning for Smartphones Using Asynchronous Ultrasound Trilateration [13] proposes a system that uses regular commercial off-the-shelf (COTS) hardware such as smartphones to determine the indoor position of the user. In their research, they have proven that a very short 21.5 kHz ultrasound “beep” emitted from a smartphone and received by four receivers in the corners of the room can lead to errors lower than 1 meter (averaging around 10 cm in their research). The receivers use a TDOA (Time-Difference-of-Arrival) or the asynchronous approach to determine the distance of each receiver and the smartphone. While this approach, so called Ultrasound trilateration, seems promising, the directional nature of ultrasound, its susceptibility to certain high frequency background noises, and the need for line-of-sight between speaker and receiver were identified as the biggest obstacles to positioning accuracy.

1.1.1.2. Wi-Fi

In order to mitigate many of the problems in Wi-Fi positioning, *WLocator: An Indoor Positioning System* [14] introduces a few improvements to the IPS system. Dealing with fluctuation, fingerprint management and location-aware application development are some of the principles and algorithms introduced, along with performance changes and lightweight software. This system is expanded in *WHLocator: Hybrid Indoor Positioning System* [15] by combining the WiFi positioning with altimeter and image sensors, and results in higher accuracies in 3D scenarios.

By implementing the transmission of multiple predefined messages *WiFi-based indoor positioning* [16] maintains the high-accuracy of other Wi-Fi based IPS, while at the same time reducing the need for a large number of antennas and relaxing the need for wide signal bandwidth. Their simulation results show that this approach can achieve 1 m accuracy, boasting no hardware changes in commercial WiFi products.

Researchers at MIT's Computer Science and Artificial Intelligence lab have managed to achieve decimeter-level IPS accuracy with their novel Chronos [17] technology. This technology works with a single access point and off-the-shelf Wi-Fi cards, and uses time-of-arrival calculation between a receiver and transmitter to localize them. It does so by making the receiver and transmitter to hop between all 35 frequency bands in the 2.4 GHz to 5.8 GHz range. This changes the rate at which signals accumulate phase for each of the frequencies, which is then used by Chronos to calculate the time-of-arrival of signals and estimate the distance. Some tests have managed to localize devices to within 65 centimeters.

1.1.1.3. Visible Light Communication

An Indoor Visible Light Communication Positioning System Using a RF Carrier Allocation Technique [18] proposes an indoor positioning system that adopts Visible Light Communication (VLC) that is based on the intensity modulation and direct detection (IM/DD) in a line-of-sight environment. They investigated this principle by simulations and experiments and found that, although it was inaccurate when estimating distance based on the effects of radiation directivity and the incidence angle, the positioning error would be reduced when the adjustment process by normalizing method is used. Their results show that the average error of estimated positions can be reduced to 2.4 cm using, which is compared with 141.1 cm without the adjustment process.

On the other hand, *Indoor Positioning System Using Visible Light and Accelerometer* [19] proposes a different approach to VLC, by complementing the IPS system with the results of the smartphone's accelerometer. The system uses the accelerometer to detect the orientation of the device, and uses the light sensor to detect the received light intensity. Their low-complexity algorithm requires no knowledge of the LED transmitters' physical parameters, and their tests show it is possible to achieve an average position error of less than 0.25 m.

1.1.1.4. Radio Frequency Identification

A Standalone RFID Indoor Positioning System Using Passive Tags [20] suggests an indoor positioning system based on RFID. This kind of IPS system proposes that small RFID tags are set up around the space. As the user moves through the space, the receiver object would pick up the

signals from these tags, and determine its location based on the signal provided by these RFID tags. *Development of an Indoor Navigation System Using NFC Technology* [21] proposes a similar solution, but uses Near-Field Communication (NFC) [22], a branch of High Frequency (HF) RFID.

1.1.1.5. Geomagnetism

Indoor positioning system using geomagnetic anomalies for smartphones [23] proposes a novel technique that makes use of the perturbations of the geomagnetic field caused by structural steel elements in a building. The advantage of this system is that it does not require any sort of physical infrastructure, which makes it a very cost-effective solution. After a building has been mapped, and its magnetic footprint recorded, a target's position could be estimated by comparing the sensor measurement of a device (e.g. smartphone) to the measurements on the magnetic footprint of the building. Their results show that the accuracy of such a system is within 3 meters.

1.1.1.6. Hybrid

Instead of building an IPS system using a single technology, some IPS systems combine more technologies that complement each other and improve the accuracy.

Hybrid Indoor Positioning with Wi-Fi and Bluetooth: Architecture and Performance [24] does just that. In their scenario, a Wi-Fi based position estimation method is used, and is enhanced by using Bluetooth hotspot devices. The Bluetooth devices help the Wi-Fi IPS by partitioning the indoor space using the divide-and-conquer method.

Redpin - Adaptive, Zero-Configuration Indoor Localization through User Collaboration [25] describes an open source indoor positioning system that was developed with an aim to allow for at least room-level accuracy. Additionally, it introduces an alternative to time-consuming training phases by incorporating a system that enables the users to train the IPS system as they use it. Redpin works with standard GSM, Wi-Fi or other wireless technologies that mobile phones implement.

1.1.2. Commercial

On the commercial side, there are a few IPS systems available, some of which will be described in this section.

1.1.2.1. Wifarer

One example of a commercial IP system is Wifarer [26]. In order to enable indoor positioning inside a closed location, Wifarer needs to map the indoor space. It does so by scanning the fingerprint of Wi-Fi or Bluetooth LE (BLE) networks. It uses the signal strength of nearby networks, and maps it to a certain point inside the indoor space. Once the whole indoor space has been mapped, it enables indoor positioning and navigation.



Figure 4: Wifarer [27]

The error of the Wifarer system greatly depends on the amount of Wi-Fi and Bluetooth LE networks present inside the indoor space, but for areas with dense Wi-Fi networks such as airports and bus stations, Wifarer's CEO boasts an error as low as half a meter. The advantages

using Wifarer are that it can be installed on any smartphone that has a magnetometer/compass, and can be used straight away.

1.1.2.2. IndoorAtlas

Another contender in the commercial space is IndoorAtlas [28]. IndoorAtlas platform takes a more innovative approach to indoor positioning by using the magnetic footprint of buildings to map the indoor space. Same as with Wifarer, the advantage of IndoorAtlas is that it can be installed on any smartphone that has a magnetometer/compass, and can be used straight away.



Figure 5: IndoorAtlas [29]

The user installs the IndoorAtlas app, uploads a map of the indoor space to the application, and starts mapping the space. For the indoor positioning to take place, the user first has to map the space by walking around the building and capturing the magnetic footprint at a large amount of points inside the building.

After the mapping is complete, the indoor positioning can take place. When off-the-shelf handsets are used, IndoorAtlas boasts an accuracy typically less than 3 meters.

1.1.2.3. Pozyx

For indoor positioning developers, another hope arose when in 2015, a new campaign started on Kickstarter. Pozyx [30] was founded by a group of developers in Brussels, Belgium, and their aim was to use the existing Ultra-wideband technology to develop an accurate IPS system.

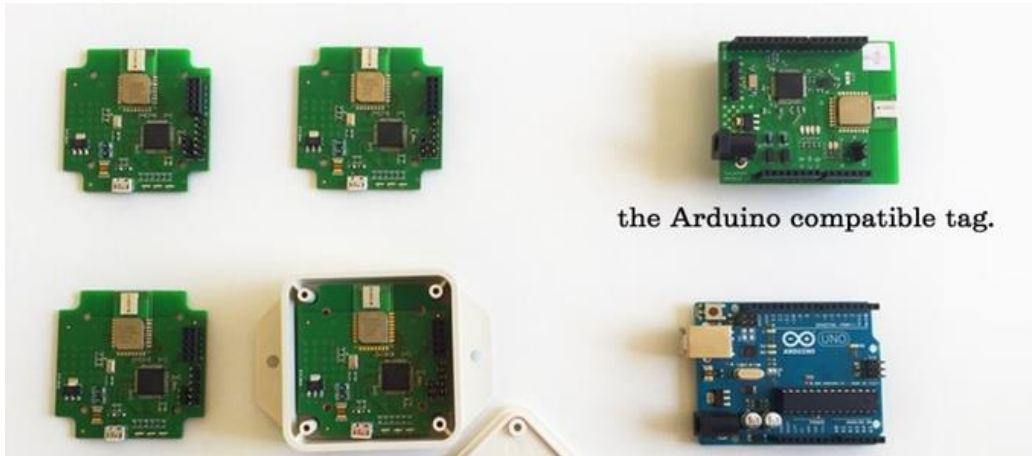


Figure 6: Pozyx system elements

The Pozyx system consists of four anchors (UWB transmitters) and a tag (UWB receiver). After the anchors are set up around the indoor scenario, the tag can be used to compute the indoor location of the device. Pozyx comes with an Arduino library and can be programmed to suit different purposes and can be embedded into different devices.

1.1.2.4. ByteLight

Developers at AcuityBrands [31] took on the approach of using Visible Light Communication to implement their indoor positioning system. They use the indoor positioning to allow the retailers to pinpoint certain objects to their clients, thereby custom-tailoring their shopping experience.

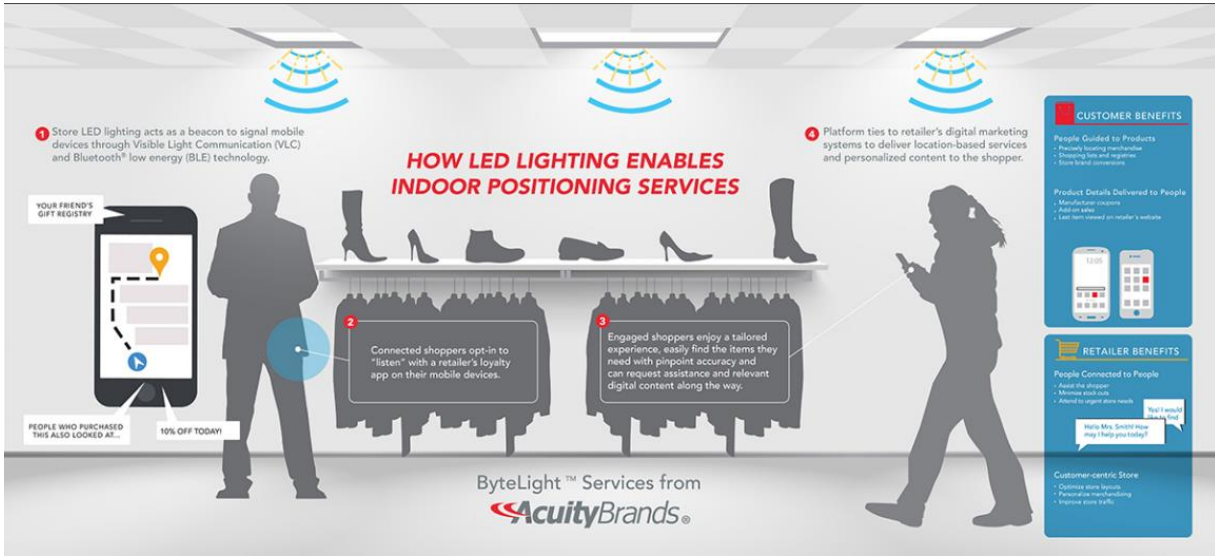


Figure 7: ByteLight business model

ByteLight uses the flickering of the light-emitting diodes (LEDs) to determine the location of the user, and uses that location to present them with special offers.

1.1.2.5. Phillips' LED-based IPS

In 2015, in a Carrefour supermarket in Lille, France, Philips has implemented their IPS system, and this enabling for one of the first IPS-enabled supermarkets.

Phillips bases their IPS on the existing VLC technologies. Every LED lamp that is a part of the IPS system emits a specific code, which is then registered by the user's smartphone (with the corresponding smartphone app) and then used to calculate the indoor position. Phillips boasts a sub-meter accuracy with their IPS.

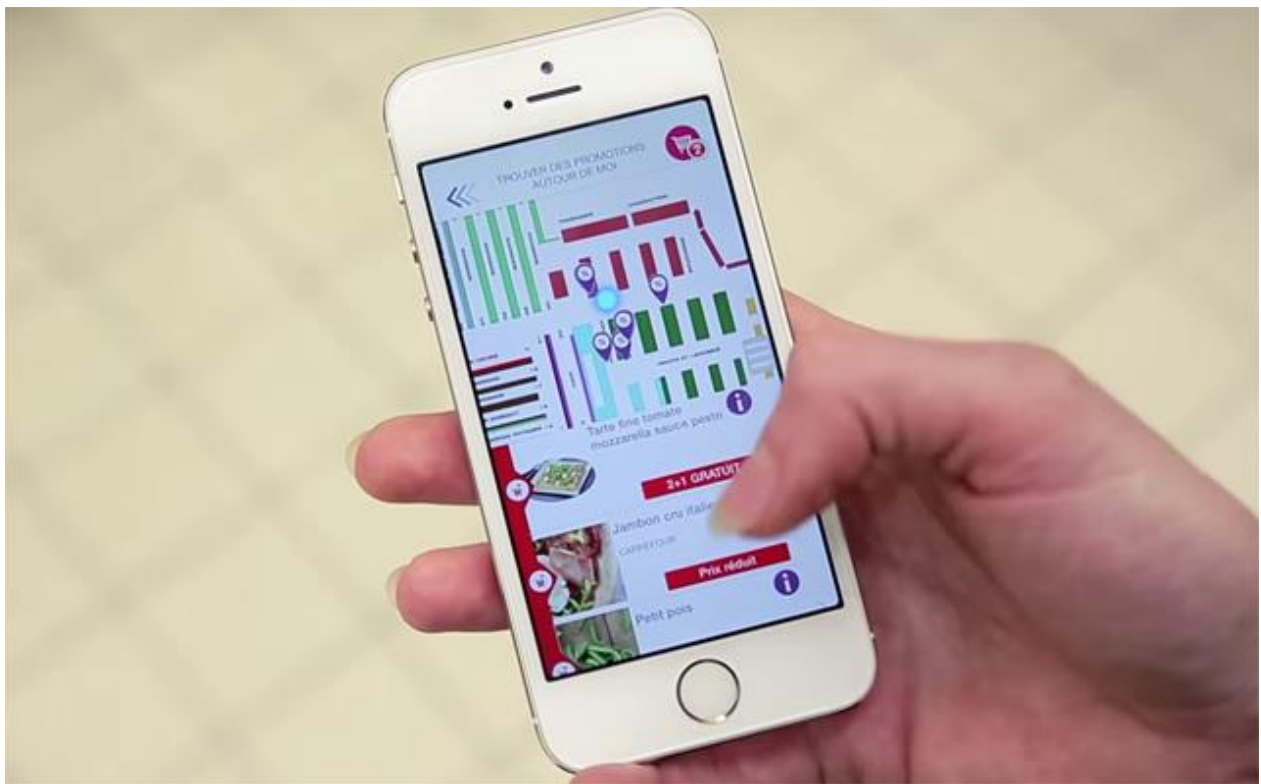


Figure 8: Carrefour smartphone app - uses Phillips' IPS

1.1.2.6. Nextome

Nextome [32] was formed by three young graduate students from Puglia, Italy. They decided to use the newly created Apple's standard called iBeacon [33] to implement their IPS, combined with Bluetooth Low Energy (BLE). iBeacons would be used as BLE transmitters and set up around the indoor scenario. After that, a BLE 4.0 enabled smartphone (Android or iOS) would be used to detect its indoor position.

Nextome use a new localization method, called MLV3. This method limits the “path fading” effect by removing signal interferences bouncing off walls, floors and other indoor objects. Additionally, they use Intelliwalk [34] technology to detect in which direction the user is moving, which requires the phone to have a gyroscope, a magnetometer, a compass and other (these days) standard phone sensors. Lastly, they use particle filtering (Sequential Montecarlo Filtering [35]) to refine the map information, which removes the odds of user being positioned in an unreachable zone and saves the energy and battery of the smartphone.

Methodology

This section describes the related technologies used inside the IPS system, as well as the methods used to achieve results.

There are a number of factors that need to be taken into account when building a quality IPS system. One of the key factors is radio signal and distance measurement method used inside the system. Different methods have been considered to solve for the positioning problem. According to [36], some of these include:

- Received signal strength (RSS) method
 - Strength of the received signal between two node deteriorates with distance between them.
- Angle-of-arrival (AOA)
 - Measuring the angle of arrival of a signal, from one node to another.
- Time-of-arrival (TOA)
 - Calculating the distance between two nodes based on the time the signal spends travelling from one node to another.
- Time-difference-of-arrival (TDOA)
 - Measuring the distance difference between an unknown node and two synchronized reference nodes.

The application of such methods can be found in [36]. This method has to meet some of the criteria imposed by the usage of radio waves for determining the position.

We combine the distance measurement method with a localization algorithm to implement the IPS. As seen in [37], some of the most common localization algorithms include:

- Trilateration

- Process of determining a location of a point by using the geometry of circles and measurement of distances.
- Triangulation
 - Process of determining a location of a point by using the geometry of circles and measurement of angles.
- Fingerprinting
 - Creation of a database with the probability distribution of signal strengths in the scenario, and usage of a map of these distributions to locate a given RSS sample.

1.2. Received Signal Strength and Triangulation

By examining the methods in Section 41, the method that was chosen for this scenario is the Received signal strength (RSS) method, combined with a modified triangulation localization algorithm.

The scenario in which this IPS system would be used is usually a closed space, such as a building. Buildings have a considerable amount of walls surrounding the rooms, and the receiver should be able to detect its location regardless of these physical obstacles. For that reason, the RSS-based positioning method would be most suitable in this scenario.

RSS-based positioning method enables us to avoid interferences. Indirect signals reach the antenna receiver with a lower signal strength than direct. We can, almost always, filter out these interferences by only accounting for the strongest (direct) signal.

1.3. Autocorrelation and Cross-correlation

One of the major problems of wireless communication is multipath interference (MPI). Transmission media, such as wireless, can bounce off certain obstacles, taking multiple paths to reach the receiver. Delays created by these obstacles can cause interference in communication. Other interference include the multicarrier interference, inter-symbol interference and multiple access interference.

The task of this IPS system is to improve accuracy above other IPS systems that use wireless communication. In indoor wireless communication, the use of code sequences that are resistant to multipath interferences is vital to achieve accuracy, due to a large number of obstacles present in the environment. In this thesis, the usage of perfect sequences [38] is proposed, whose correlation properties render them immune to multipath interferences, as opposed to the more commonly used coding sequences.

In this section, autocorrelation and cross-correlation properties of coding sequences will be explained.

Cross-correlation is defined as a measure of similarity between two series of data (signals, or waveforms) as a function of time-lag applied to one of them.

Autocorrelation, on the other hand, is a cross-correlation of a signal with itself. In autocorrelation, there will be a peak at a lag of zero, and its size will be the signal power, as can be seen in Figure 9.

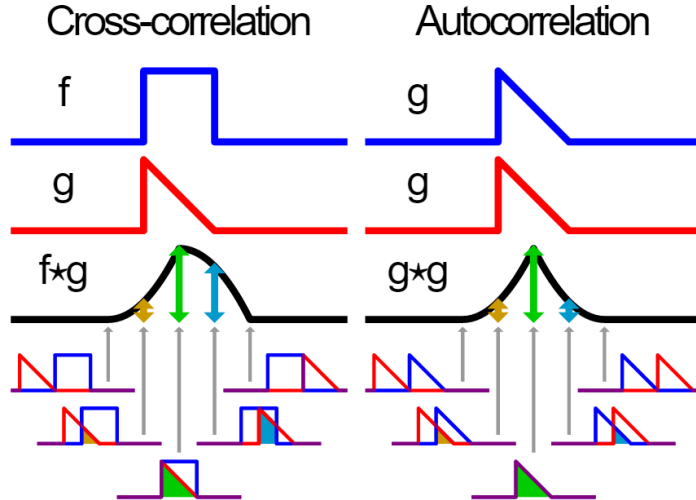


Figure 9: Autocorrelation vs. Cross-correlation [39]

A sequence x is a periodic sequence with a period M when, where $x(n) = x(\text{mod}(n, M))$ where $\text{mod}(a, b)$ is the remainder of a divided by b .

Let $x[n]$ with $n = 0, 1, 2, \dots, M - 1$, be one of the M values of a periodic sequence x . The DFT (Discrete Fourier Transform) of $x[n]$ is defined as

$$X[k] = DFT\{x[n]\} = \sum_{n=0}^{M-1} x[n] W_M^{kn},$$

Equation 1: Discrete Fourier Transform (DFT)

where $W_M = \exp(-j2\pi/M)$, $k = 0, 1, 2, \dots, M - 1$, with $j = \sqrt{-1}$ for convenience of notation. The IDFT (Inverse Discrete Fourier Transform) of $X[k]$ is then given by

$$IDFT\{X[n]\} = x[n] = \frac{1}{M} \sum_{k=0}^{M-1} X[k] W_M^{-kn}.$$

Equation 2: Inverse Discrete Fourier Transform (IDFT)

Using Equation 1 and Equation 2 the periodic cross-correlation between two different sequences $x(r)$ and $x(s)$ is defined as

$$R_{x^{(s)}x^{(r)}}[n] = \sum_{k=0}^{M-1} x^{(r)}[k] x^{*(s)}[\text{mod}(k+n, M)] = \sum_{k=0}^{M-1} x_k^{(r)} x_{k+n}^{*(s)}.$$

Equation 3: Periodic cross-correlation between two different sequences

Alternatively, it can be defined as

$$R_{x^{(s)}x^{(r)}}[n] = IDFT \{ X^{(r)} X^{*(s)} \}$$

Equation 4: Periodic cross-correlation between two different sequences (alternate)

where the superscript * denotes the complex conjugate.

The autocorrelation of a periodic sequence can also be calculated using Equation 4, when $r = s$.

When a periodic sequence has an autocorrelation of zero for any non-zero delay, the sequence is said to be a perfect sequence. Additionally, the two different sequences are called orthogonal if the cross-correlation between them is zero for a null delay.

1.4. Orthogonal Perfect DFT Golay coding sequences

This section explains how the Orthogonal Perfect DFT Golay (OPDG) coding sequences were formed.

Any sequence set with perfect [40] or near-perfect autocorrelation values, which is also orthogonal or near-orthogonal, is a good candidate to be used in asynchronous communication systems, such as DS-CDMA (Direct-Sequence Code-Division Multiple Access), or any other system where the signal reception may be contaminated by the multi-path problem. Another important property of the sequence set is the number of orthogonal sequences available. The Gold sequences [41] are a good example of a set of sequences having these properties, since they have excellent correlation properties while being possible to generate in large numbers. For instance, it is possible to create 32 orthogonal Gold sequences [42] with a length of 32. However, sequences with low cross-correlation values usually have high out-of-phase autocorrelation values. Likewise, low out-of-phase autocorrelation values are usually achieved at the cost of higher cross-correlation values. A compromise between these properties must be carefully selected for usage on a CDMA-based communication system.

Golay sequences [43] are bipolar complementary sequences. Additionally, the autocorrelation of a single sequence of a Golay pair is not zero with all non-null delays, for any length $L = 2N$. However, the sum of the out-of-phase autocorrelations of both sequences in the pair is zero. Therefore, Golay sequences are not perfect sequences. Nevertheless, they are interesting for their properties. A generic algorithm for Golay sequence generation was presented by Budisin [44] as follows

$$\begin{aligned}a_0[k] &= \delta[k] \\b_0[k] &= \delta[k] \\a_n[k] &= a_{n-1}[k] + w_n b_{n-1}[k - D_n] \\a_n[k] &= a_{n-1}[k] - w_n b_{n-1}[k - D_n]\end{aligned}$$

Equation 5: Generic algorithm for Golay sequence generation

where $\delta[k]$ is the unit pulse function that works as a trigger signal, $a_n[k]$ and $b_n[k]$ are the Golay sequences, w_n is a generation seed (either 1 or -1), and D_n is a delay ($2n - 1$).

An example of a Golay complementary sequence of length 4 is the following pair: (+1,+1,+1,-1) and (+1,+1,-1,+1). The amplitude of a Golay sequence $a_n[k]$ is a constant value given by $|a_n[k]|=1$.

It is well-known that any constant amplitude sequence, defined in the frequency domain, corresponds to a perfect sequence in the time domain [45].

Applying an IDFT to Golay sequences creates two new polyphase perfect sequences, which are

$$\begin{aligned} OPDG_1 &= IDFT\{a_n[k]\} \\ OPDG_2 &= IDFT\{b_n[k]\} \end{aligned}$$

Equation 6: Polyphase perfect sequences

It should be noted that it is possible to find the IDFT of any sequence X using also a DFT, because

$$IDFT\{X(n)\} = \frac{1}{N} \left[DFT\{X^*(n)\} \right]^*$$

Equation 7: IDFT to DFT

The same sequences can be achieved by a recursive algorithm as follows

$$\begin{aligned} a_0[k] &= A \\ b_0[k] &= A \\ a_n[k] &= a_{n-1}[k] + q \cdot W_{2^N}^{-k \cdot 2^{n-1}} b_{n-1}[k] \\ b_n[k] &= a_{n-1}[k] - q \cdot W_{2^N}^{-k \cdot 2^{n-1}} b_{n-1}[k] \end{aligned}$$

Equation 8: Recursive algorithm

where A is a constant signal or vector , $W_L = \exp(-j2\pi/L)$, $j = \sqrt{-1}$ and $0 < n \leq N$. The resulting sequences a_n and b_n are the OPDG1 and OPDG2 as per Equation 6 scaled by $A \times L$. They can be on the same scale as Equation 6 using $A = 1/L$, with $L = 2N$.

Several operations can be applied to the OPDG sequences to generate different sequences. One can create a real code by ignoring the imaginary part of the complex valued sequences and keeping only the real part ($Re\{OPDGx\}$). Likewise, one can ignore the real part of the sequence and keep only the imaginary part ($Im\{OPDGx\}$). One can also add the real part to the imaginary part ($Re\{OPDGx\}+Im\{OPDGx\}$). It is also possible to apply a sign function to any of the previous sequences. A sign function ($Sgn(x)$) returns -1 to negative inputs, and 1 to positive ones. Another possibility is to make a cyclic shift of the imaginary part of each code, prior to the sum, thus generating $L - 1$ new complex valued sequences.

It is also possible to decode the original input value A , from Equation 8, back from the OPDG codes. A recursive decoding method can be used as follows

$$\begin{aligned} a_{n-1}[k] &= q \cdot W_{2^N}^{-k \cdot 2^{n-1}} \cdot \{a_n[k] + b_n[k]\} \\ b_{n-1}[k] &= a_n[k] - b_n[k], \end{aligned}$$

Equation 9: Recursive decoding method

where $1 \leq n \leq N$, a_n and b_n are the OPDG1 and OPDG2 that resulted from Equation 8, and, as previously, $W_L = \exp(-j2\pi/L)$. Notice that in Equation 9, n varies from N down to 1. From a_0 and b_0 , a vector A' can be created by

$$A'[k] = a_0[k] + b_0[k]$$

Equation 10: Vector A

The resulting A' is an interesting vector because it presents two different method decoding processes:

$$\text{Re}\{DFT(A')\} = A[q]^N 2^{2N+1} \delta[k - 2^N + 1]$$

Equation 11: Decoding process - First method

and

$$|A'|^2 = A^2 2^{2N+2}$$

Equation 12: Decoding process - Second method

As seen in Equation 11, the real part of a DFT applied to A' is proportional to a Dirac pulse delayed by $2N - 1$. This property allows an enhanced detection process in spite of MPI.

1.5. Autocorrelation Crest Factor (ACCF)

The novel OPDG [46] codes are derived from real orthogonal perfect DFT sequences. To be more precise, the first OPDG code is obtained by making the sum of the real and imaginary part of OPDG1. The second OPDG code is built using the addition of the real and imaginary part of OPDG2. These novel codes are real, orthogonal and perfect. As such, they should be optimum alternative codes to the ZigBee [47] codes, which are widely used in the mainstream.

An autocorrelation crest factor [6] can be used as a parameter of autocorrelation efficiency. The autocorrelation crest factor ACCF is defined as a ratio of the maximum peak A_{peak} and the root mean square of the autocorrelation function A_{rms} as:

$$ACCF = \frac{A_{peak}}{A_{rms}}$$

Equation 13: Autocorrelation Crest Factor (ACCF)

When the autocorrelation is perfect, like a Dirac pulse, the ACCF of a periodic sequence of length L is equal to \sqrt{L} .

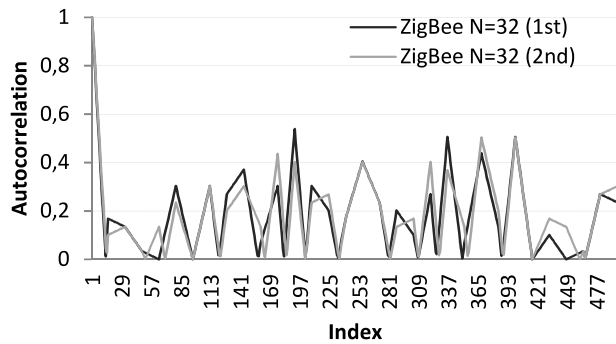


Figure 10: Normalized absolute periodic autocorrelation - ZigBee pseudorandom noise (PN) codes, with a resolution of 16 bits.

A comparison between these two codes follows. Figure 10 shows the normalized periodic autocorrelation properties of the standard ZigBee codes with the code length of 32. The ACCF average is 7.77.

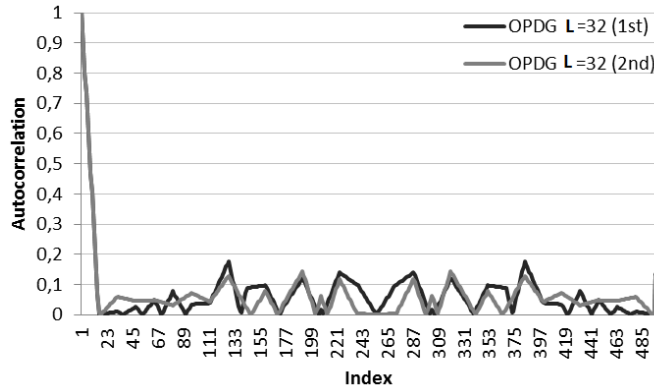


Figure 11: Normalized absolute periodic autocorrelation – OPDG codes, with a resolution of 16 bits.

Figure 11 shows the normalized periodic autocorrelation properties of the OPDG codes with the length of 32. The ACCF average is 9.48. Furthermore, by increasing the code length, autocorrelation properties (or ACCF) increase greatly. Increasing the code length of the OPDG codes results in a reduction of fluctuation in the normalized periodic autocorrelation function, as can be seen in Figure 12. This last ACCF average - 18.62 - is much higher.

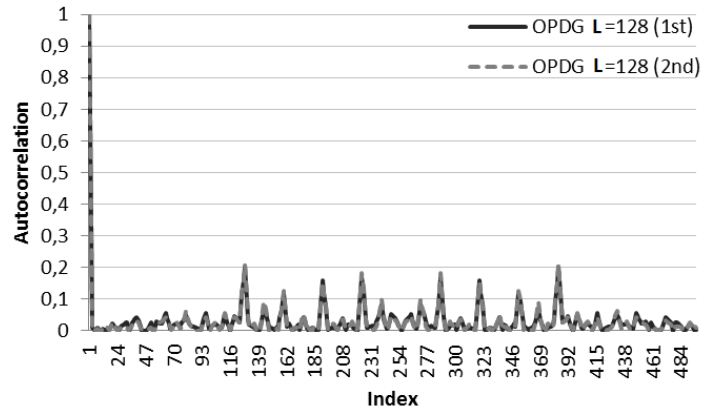


Figure 12: Normalized absolute periodic autocorrelation - OPDG codes with the code length of 128, with a resolution of 16 bits

The ACCF enables us to find the better code set, and helps us minimize the MPI effect, as can be indicated by the lower amplitudes of the out-of-phase autocorrelation values in Figure 12 when compared to Figure 10 and Figure 11.

1.6. Standing Wave Cancellation

A common occurrence in the field of wireless communication is the standing wave. In environments that contain many obstacles, such as closed spaces, the wave that is being sent from the transmitter to the receiver propagates through space and gets reflected from different kinds of surfaces. These reflections cause the receiving end to receive multiple instances of the same wave, some of them arriving directly, while others arriving after being reflected from a certain object. This occurrence is commonly called MPI, and represents a common issue in indoor positioning systems that use wireless technology.

The MPI has another side-effect, which is called the standing wave. When a wave gets reflected from a surface, it generates another wave that propagates back in the opposite direction. If one puts a receiver somewhere between the transmitter and the reflective surface, detecting the strength of the signal would vary on the position in which the receiver is placed because of the standing wave effect. Certain positions, particularly those that are half wavelength apart, would show no oscillations in the signal strength when measured multiple times. These points along the medium are called nodes (N). Some other points along the medium would yield different results, showing high oscillations in signal strength. The points that contain the highest amount of oscillations are called the antinodes (AN) [48].

In order to achieve accurate and consistent indoor positioning estimation using signal strength, inside closed spaces, mitigating the effect of the standing wave is one of the problems that needs to be addressed. Currently, a technical solution to this problem does not exist, and as a part of this thesis, a way to solve the problem of the standing wave will be introduced, in cases where wireless communication is used in indoor positioning systems.

To solve this problem, a different kind of wireless transmitter and receiver is used within the IPS system. The functioning of this transmitters and receivers will be furtherly explained.

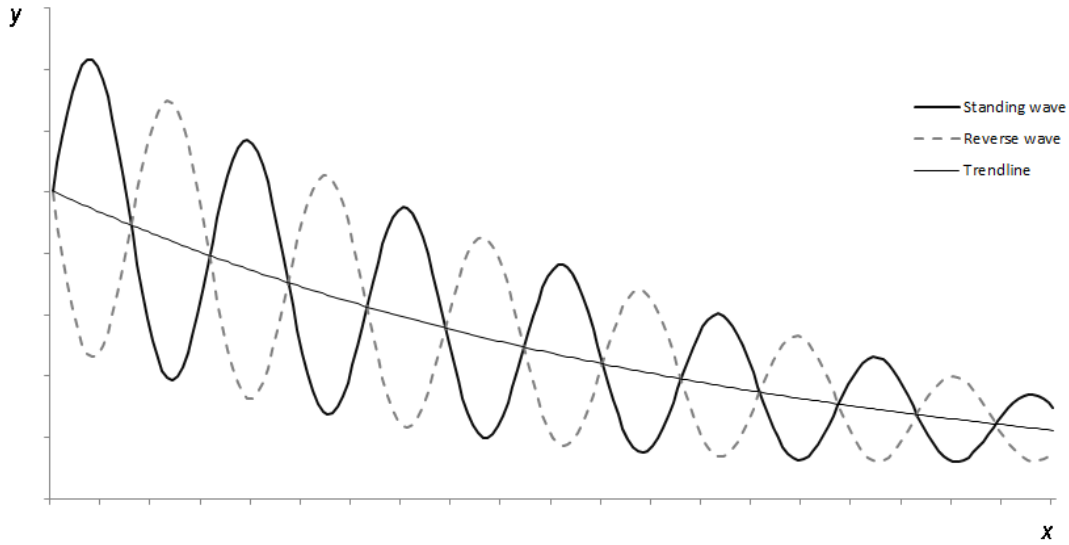


Figure 13: Standing wave cancellation

The standing wave cancellation wireless transmitter consists of a signal generator suitable for creating a signal with wavelength λ , an output and a relay switch, connected so that a relay switch alternatively connects the signal generator through a first path generating a first wave and through a second path to the output to generate the second wave. These two paths deliver two different signals. The first wave is created with a wavelength of λ , whereas the second wave is created with half the wavelength λ , by guiding the signal through a different path towards the output, as seen in Figure 14.

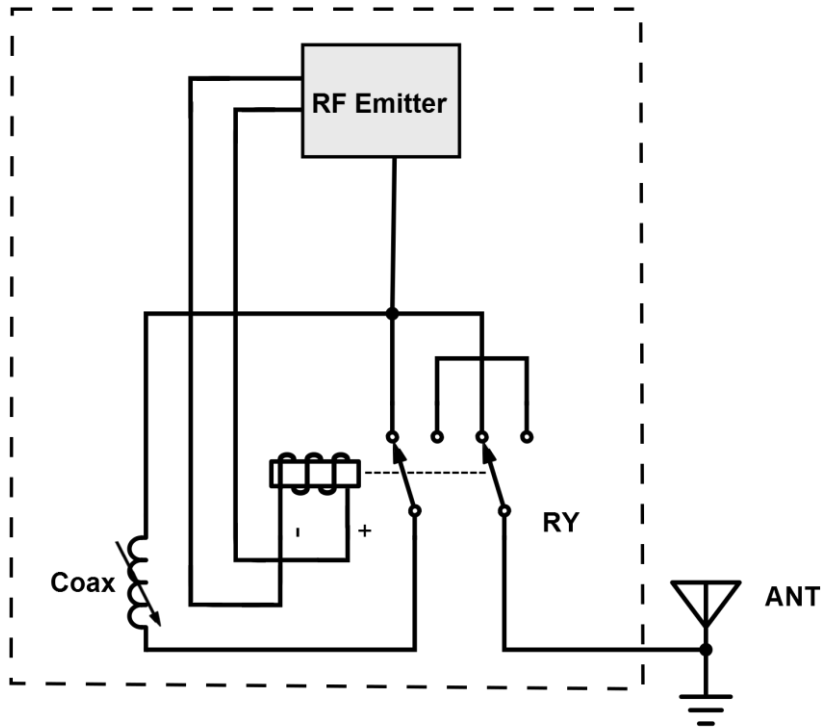


Figure 14: Standing Wave Cancellation - Mechanism

To generate the signal, a radio signal generator is used. The signal that the generator generates is then either sent directly to the antenna, or a relay switch (Double Pole Double Throw - DPDT) redirects the signal through a coaxial cable which has a length such as to generate a wave shifted in half the wavelength λ , again to the same antenna. The relay switch is then used in such a way to emit these two radio waves in time-division multiplexing, thus enabling the receiver to mitigate the effect of the standing wave by summing up the two waves before processing them.

A Portuguese patent under the number #109137 has been submitted for this mechanism. More information is available in the appendix.

1.7. Indoor Positioning System

In order to accurately determine the indoor position of an entity in closed space, a number of problems need to be solved. One of the problems is the MPI, which we believe can be mitigated using the OPDG codes. The other problem is the standing wave, which can be mitigated using the method described in section 1.6.

We propose a system that can use the communication of Frequency Modulation (FM) transmitters and receivers with OPDG codes to determine the indoor location of a device. The computing device we use to receive and process the codes is a small, low-powered single-board computer Raspberry Pi [49] equipped with a transceiver. A second Raspberry Pi is also used to control the transmissions of all transmitter pairs.

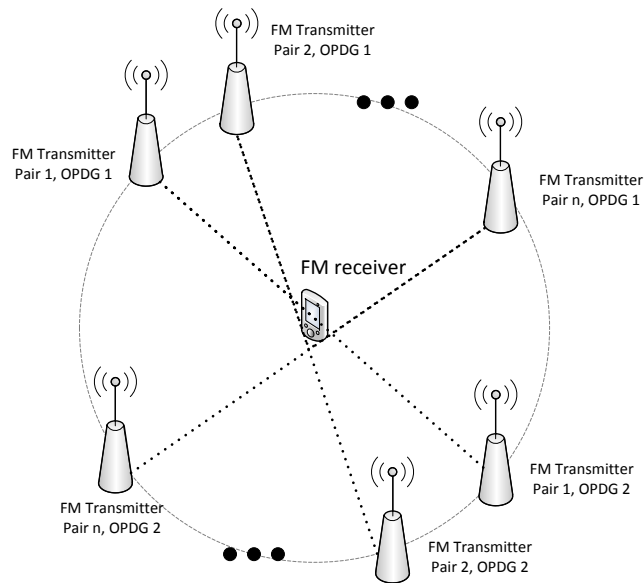


Figure 15: Indoor Positioning System - Network Topology

Figure 15 displays the network topology of our indoor positioning system. The topology consists of transmitters and receivers (both built with the Raspberry Pi computers).

1.7.1. Raspberry Pi

The Raspberry Pi is a low cost, credit-card sized computer developed with the intention of promoting the teaching of basic computer science in schools. Taking its size into consideration, it is a capable device that enables people of all ages to explore computing, and to learn how to program, as well as getting started with all kinds of electronics projects. It is capable of doing everything you would expect a desktop computer to do, from browsing the internet and playing high-definition video, to making spread sheets, word-processing, and playing games, and much more.

It was developed by The Raspberry Pi Foundation [49] (a charity association) and is manufactured through licensed manufacturing deals with Newark element14, RS Components and Egoman. These companies sell the Raspberry Pi online.

The form factor of the Raspberry Pi can be seen in Figure 16 below.



Figure 16: The Raspberry Pi

Due to the available resources, we have used two different model of the Raspberry Pi. The first model, Model B, can be seen on the left of the figure, while the second model, Model B+ can be seen on the right.

Raspberry Pi's have been used as both the receivers, as well as the transmitters inside the IPS system.

1.7.2. FM Receiver

It has been mentioned that the Raspberry Pi will be used as a computing device in order to process the FM signals it receives from the transmitters in order to determine its indoor position. In order to use the Raspberry Pi as a computing device for the received FM signal, we need some kind of way to receive the FM signal and forward it to the Raspberry Pi for further processing. Out-of-the-box, the Raspberry Pi does not offer any way of receiving a FM signal. Hence, in order to receive the FM signal, an external receiver should be used.

In this case, a cheap FM tuner evaluation board was bought online and used to receive the signal. The SparkFun FM Tuner Evaluation Board (Si4703) [50] is an evaluation board that enables us to tune into FM radio stations. It breaks out all the major pins and makes it easy to incorporate the chip as a part of a bigger project. The board is powered by 3.3V, which matches the output of the Raspberry Pi's general-purpose input/output (GPIO) pins and makes a great match with the Raspberry Pi. The board, displayed in Figure 17, also allows us to tune and seek for FM signals using a few built-in GPIO pins. By plugging the headphones into the 3.5 mm jack, we can effectively use the headphones cable as an antenna for the receiver.

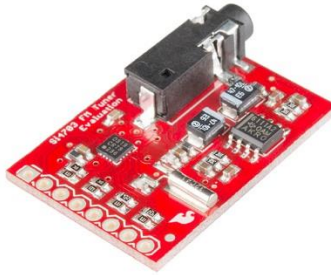


Figure 17: Si4703 FM Tuner

In order to forward the signal from the FM module to the Raspberry Pi, we have used a male-to-male 3.5 mm jack cable, as displayed in Figure 18. One end of the cable was connected to the 3.5 mm female port on the FM module, while the other end was connected to the Mic input of an

external USB soundcard. This external sound card was connected via USB to the Raspberry Pi, since out-of-the-box the Raspberry Pi does not feature any audio input ports.

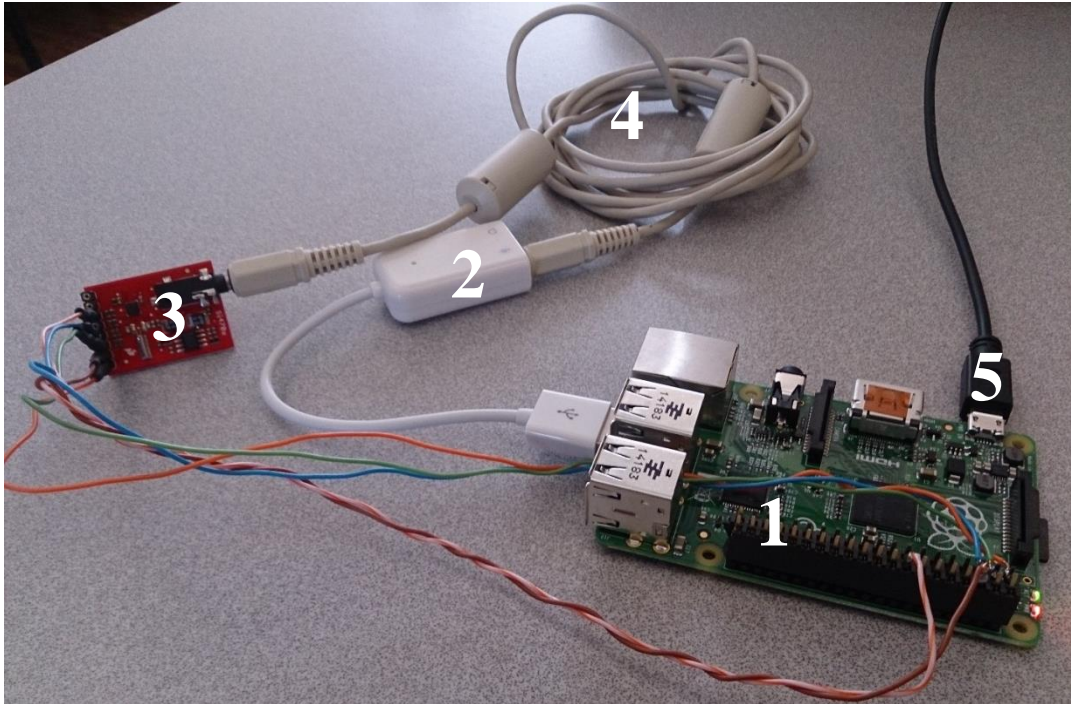


Figure 18: FM receiver module

Figure 18 also shows all the components that make up the receiver. These components are:

1. Raspberry Pi
2. External sound card
3. Si4703 FM receiver module
4. 3.5 mm jack cable
5. Power supply

The receiver would be usually powered through a USB 3.0 port on a laptop, since both the laptop and the receiver have to be carried around when performing measurements around a scenario.

The Si4703 module was connected to the Raspberry Pi using the connections seen in Figure 19 below.

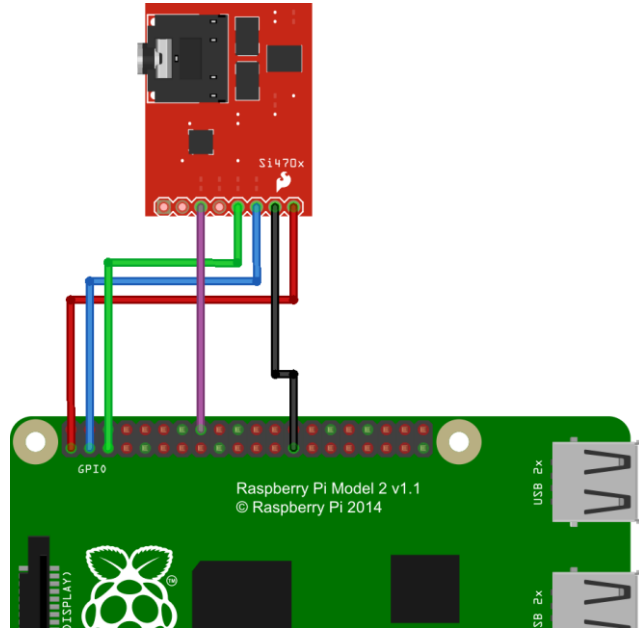


Figure 19: Si4703 to Raspberry Pi connection

1.7.3. FM Transmitter

Now that we have the hardware of the receiver set up, we need to set up the transmitters. In order to add functionality and modularity to the FM transmitter, we have opted to, again, use the Raspberry Pi's.

One of the features that was not originally intended for the Raspberry Pi was the transmission of radio signals. Using a piece of code [51] hacked together at Code Club, it is possible to turn the Raspberry Pi into an FM transmitter. By connecting a short piece of wire to the GPIO 4 (GPCLK0) pin of the Raspberry Pi, and running the piece of code, you effectively get a FM transmitter.

Since the code is written in Python, it is easy to expand the functionality of the FM transmitter by adding mode features to the code, which is exactly what has been done in this case. Functionality to start/stop the receiver remotely has been included, as well as a few tweaks that help us build the IPS scenario.



Figure 20: FM Transmitter

The transmitter, displayed in Figure 20, consists of the following parts:

1. Raspberry Pi
2. Antenna
3. Power supply

The antenna of the transmitter can be any piece of wire. In this case, we used a 35 cm long piece of copper wire.

1.7.4. Control Software

In order for the system to work seamlessly, we need to connect all the nodes (receivers and transmitters) into a coherent system. To see that all of our tests for the IPS scenario have been successful, we need to find a way to monitor and control all the nodes.

While testing this software and different measurement mechanisms, there were many iterations of the software as well. For the simplicity of explaining, only the software for one scenario will be explained.

Since this software requires communication between the transmitters and the receiver. We have to make sure that all the transmitters and the receiver are connected to the same network, and that the receiver software has all the IP addresses of the transmitters defined.

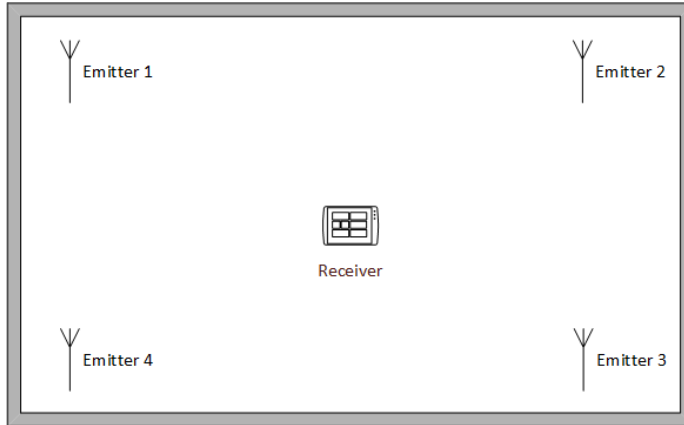


Figure 21: IPS - simplified scenario

Figure 21 above displays a scenario in which most of the tests were performed, and the software for this scenario will be explained.

The software will be divided into two parts:

- Transmitter software
- Receiver software

1.7.4.1. Transmitter software

As mentioned, in order to make the Raspberry Pi transmitters emit radio signals, a piece of code developed by Code Club PiHack was used as a base, after which it was upgraded to meet the needs of the IPS scenario.

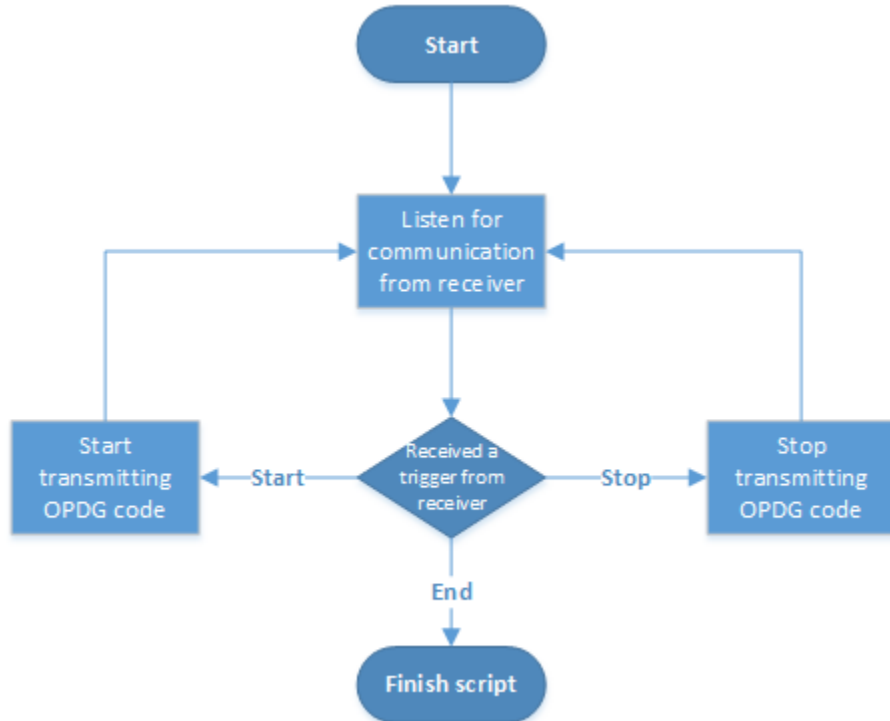


Figure 22: Transmitter software flowchart

Figure 22 shows the flowchart that explains the way the transmitter communicates with the receiver. The transmitter waits for the signal from the receiver to know when it needs to start emitting the OPDG code. The signal is received through a Transmission Control Protocol (TCP) connection between the transmitters and the receiver.

1.7.4.2. Receiver software

The second part of the system is the receiver. Functions of the receiver are the following:

- Controls the transmitters (start/stop signaling) using TCP;
- Captures and processes the FM signal coming from the transmitters.

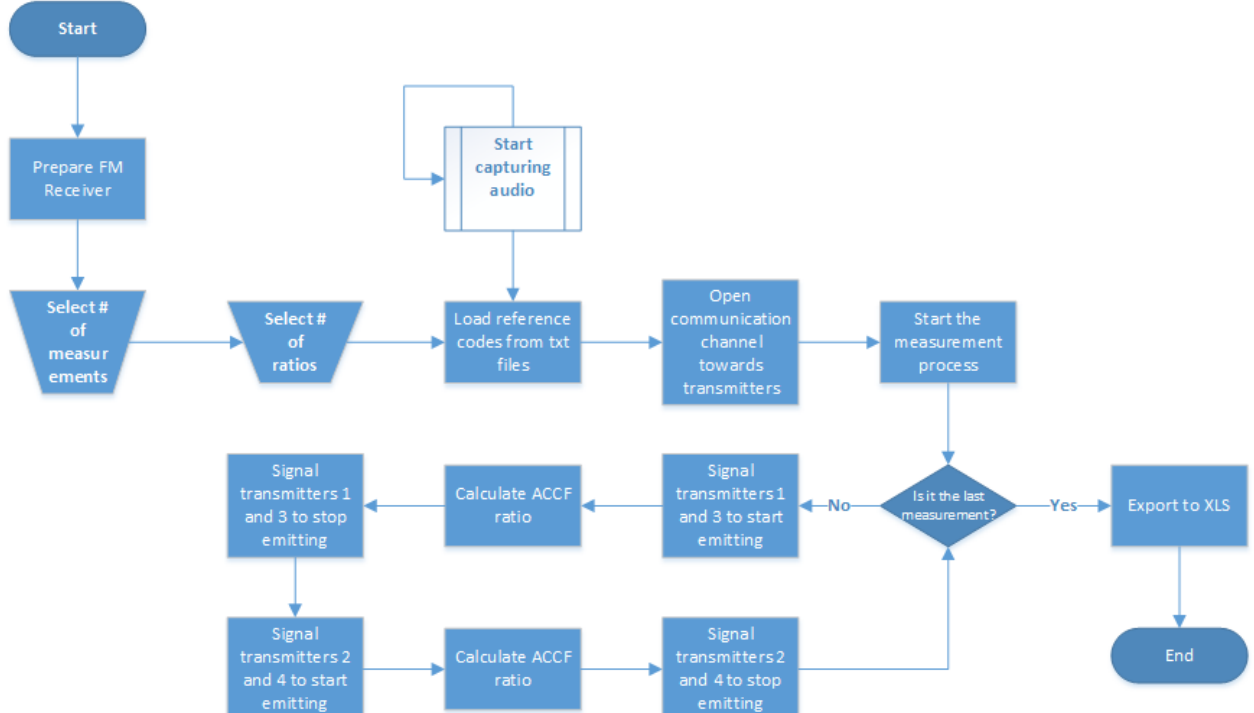


Figure 23: Receiver software flowchart

Figure 23 shows the flow of functions in the implementation of the receiver. After requesting some initial information from the user (amount of measurements, etc.) it starts capturing the FM signal coming from the transmitters.

Following the initial setup, the control software opens TCP communications towards the transmitters. It then uses this TCP communication to signal the transmitters when to transmit. The message sequence can be seen in Figure 24 below.

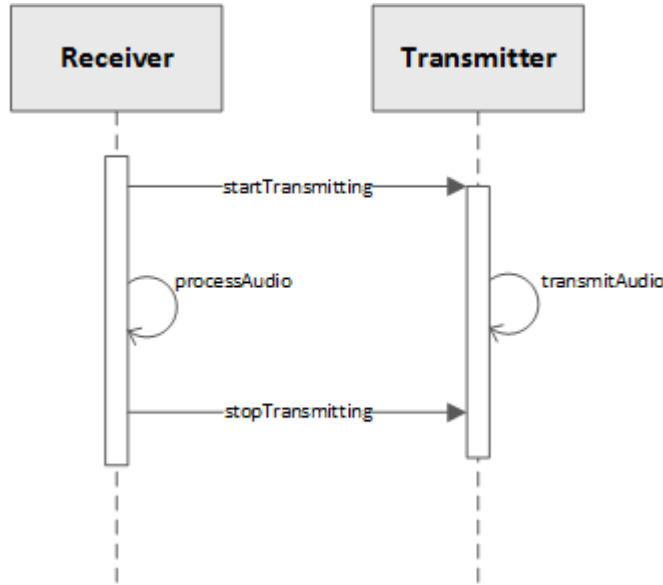


Figure 24: TCP Communication - Transmitter to Receiver

After the measurements start, at the end of each measurement the receiver is moved to a different position (due to a lack of available equipment). For each of these positions, it calculates the ratio of OPDG1/OPDG2 codes which are transmitted on only 2 transmitters at a time. The process of calculating the ACCF ratios is shown in Figure 25 below.

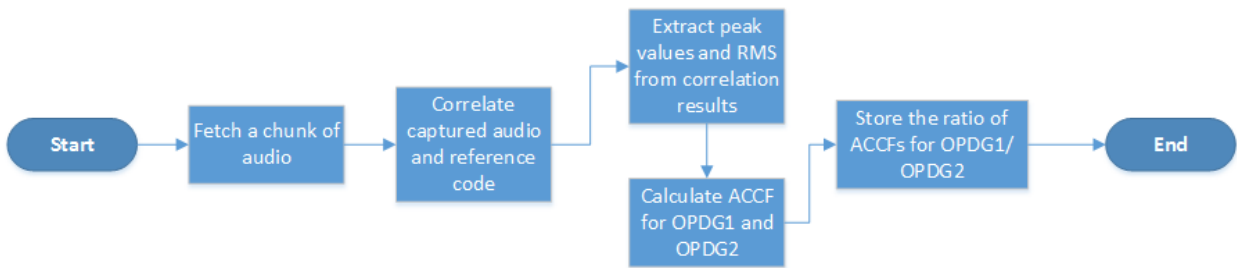


Figure 25: ACCF Ratio calculation

This part uses raw audio and reference codes (text files with signal amplitudes defined) to calculate the ACCF ratios. First it extracts the peaks from the correlation of the two signals. After extracting the signals, it uses the formula for the autocorrelation crest factor (defined in the Methodology section) to calculate the ACCF of each of the codes (OPDG1 and OPDG2). Finally, it calculates the ratio between the two signals and stores it.

After all the positions were measured, it exports the results into an Excel file. From this Excel file we can then further process the information and create some graphs to see the results.

Setting up

This section will deal with how the indoor positioning system was set up. The instructions will be laid out step by step and each of the steps explained.

Things we need:

- 5x Raspberry Pi
- 5x USB WiFi dongle
- 4x 5V power supply
- 4x antenna
- 1x external sound card
- 1x SparkFun FM Tuner Evaluation Board (Si4703)
- 1x 3.5mm jack cable
- Transmitter and receiver files (provided in the attached DVD)

1.8. Transmitters

Setting up the transmitters is pretty simple and straightforward. The setup will be divided into multiple parts.

1.8.1. Hardware

The transmitter contains the elements explained in 1.7.3. The antenna has to be connected to the Pin 7 on the Raspberry Pi GPIO header, as displayed in Figure 26.



Figure 26: FM Transmitter - Antenna connection

In order to establish the communication between the transmitter and the receiver, they need to be connected to the same network.

1.8.2. Software

The software package for the transmitter contains the following:

- PiFm binary (“pifm”)
- PiFm source code (“pifm.c”)
- Transmitter program (“transmitter.py”)
- Audio (WAV) files of the OPDG1 and OPDG2 codes

To set up the transmitter, continue with the following steps:

1. Transfer the files from the transmitter folder to the Raspberry Pi. Files can be transferred over the network (using Secure Copy – SCP or SSH File Transfer Protocol – SFTP) or using removable media (Universal Serial Bus – USB flash drive, etc.). Transfer them to the folder `~/transmitter`.

2. The Raspberry Pi should come preinstalled with Python 3.x. If that is not the case, make sure it is installed with the following commands:

```
sudo apt-get update  
sudo apt-get install python3
```

3. Run the transmitter script:

```
sudo python3 ~/transmitter/transmitter.py <wav_file>
```

An example would be:

```
sudo python3 ~/transmitter/transmitter.py OPDG1_N128_c4_x256.wav
```

At this point, the script is running, and our transmitter is waiting for the signal from the receiver on when it should transmit the code. This concludes setting up the transmitter.

1.9. Receiver

As with the transmitters, we will divide the setup of the receiver into hardware and software.

1.9.1. Hardware

The receiver contains the elements described in 1.7.2. Before setting up the software, make sure that the receiver's hardware components are connected in a proper manner, as described in 1.7.2.

1.9.2. Software

The software package for the receiver contains the following:

- Receiver program (“receiver.py”)
- Configuration file (“config.cfg”)
- Textual representations of the amplitudes in audio (WAV) files of the OPDG1 and OPDG2 codes from the transmitter – Reference file

To set up the receiver, continue with the following steps:

1. Transfer the files from the receiver folder to the Raspberry Pi. Files can be transferred over the network (SCP, SFTP) or using removable media (USB flash drive, etc.). Transfer them to the folder `~/receiver`.

2. The Raspberry Pi should come preinstalled with Python 3.x. If that is not the case, make sure it is installed with the following commands:

```
sudo apt-get update  
sudo apt-get install python3
```

3. Turn on all the transmitters and make sure they are connected to the same network as the receiver.
4. Define the IP addresses of all the transmitters in `config.cfg` configuration file.
5. Run the transmitter script:

```
sudo python3 ~/receiver/receiver.py <reference_file_1> <reference_file_2>
```

An example would be:

```
sudo python3 ~/receiver/receiver.py OPDG1.txt OPDG2.txt
```

6. Input the number of wanted measurements and wanted ratios when the program asks for it.

Tests

To test out our IPS system, a number of real-world indoor scenarios were set up, starting with a simple scenario with two transmitters, and then moving to the 2D scenario with four transmitters.

1.10. Linear scenario tests

For the first scenario, we placed two FM transmitters at a defined distance away from each other. Each transmitter was transmitting one code from a code pair on the frequency of 106.9 MHz, which has been chosen to minimize the problem of MPI due to the absence of commercial FM radio transmitters in the measurement zone. The receiver, a Raspberry Pi with a FM receiver module, was moved from one transmitter to the other, and measurements were taken at specific interval lengths. Measurements were made by simultaneously calculating the ACCF for both codes in the pair, after which a ratio was made between the two obtained values in order to cancel the FM automatic gain control. In Figure 27, the dots in between the transmitters denote the positions of the measurements taken.

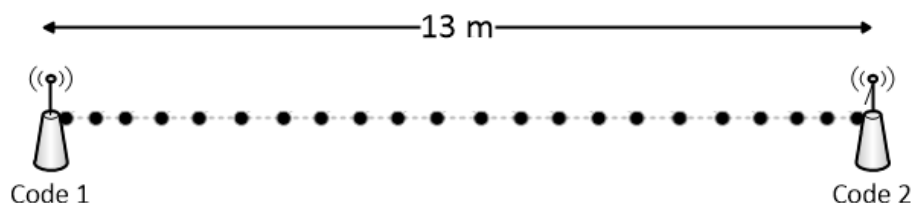


Figure 27: Linear scenario

The transmitters transmit their signals in two ways:

- Simultaneous;
- TDM.

The test scenarios will cover both of the approaches, after which the best approach will be used for further testing.

1.10.1. Test scenario 1

Table 1 below displays the parameters of this test scenario.

Table 1: Test scenario 1 - Parameters

Distance between transmitters	10 meters
Code families tested	OPDG
Measurements taken every	1.25 meters
Emitting type	Simultaneous
Antenna length	0.15 m

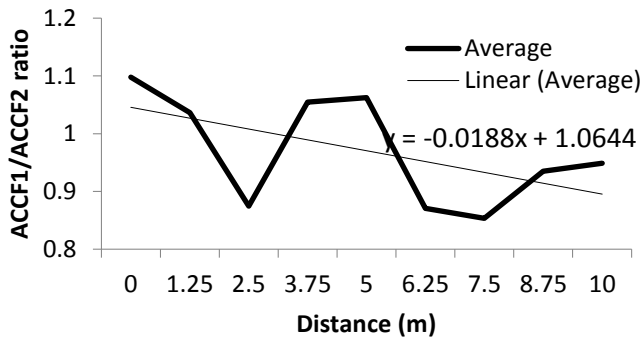


Figure 28: Test scenario 1 - Results

Results gained in this first scenario, displayed in Figure 28, show the potential of the ACCF, and how it can be used to estimate the location of the receiver between two transmitters.

If we take into account the trend line of the actual results (y), we can see that the ratio of the two ACCFs slowly drops as we move from the first to the second antenna (0 to 10 m). Using the equation of the trend line y , we are able to give a rough estimation of the receiver between the two transmitters.

The following scenarios look into alternative ways of measuring the results in order to improve the location estimation.

1.10.2. Test scenario 2

Table 2 below displays the parameters of this test scenario.

Table 2: Test scenario 2 - Parameters

Distance between transmitters	10 meters
Code families tested	OPDG
Measurements taken every	1.25 meters
Emitting type	Simultaneous
Antenna length	0.125, 0.25, 0.5, 1 meters

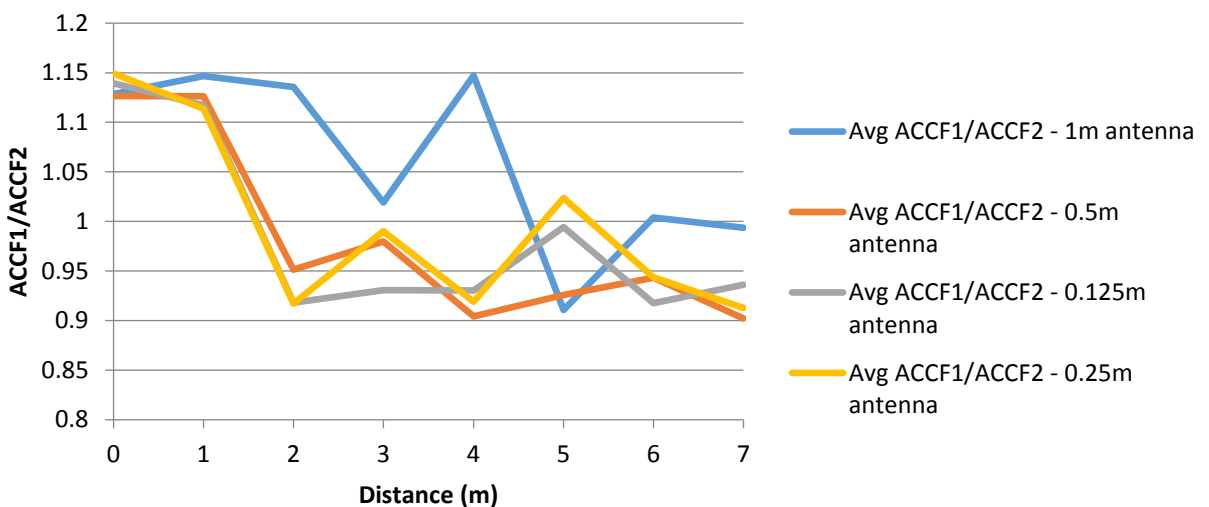


Figure 29: Test scenario 2 - Results

In Figure 29 we can see the results of testing the same 2-transmitter scenario, at a distance of 7 meters between each other, and with different antenna lengths.

For the antennas, we used a piece of thin copper wire that was cut to the appropriate length.

From this graph we can concluded that antennas between 0.25 and 0.5 meters of length gave better results in terms of ACCF1/ACCF2 to distance ratio.

1.10.3. Test scenario 3

Table 3 below displays the parameters of this test scenario.

Table 3: Test scenario 3 - Parameters

Distance between transmitters	21 meters
Code families tested	OPDG
Measurements taken every	3 meters
Emitting type	Simultaneous
Antenna length	0.35 m

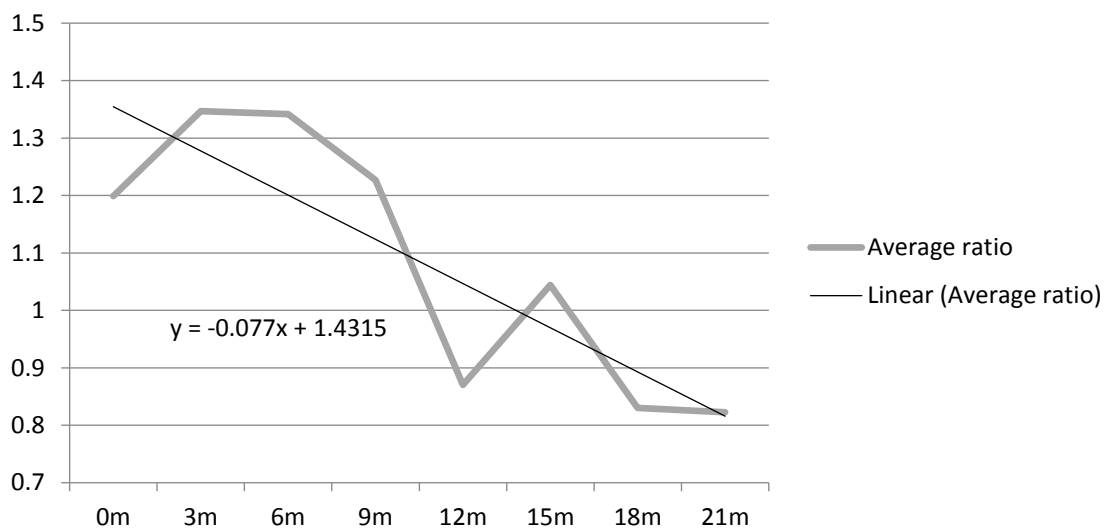


Figure 30: Test scenario 3 - Results

This test scenario was built with the purpose of testing how the distance between the transmitters affects the ACCF1/ACCF2 ratio. From Figure 30 we can clearly conclude that, with distance, results improve significantly, judging by the linear trend line.

We can see a larger difference in the ACCF1/ACCF2 ratio between each measurement, which makes it easier for us to estimate the location of the receiver between the transmitters.

1.11.Two-dimensional scenario tests

Following the linear tests, the next logical step is to test out the same methods and principles in a two-dimensional scenario.

1.11.1. Test scenario 4 - TDM

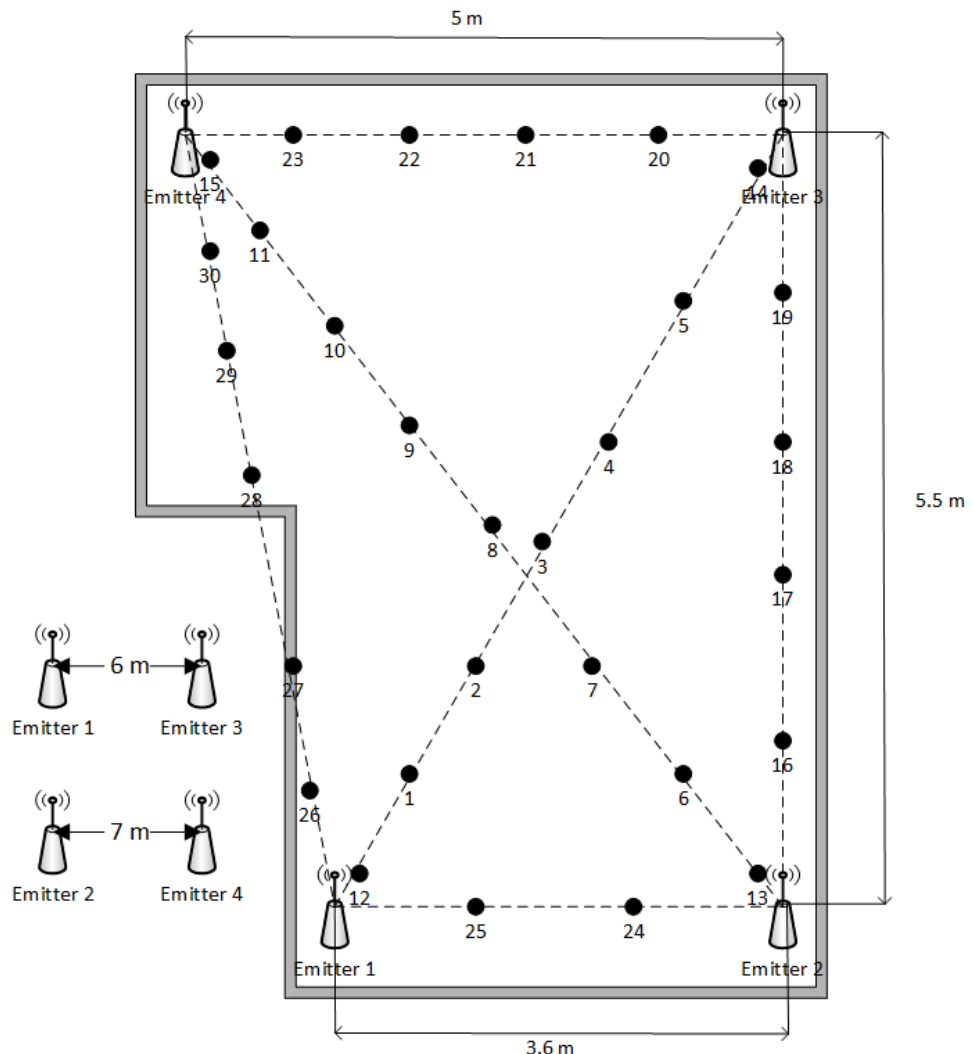


Figure 31: Test scenario 4

Based on the conclusion from the linear tests, which show that accuracy increases with length, this test was performed in the biggest room at disposal at the time. Unfortunately, the room in this test, Figure 31, was of an irregular shape, but still served the purpose.

Transmitters were placed in the far corners of the room, in order to achieve maximum distance between transmitters.

The first method that was tested was Time-division Multiplexing (TDM). The approach taken in this test was to make the transmitters emit the signal only one transmitter at a time. The algorithm would go as follows:

1. The receiver would be placed in a certain position inside the room.
2. The transmitters that are placed in the corners of the room would start emitting the signal in the following order:
 - Transmitter 1 – emitting the first generated OPDG code (OPDG1);
 - Transmitter 3 – emitting the second generated OPDG code (OPDG2);
 - Transmitter 2 – emitting the first generated OPDG code (OPDG1);
 - Transmitter 4 – emitting the second generated OPDG code (OPDG2).

Each of the transmitters would emit the signal for 15 seconds.

3. The receiver would detect the signal of Transmitter 1 and start processing it. During these 15 seconds the receiver would process the signal and calculate the ACCF.
4. After this is done, it would process the signal of Transmitter 3 immediately afterwards and calculate its ACCF. After both of these would be calculated, it would calculate the ratio of these ACCFs. This way we get the ratio of two signals.
5. Steps 3 and 4 would be repeated for Transmitters 2 and 4.
6. The whole procedure would be repeated for all of the marked positions inside the scenario.

These results were proven to be unusable, because we didn't find any significant change in the ratio of the OPDG1 and OPDG2 signals between neither of the pairs, as can be seen in Figure 32 below.

Ant2 (OPDG1) -> Ant4 (OPDG2)

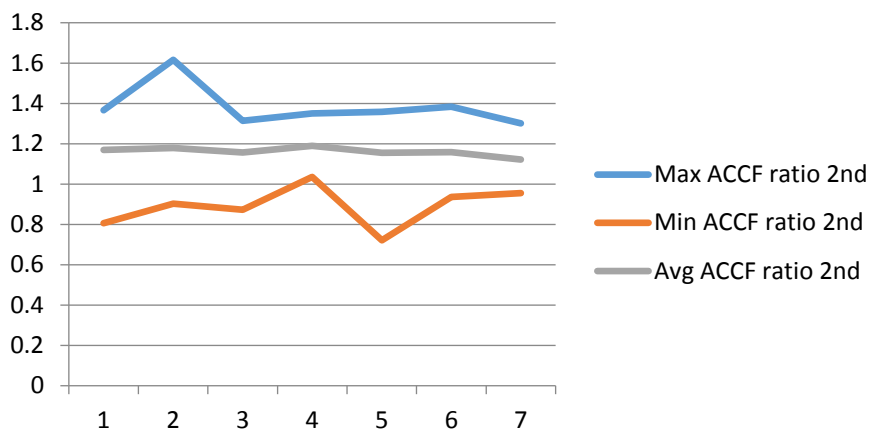


Figure 32: Test scenario 4 - Results

1.11.2. Test scenario 5 – Simultaneous emitting

To setup the second two-dimensional scenario, we used 4 transmitters again, which were placed in the corners of a large classroom filled with tables and chairs with metallic legs. The codes were transmitting simultaneously in pairs, and all transmitters were put on corner tables.

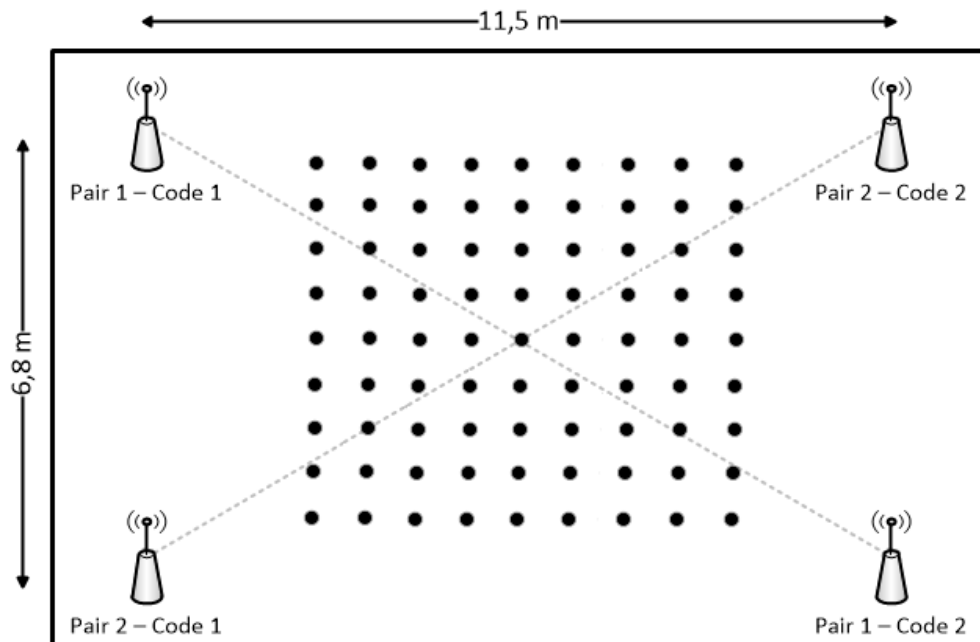


Figure 33: Test scenario 5

In the this test scenario, displayed in Figure 33 above, a pair of real OPDG codes $\{\text{Re}[\text{OPDG1}] + \text{Im}[\text{OPDG1}]\}$ and $\{\text{Re}[\text{OPDG2}] + \text{Im}[\text{OPDG2}]\}$ has been used. The first FM transmitter of the pair, with the code $\{\text{Re}[\text{OPDG1}] + \text{Im}[\text{OPDG1}]\}$, was located at -3.5 meters of the central point zero. The second FM transmitter of the pair, with the code $\{\text{Re}[\text{OPDG2}] + \text{Im}[\text{OPDG2}]\}$, was located at +3.5 meters. Both transmitters were in LOS, with some walls around them, creating a real indoor environment with some MPI.

The transmitters were placed 6.8 and 11.5 meters apart, and the pairs were transmitting the signals interchangeably. The receiver, in this case, was moved around a number of points in the middle of the scenario. Positions closer to the transmitters (less than a 1.25 m) were avoided in order to minimize the near-field effect of the transmitters which is a well-known issue [52]. Measurements were taken in these points in a similar fashion as the ones in the scenario with two transmitters. For each point, two ACCF ratios were measured. The first ratio was calculated as a ratio of the ACCF of the first code and the ACCF ratio of the second code, for the first pair of antennas. The second ratio was calculated as a ratio of the ACCF of the first and the ACCF of the second code for the second pair.

For this test, we took a sample of 30 measurements per position, meaning each of the ratios were measured and calculated 30 times, and average values were taken in account for further calculations in order to decrease the error of measurement. Taking into consideration the time that was available to do the tests, we evaluated that 30 measurements per position would be enough to give a proper average reading.

This scenario yielded better results, which will be explained in the Results section of the thesis.

Results

Our IPS measurements of the ACCF, shown in Figure 34, show that OPDG codes with the same code length as ZigBee codes give an average of 8% better ACCF, while increasing the code length of the OPDG codes to 128 highly improves the ACCF to an average of 7.1. These measurements were made during 30 seconds.

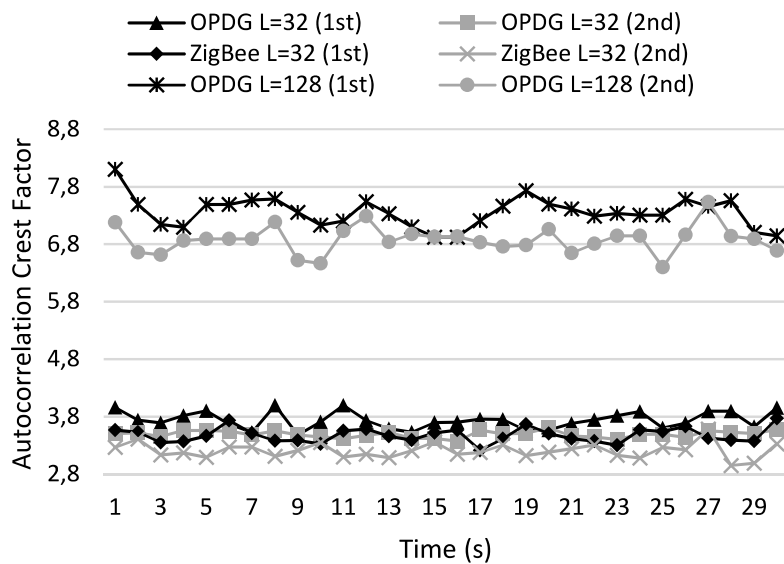


Figure 34: ACCF measurements - ZigBee vs. OPDG

Furthermore, while testing the proposed 2D scenarios, results show that, using the linear trend line of the ACCF1/ACCF2 ratios, we are able estimate the position of the receiver between the two transmitters and calculate the error. OPDG codes have shown better properties in this scenario by trend line with a higher absolute slope, which can be used to approximate the position between the two transmitters.

The tests were performed with Golay, Chu, ZigBee and OPDG codes, and the results are shown in Figure 35 below.

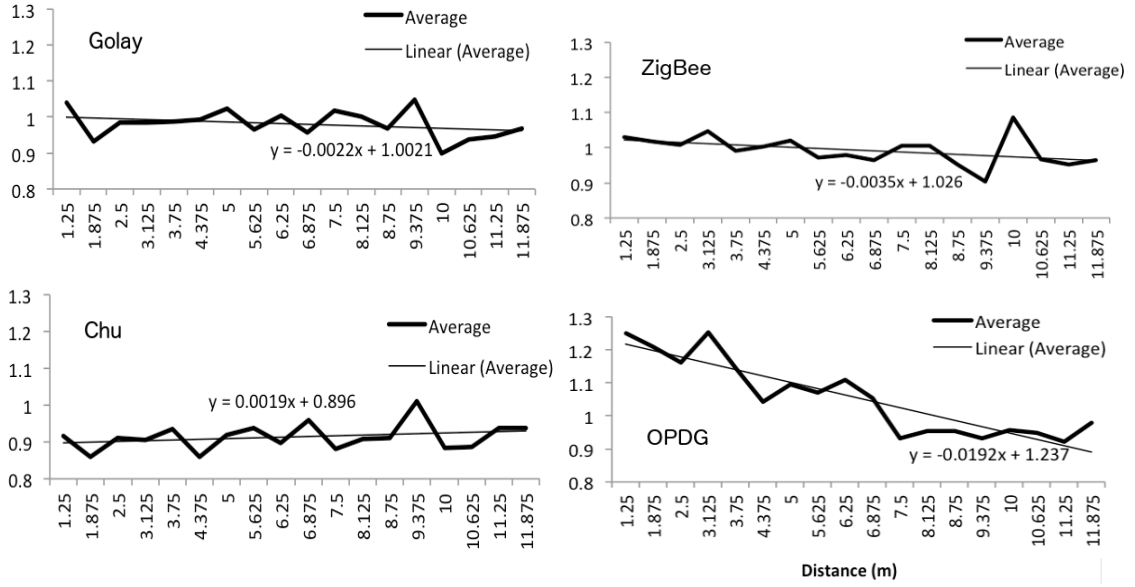


Figure 35: Test results – Golay, Chu, ZigBee and OPDG

To estimate the position of the receiver between the two transmitters the trend line equation y has been used. By doing that, the x value in the equation would provide us with the estimated location. A few measurements that are close to the transmitters were discarded in order to avoid the near-field effect.

By calculating the average estimation error using the trend line equation and the ACCF1/ACCF2 ratio for each of the code family, we can determine the efficiency of the code family.

All codes used are real codes and they have been selected with the same length of 128 chips. The 128-length ZigBee codes have been constructed using a Hadamard transform [53] based on 32-length ZigBee codes. All codes have been transmitted with the same power in our TDM-CDMA system with a mono FM transmission at 106.9 MHz. The transmission rate for all different codes was 4000 samples/sec.

Code Family	Average estimation error
Golay	13.48 m
Chu	14.28 m
ZigBee	7.99 m
OPDG	3.67 m

Table 4: Average indoor location estimation error between two transmitters - Golay, Chu, ZigBee and OPDG

Results, displayed in Table 4, show that using the OPDG codes we were able to estimate the position of the receivers between two transmitters with an error near 3.5 meters (almost the same error as the commercial GPS). This shows better estimation properties than ZigBee, Golay and Chu codes, which had an error higher than 7, 13 and 14 meters respectively. The error averages were calculated without discarding the estimated distances that were higher than our real scenario (classroom distances).

The same method can be used to estimate positions inside a 2D scenario with 4 transmitters. Since we are using 4 transmitters, the transmitters emit the codes in pairs in order to cover the whole scenario.

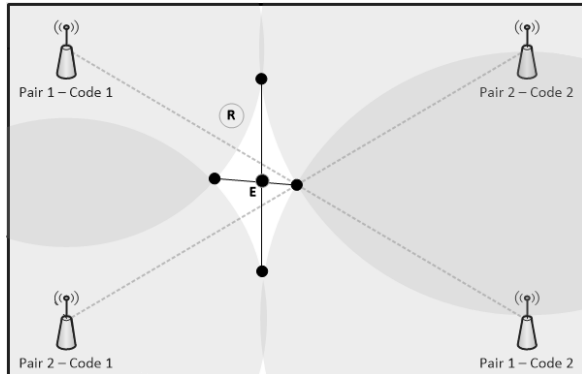


Figure 36: Triangulation process

In order to estimate the location of the receiver, we used the average ACCF ratios for each one of the pairs to estimate the power coverage area to that specific location. The location process was calculated using a representation of transmitter influence radiiuses. An example of the triangulation

process for the influence radii can be seen in Figure 36 above. Shaded areas represent the influence radius of each of the transmitters on the two-dimensional scenario. In our calculation, we have assumed that the influence radius of the second transmitter in the pair reaches half way to the other transmitter. By setting those influence radii to fixed values, we can use the ACCF1/ACCF2 ratio of that pair to estimate influence radius of the other transmitter in the pair. If we define the distance between the two transmitters in the pair as d , then the influence radius (IR) of the second transmitter in each of the pairs would be half the distance between those transmitters.

Transmitter	Influence radius
Pair 1 – Code 1	$IR_{e_{11}} = IR_{e_{12}} + \frac{ACCF - 1}{ACPM_{e_{11}e_{12}}}$
Pair 1 – Code 2	$IR_{e_{12}} = \frac{1}{2}d_{e_{11}e_{12}}$
Pair 2 – Code 1	$IR_{e_{21}} = IR_{e_{22}} + \frac{ACCF - 1}{ACPM_{e_{21}e_{22}}}$
Pair 2 – Code 2	$IR_{e_{22}} = \frac{1}{2}d_{e_{21}e_{22}}$

Table 5: Influence radii of transmitters

The IR distance used in Table 5: Influence radii of transmitters is in function of e_{xy} , where x indicates the number of the pair and y indicates the transmitter number inside the pair. ACCF represents the calculated ACCF1/ACCF2 ratio of the pair in the measuring position, and ACPM represents the change of ACCF1/ACCF2 ratio values per meter when moving from one transmitter in the pair to the other (calculated from the linear equation of the trend line).

After calculating the influence radii of all the transmitters, we use the intersection points of the radii to estimate the position of the receiver. The position is estimated using a method similar to the triangulation process, by calculating the intersection of the lines that pass through the intersection points. E marks the estimated position and R marks the real position of the receiver.

Code Family	Average estimation error	Successful estimations
Golay	4.29 m	19/81 (23.5%)
Chu	2.27 m	6/81 (7.4%)
ZigBee	2.90 m	23/81 (28.4%)
OPDG	2.78 m	21/81 (25.9%)

Table 6: Average indoor location estimation error in a scenario with four transmitters – Golay, Chu, ZigBee and OPDG

Following the 2D scenario tests with four transmitters, we were able to calculate the error estimation for each of the code families using the calculation methods described in Table 5. The results have shown that OPDG codes display better ratio of average localization estimation errors (2.78 m) and the number of successful estimations (25.9%), as presented in Table 6. Unsuccessful estimations occur when transmitter influence radiiuses do not intersect. In spite of presenting a lower error (2.27 m), the Chu sequences reveal the lowest successful estimation (7.4%) inside the classroom.

Conclusion

Results of testing the indoor position estimation properties of the new OPDG codes have led to encouraging results. We have shown that the OPDG coding sequences, used in a TDM/CDMA network with FM modulation, have shown superior location estimation properties when compared to other well-known coding sequences such as ZigBee, Golay, due to their natural immunity to multipath interference.

Besides the location estimation accuracy, OPDG codes have shown to be good candidates for usage in this scenario by displaying one of the highest successful estimation rates within the test area (even higher than Chu codes). We have also shown that improving our IPS scenario could give way to a viable low cost alternative to existing indoor positioning systems based on the signal strength of a FM signal. Future work will show how to improve the location precision and success rate by deploying additional pairs of transmitters, by mitigating the negative effects of the standing wave, as well as introducing a more realistic indoor scenario with some walls between each transmitter pair.

Future work

If we are to take into consideration the result of using OPDG codes in a TDM-CDMA network with FM modulation as a method for positioning, development of the system is still needed if we were to use this system in a real world scenario. The error of 2.78 meters is still too big to be considered as a good option for indoor positioning.

In order to improve the accuracy of the system, additional sensor mechanisms can be added which would complement the existing system.

An additional mechanism could use a similar approach to the first one, but use ultrasonic waves instead of radio waves. This type of a mechanism would be similar to the RF mechanism, except it would implement microphones instead of antennas.

A third mechanism could be added, which would be equipped with magnetometers. These magnetometers would detect the magnetic footprint and associate it with a certain position inside the scenario.

Lastly, this system could be improved by adding a final mechanism. This fourth mechanism would start off with a large number of photos being taken from different points of the environment. The photos taken would then be stored into a database, with each of the photos mapped to the location in the environment. In order to accomplish that, the receiver would be equipped with two cameras, facing in opposite directions. After receiving the location estimation from the three mechanisms (radio waves, ultrasound, and local magnetic variations), the image capture mechanism activates and takes photos from the two mounted cameras. These photos are then compared to the photos in the database, for the locations around the estimated position. After being compared, the location estimation improves significantly due to the photo comparison.

The combination of these four mechanisms could enhance the location estimation accuracy and bring it to a level that is usable in the real world. A model of this IPS can be seen in Figure 37 below.

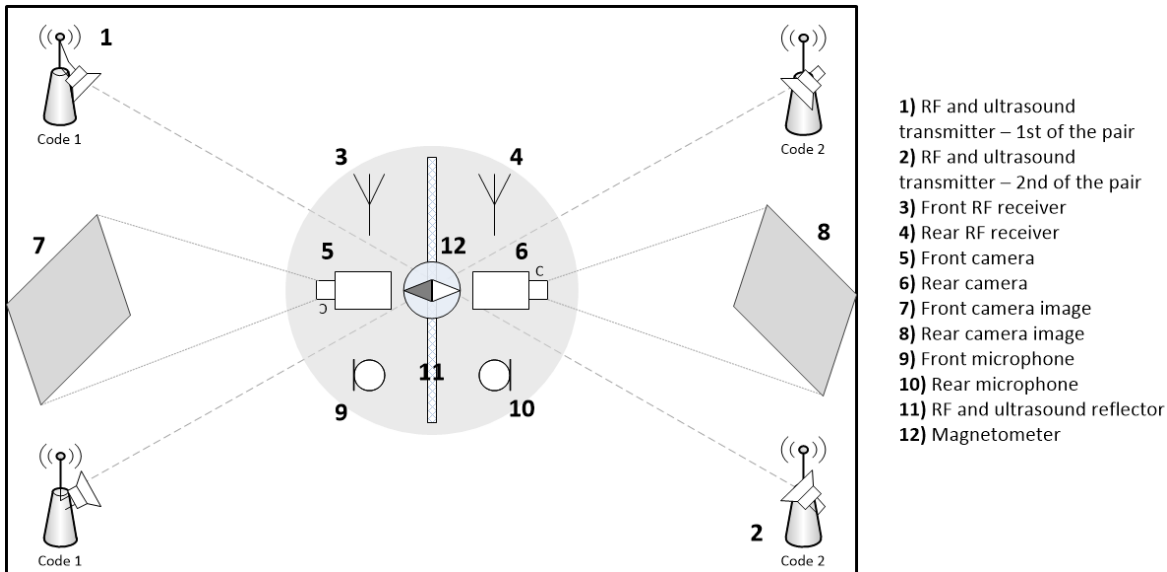


Figure 37: Theoretical four mechanism IPS

The downside of an indoor positioning such as this one would be the complexity of the system. To make four different mechanisms work in a seamless fashion would be no easy task. Furthermore, taking into consideration all the components in the system, many of these components are not readily available in existing indoor scenarios, and would have to be purchased separately. Ideally, it would be possible to build a system like this using consumer off-the-shelf hardware, but at the current state of technology it is still not the case.

Bibliography

- [1] W. H. Dutton, E. M. Rogers, and S.-H. Jun, “Diffusion and social impacts of personal computers,” *Commun. Res.*, vol. 14, no. 2, pp. 219–250, 1987.
- [2] F. Cristian, “Understanding fault-tolerant distributed systems,” *Commun. ACM*, vol. 34, pp. 56–78, 1991.
- [3] G. H. Forman and J. Zahorjan, “The challenges of mobile computing,” *Computer (Long Beach. Calif.)*, vol. 27, no. 4, pp. 38–47, 1994.
- [4] M. Satyanarayanan, “Pervasive computing: Vision and challenges,” *IEEE Personal Communications*, vol. 8, no. 4. pp. 10–17, 2001.
- [5] H. Liu, H. Darabi, P. Banerjee, and J. Liu, “Survey of wireless indoor positioning techniques and systems,” *IEEE Transactions on Systems, Man and Cybernetics Part C: Applications and Reviews*, vol. 37, no. 6. pp. 1067–1080, 2007.
- [6] M. Ferreira, J. Bagaric, J. M. Lanza-Gutierrez, J. S. Pereira, J. A. Gomez-Pulido, and S. Priem-Mendes, “On the Use of Perfect Sequences and Genetic Algorithms for Estimating the Indoor Location of Wireless Sensors,” *Int. J. Distrib. Sens. Networks*, vol. 2015, pp. 2–5, 2015.
- [7] J. Bagaric, M. Ferreira, J. da S. Pereira, and S. P. Mendes, “On estimating indoor location using wireless communication between sensors,” *Proc 10th Conference on Telecommunications Conftele*, 2015. .
- [8] J. Bagaric, J. da S. Pereira, and S. Priem-Mendes, “Standing wave cancellation - Wireless transmitter, receiver, system and respective method,” 109137, 2016.
- [9] P. K. Enge, “The Global Positioning System: Signals, measurements, and performance,” *Int. J. Wirel. Inf. Networks*, vol. 1, no. 2, pp. 83–105, 1994.
- [10] J. Hallberg, M. Nilsson, and K. Synnes, “BLUETOOTH POSITIONING,” *10th Int. Conf. Telecommun. 2003 ICT 2003*, vol. 2, pp. 954–958, 2003.
- [11] B. Srivastava, “Radio frequency ID technology: The next revolution in SCM,” *Bus. Horiz.*,

vol. 47, no. 6, pp. 60–68, 2004.

- [12] D. Porcino and W. Hirt, “Ultra-wideband radio technology: Potential and challenges ahead,” *IEEE Communications Magazine*, vol. 41, no. 7, pp. 66–74, 2003.
- [13] V. Filonenko, C. Cullen, and J. Carswell, “Indoor Positioning for Smartphones Using Asynchronous Ultrasound Trilateration,” *ISPRS Int. J. Geo-Information*, vol. 2, no. 3, pp. 598–620, 2013.
- [14] S. Phillips, M. Katchabaw, and H. Lutfiyya, “WLocator: An indoor positioning system,” in *3rd IEEE International Conference on Wireless and Mobile Computing, Networking and Communications, WiMob 2007*, 2007.
- [15] N. Lemieux and H. Lutfiyya, “WHLocator: hybrid indoor positioning system,” *Proc. 2009 Int. Conf. Pervasive Serv.*, pp. 55–63, 2009.
- [16] C. Yang and H. R. Shao, “WiFi-based indoor positioning,” *IEEE Commun. Mag.*, vol. 53, no. 3, pp. 150–157, 2015.
- [17] D. Vasisht, S. Kumar, and D. Katabi, “Decimeter-Level Localization with a Single WiFi Access Point,” *Proc. 13th USENIX Symp. Networked Syst. Des. Implement.*, pp. 165–178, 2016.
- [18] H. S. Kim, D. R. Kim, S. H. Yang, Y. H. Son, and S. K. Han, “An indoor visible light communication positioning system using a RF carrier allocation technique,” *J. Light. Technol.*, vol. 31, no. 1, pp. 134–144, 2013.
- [19] M. Yasir, S.-W. Ho, and B. N. Vellambi, “Indoor Positioning System Using Visible Light and Accelerometer,” *J. Light. Technol.*, vol. 32, no. 19, pp. 3306–3316, 2014.
- [20] S. S. Saad and Z. S. Nakad, “A standalone RFID indoor positioning system using passive tags,” *IEEE Trans. Ind. Electron.*, vol. 58, no. 5, pp. 1961–1970, 2011.
- [21] B. Ozdenizci, K. Ok, V. Coskun, and M. N. Aydin, “Development of an indoor navigation system using NFC technology,” in *Proceedings - 4th International Conference on Information and Computing, ICIC 2011*, 2011, pp. 11–14.
- [22] R. Want, E. Engineering, B. Bilginer, P. Ljunggren, S. M. Sadik, J. Nilsson, E. T. Jansson, M. Technology, I. Electrical, S. Ericsson, and M. Communications, “Near field communication,” *IEEE Pervasive Comput.*, vol. 10, no. 3, pp. 4–7, 2011.
- [23] S. E. Kim, Y. Kim, J. Yoon, and E. S. Kim, “Indoor positioning system using geomagnetic

- anomalies for smartphones,” in *2012 International Conference on Indoor Positioning and Indoor Navigation, IPIN 2012 - Conference Proceedings*, 2012.
- [24] A. Baniukevic, C. S. Jensen, and H. Lu, “Hybrid indoor positioning with Wi-Fi and Bluetooth: Architecture and performance,” in *Proceedings - IEEE International Conference on Mobile Data Management*, 2013, vol. 1, pp. 207–216.
 - [25] P. Bolliger, “Redpin-adaptive, zero-configuration indoor localization through user collaboration,” ... *Work. Mob. entity localization Track*. ..., p. 55, 2008.
 - [26] W. Inc., “Wifarer.” [Online]. Available: <http://www.wifarer.com/>. [Accessed: 12-Aug-2016].
 - [27] W. Inc., “Wifarer - Image.” .
 - [28] IndoorAtlas USA Inc., “IndoorAtlas.” [Online]. Available: <https://www.indooratlas.com/>. [Accessed: 13-Aug-2016].
 - [29] IndoorAtlas USA Inc., “IndoorAtlas - Image.” .
 - [30] Pozyx Labs, “Pozyx.” [Online]. Available: <http://pozyx.io/>.
 - [31] Acuity Brands, “ByteLight.” [Online]. Available: <http://www.acuitybrands.com/solutions/services/bytelight-services-indoor-positioning>. [Accessed: 14-Aug-2016].
 - [32] nextome SRL, “Nexttome.” [Online]. Available: <https://www.nextome.net/en/indoor-positioning-technology.php>.
 - [33] ibeacon.com, “WHAT IS IBEACON? A GUIDE TO BEACONS,” *ibeaconinsider*, 2016. .
 - [34] Ludovic Privat, “Nextome: Bluetooth Indoor Location Made in Italy.” [Online]. Available: http://www.gpsbusinessnews.com/Nextome-Bluetooth-Indoor-Location-Made-in-Italy_a5322.html. [Accessed: 14-Aug-2016].
 - [35] A. Doucet, N. de Freitas, and N. Gordon, “An Introduction to Sequential Monte Carlo Methods,” *Seq. Monte Carlo Methods Pract.*, pp. 3–14, 2001.
 - [36] M. R. Gholami, “Positioning Algorithms for Wireless Sensor Networks,” Chalmers University of Technology, Gothenburg, Sweden, 2011.
 - [37] R. Dalce, “Comparison of Indoor Localization Systems Based on Wireless Communications,” *Wirel. Eng. Technol.*, vol. 2, no. 4, pp. 240–256, 2011.
 - [38] “Perfect and almost perfect sequences.” [Online]. Available:

http://qh.eng.ua.edu/e_paper/phd_research/pinhole_image/perfect_almost_perfect_Jungnickel_1999.pdf. [Accessed: 14-Feb-2016].

- [39] Wikipedia, “Autocorrelation vs. Cross-correlation - Image.” .
- [40] J. da S. Pereira, *Sequências perfeitas para sistemas de comunicação*. 2015.
- [41] Z. Zhou and X. Tang, “Generalized modified Gold sequences,” *Des. Codes, Cryptogr.*, vol. 60, no. 3, pp. 241–253, 2011.
- [42] J. S. Pereira and H. J. A. Da Silva, “M-ary mutually orthogonal complementary gold codes,” in *European Signal Processing Conference*, 2009, pp. 1636–1640.
- [43] S. Kounias, C. Koukouvinos, and K. Sotirakoglou, “On Golay sequences,” *Discrete Math.*, vol. 92, no. 1–3, pp. 177–185, 1991.
- [44] S. Z. Budisin, “Efficient pulse compressor for Golay complementary sequences,” *Electron. Lett.*, vol. 27, no. 3, pp. 219–220, 1991.
- [45] H. Dieter Like, “Sequences and Arrays with Perfect Periodic Correlation,” *IEEE Trans. Aerosp. Electron. Syst.*, vol. 24, no. 3, pp. 287–294, 1988.
- [46] J. S. Pereira and H. J. A. Da Silva, “Alternative Zigbee codes derived from orthogonal perfect DFT sequences,” in *Proceedings of 6th International Conference on Wireless Communication and Sensor Networks, WCSN-2010*, 2010.
- [47] C. M. Ramya, M. Shanmugaraj, and R. Prabakaran, “Study on ZigBee technology,” in *ICECT 2011 - 2011 3rd International Conference on Electronics Computer Technology*, 2011, vol. 6, pp. 297–301.
- [48] R. P. Feynman, R. B. Leighton, and M. L. Sands, *The Feynman Lectures on Physics*, vol. 1. 1963.
- [49] Raspberry Pi Foundation, “Raspberry Pi - Teach, Learn, and Make with Raspberry Pi,” *Www.Raspberrypi.Org*, 2012. .
- [50] I. Silicon Laboratories, “Si4702/03-C19,” 2009.
- [51] C. C. PiHack, “Turning the Raspberry Pi Into an FM Transmitter.” [Online]. Available: http://www.icrobotics.co.uk/wiki/index.php/Turning_the_Raspberry_Pi_Into_an_FM_Transmitter. [Accessed: 01-Sep-2015].
- [52] C. Girard, C. Joachim, and S. Gauthier, “The physics of the near-field,” *Reports Prog. Phys.*, vol. 63, no. 6, pp. 893–938, 2000.

- [53] W. K. Pratt, J. Kane, and H. C. Andrews, “Hadamard transform image coding,” *Proc. IEEE*, vol. 57, no. 1, pp. 58–67, 1969.
- [54] S. Hara, “Overview of Multicarrier CDMA,” *IEEE Communications Magazine*, vol. December, pp. 126–130, 1997.
- [55] J. S. Pereira and H. A. Silva, “Codificador e descodificador eletrônico de sinais ortogonais e perfeitos,” 106755, 2015.
- [56] P. Kinney, “ZigBee Technology : Wireless Control that Simply Works,” *Communications Design Conference*, no. October, pp. 1–20, 2003.
- [57] A. V. Alejos, D. Muhammad, and H. U. R. Mohammed, “Design and implementation of Ground Peneration Radar system using coded Sequences and improved target detection using Golay codes,” in *2008 IEEE Region 5 Conference*, 2008, pp. 318–321.
- [58] B. M. Popovic, “Generalized Chirp-Like Polyphase Sequences with Optimum Correlation Properties,” *IEEE Trans. Inf. Theory*, vol. 38, no. 4, 1992.
- [59] A. Yaghjian, “An overview of near-field antenna measurements,” *IEEE Transactions on Antennas and Propagation*, vol. 34, no. 1. pp. 30–45, 1986.
- [60] J. Hightower and G. Borriello, “Location Sensing Techniques,” *Computer (Long. Beach. Calif.)*, no. August, pp. 1–4, 2001.

Appendices and attachments

This chapter contains all of the additional work that has been created while researching into the topic of this thesis.

Appendix I – Scientific Paper

Hindawi Publishing Corporation
 International Journal of Distributed Sensor Networks
 Volume 2015, Article ID 720574, 12 pages
<http://dx.doi.org/10.1155/2015/720574>

On the use of perfect sequences and genetic algorithms for estimating the indoor location of wireless sensors

M. Ferreira^{1,2}, J. Bagarić^{1,3}, Jose M. Lanza-Gutierrez^{2,4}, S. Priem-Mendes^{1,2}, J. S. Pereira^{1,2,3}, Juan A. Gomez-Pulido^{2,4}

¹Polytechnic Institute of Leiria, School of Technology and Management, Leiria, Portugal

² Center for research in Informatics and Communications, Polytechnic Institute of Leiria, Portugal

³Instituto de Telecomunicações, Leiria Branch, Portugal

⁴University of Extremadura, Dep. of Technologies of Computers and Communications, Polytechnic School, Caceres, Spain.

Abstract – Determining the indoor location is usually performed by using several sensors. Some of these sensors are fixed to a known location and either transmit or receive information that allows other sensors to estimate their own locations. The estimation of the location can use information such as the time-of-arrival of the transmitted signals, or the received signal strength, among others. Major problems of indoor location include the interferences caused by the many obstacles in such cases, causing among others the signal multipath problem and the variation of the signal strength due to the many transmission media in the path from the emitter to the receiver. In this paper, the creation and usage of perfect sequences that eliminate the signal multipath problem is presented. It also shows the influence of the positioning of the fixed sensors to the precision of the location estimation. Finally, genetic algorithms were used for searching the optimal location of these fixed sensors, therefore minimizing the location estimation error.

1. Introduction

The GPS (Global Positioning System) receivers work well in line-of-sight (LOS) conditions, meaning they cannot be used in an indoor scenario or locations in which there is limited LOS to the GPS satellites. Current GPS outdoor location accuracy is around 3 meters and is too high for most home automation purpose tasks. Additionally, a GPS signal cannot be caught clearly in indoor scenarios.

The type and quality of measurements have a considerable effect on the performance of a positioning algorithm in a Wireless Sensor Network (WSN). Different types of measurements have been considered in the literature -[5] for the positioning problem, e.g., received signal strength (RSS), angle-of-arrival (AOA), time-of-arrival (TOA), and time-difference-of-arrival (TDOA). The application of such techniques can be found in [6].

Since designing an estimator for the positioning problem strongly depends on the model of measurements, it is of great importance to use an accurate model for measurements. The sensor nodes can be either stationary or moving. They might also be able to make more than one type of measurement. Our project started with RSS-based measurement because it is the only accepted measurement that does not suffer from NLOS conditions. Our real scenario work instance is a building with a considerable set of walls where a wireless sensor should be able to locate itself.

The performance of communication systems using Code Division Multiple Access (CDMA) and Orthogonal Frequency Division Multiple Access (OFDMA) is directly related to the coding sequence they use. These sequences should have a perfect autocorrelation and excellent cross-correlation properties for synchronization or code detection in noisy environments. The importance of code detection accuracy in these coding sequences becomes evident when they are applied in WSN environments that have much interference.

In this paper, the general issue of implementing an accurate Indoor Positioning System (IPS) will be tackled, using a small TDM-CDMA (Time Division Multiplexing – Code Division Multiple Access) distributed sensor network. This IPS system will be implemented using low cost FM (Frequency Modulation) transmitters and receivers.

Several sequences have been proposed and used in communication and localization systems. In the third generation of mobile communication (3G), Walsh-Hadamard Sequences are used in UMTS [7]. This system has been further improved in what is now called 4G Long Term Evolution (LTE), using Zadoff-Chu sequences instead of the Walsh-Hadamard [7]. Another set of sequences, the Gold Sequences, are currently used in the Global Positioning System (GPS) for outdoor localization [8]. Golay sequences are also widely considered in many areas, including radar systems [9].

An analysis was performed by comparing the behavior of novel OPDG (Orthogonal Perfect DFT Golay) codes to the ZigBee codes (32-length Pseudo Noise code of a WSN), demonstrating that OPDG codes have better correlation properties. Afterwards, a scenario of an IPS is set up, and the significance of using OPDG codes with better correlation properties is presented. We start the paper by explaining the intention of using a novel code family (OPDG), comparing it to the well-known PN (Pseudo Noise) ZigBee codes. Afterwards, a scenario of our IPS system is introduced, and testing results are presented. To further improve the IPS system, we introduce a genetic algorithm that helps us locate the optimum FM transmitter placement positions within the indoor scenario.

At the end, it is pointed out how the presented results indicate that this system is a viable alternative to existing IPS systems, with the additional advantage of its low implementation cost.

2. OPDG IPS Model

One of the major problems of wireless communication is multipath Interference (MPI). Transmission media, such as wireless, can bounce off certain obstacles, taking multiple paths to reach the receiver. Delays created by these obstacles can cause interference in communication. Other interferences include the multi-carrier interference, inter-symbol interference and the multiple access interference. These interferences can be reduced by using perfect sequences for transmission [10]. The latter two interferences can be reduced if those sequences are also orthogonal for any delay between them [11].

Our task is to improve accuracy in IPS systems that use wireless communication. In indoor wireless communication, the use of code sequences that are resistant to multi-path interferences is vital to achieve accuracy, due to a large number of obstacles present in the environment. We propose the use of perfect sequences, whose correlation properties render them immune to multipath interferences, as opposed to commonly used coding sequences.

In this section, autocorrelation and cross-correlation properties of coding sequences will be explained. Further on, a comparison will be made between the widely-used ZigBee coding sequences and the novel OPDG sequences. Lastly, a low cost IPS scenario will be set up and explained.

A. Autocorrelation and cross-correlation

A sequence x is a periodic sequence with a period M when, where $x(n) = x(\text{mod}(n, M))$ where $\text{mod}(a, b)$ is the remainder of a divided by b .

Let $x[n]$ with $n = 0, 1, 2, \dots, M - 1$, be one of the M values of a periodic sequence x . The DFT (Discrete Fourier Transform) of $x[n]$ is defined as

$$X[k] = DFT\{x[n]\} = \sum_{n=0}^{M-1} x[n]W_M^{kn}, \quad (1)$$

where $W_M = \exp(-j2\pi/M)$, $k = 0, 1, 2, \dots, M - 1$, with $j = \sqrt{-1}$ for convenience of notation. The IDFT (Inverse Discrete Fourier Transform) of $X[k]$ is then given by

$$IDFT\{X[n]\} = x[n] = \frac{1}{M} \sum_{k=0}^{M-1} X[k] W_M^{-kn}. \quad (2)$$

Using (1) and (2), the periodic cross-correlation between two different sequences $x^{(r)}$ and $x^{(s)}$ is defined as

$$\begin{aligned} R_{x^{(s)}x^{(r)}}[n] &= \sum_{k=0}^{M-1} x^{(r)}[k] x^{*(s)}[\text{mod}(k+n, M)] \\ &= \sum_{k=0}^{M-1} x_k^{(r)} x_{k+n}^{*(s)}. \end{aligned} \quad (3)$$

Alternatively, it can be defined as

$$R_{x^{(s)}x^{(r)}}[n] = IDFT\{X^{(r)} X^{*(s)}\}, \quad (4)$$

where the superscript * denotes the complex conjugate.

The autocorrelation of a periodic sequence can also be calculated using (4), when $r = s$.

When a periodic sequence has an autocorrelation of zero for any non-zero delay, the sequence is said to be a perfect sequence. Additionally, the two different sequences are called orthogonal if the cross-correlation between them is zero for a null delay. Because of these correlation properties, orthogonal perfect sequences are ideal to be used in several applications, such as radar systems, sonar systems, communication synchronization systems, etc.

B. OPDG code

Any sequence set with perfect or near-perfect autocorrelation values, which is also orthogonal or near-orthogonal, is a good candidate to be used in asynchronous communication systems, such as DS-CDMA (Direct-Sequence Code-Division Multiple Access), or any other system where the signal reception may be contaminated by the multi-path problem. Another important property for the sequence set is the number of orthogonal sequences available. The Gold sequences are a good example of a set of sequences having these properties, since they have excellent correlation properties while being possible to generate in large numbers. For instance, it is possible to create 32 orthogonal Gold sequences with a length of 32. However, sequences with low cross-correlation values usually have high out-of-phase autocorrelation values. Likewise, low out-of-phase autocorrelation values are usually achieved at the cost of higher cross-correlation values. A compromise between these properties must be carefully selected for usage on a CDMA-based communication system.

Golay sequences are bipolar complementary sequences. Additionally, the autocorrelation of a single sequence of a Golay pair is not zero with all non-null delays, for any length $L = 2^N$. However, the sum of the out-of-phase autocorrelations of both sequences in the pair is zero. Therefore, Golay sequences are not perfect sequences. Nevertheless, they are interesting for their properties. A generic algorithm for Golay sequence generation was presented by Budisin [12] as follows

$$\begin{aligned} a_0[k] &= \delta[k] \\ b_0[k] &= \delta[k] \\ a_n[k] &= a_{n-1}[k] + w_n b_{n-1}[k - D_n] \\ a_n[k] &= a_{n-1}[k] - w_n b_{n-1}[k - D_n] \end{aligned} \quad (5)$$

where $\delta[k]$ is the unit pulse function that works as a trigger signal, $a_n[k]$ and $b_n[k]$ are the Golay sequences, w_n is a generation seed (either 1 or -1), and D_n is a delay (2^{n-1}).

An example of a Golay complementary sequence of length 4 is the following pair: (+1,+1,+1,-1) and (+1,+1,-1,+1). The amplitude of a Golay sequence $a_n[k]$ is a constant value given by $|a_n[k]|=1$.

It is well-known that any constant amplitude sequence, defined in the frequency domain, corresponds to a perfect sequence in the time domain.

Applying an IDFT to Golay sequences creates two new polyphase perfect sequences, which are

$$\begin{aligned} OPDG_1 &= IDFT\{a_n[k]\} \\ OPDG_2 &= IDFT\{b_n[k]\}. \end{aligned} \quad (7)$$

It should be noted that it is possible to find the IDFT of any sequence X using also a DFT, because

$$IDFT\{X(n)\} = \frac{1}{N} [DFT\{X^*(n)\}]^*. \quad (8)$$

The same sequences can be achieved by a recursive algorithm as follows

$$\begin{aligned} a_0[k] &= A \\ b_0[k] &= A \\ a_n[k] &= a_{n-1}[k] + q \cdot W_{2^n}^{-k \cdot 2^{n-1}} b_{n-1}[k] \\ b_n[k] &= a_{n-1}[k] - q \cdot W_{2^n}^{-k \cdot 2^{n-1}} b_{n-1}[k] \end{aligned} \quad (9)$$

where A is a constant signal or vector, $W_L = \exp(-j2\pi/L)$, $j = \sqrt{-1}$ and $0 < n \leq N$. The resulting sequences a_n and b_n are the $OPDG_1$ and $OPDG_2$ as per (7) scaled by $A \times L$. They can be on the same scale as (7) using $A = 1/L$, with $L = 2^N$.

Several operations can be applied to the OPDG sequences to generate different sequences. One can create a real code by ignoring the imaginary part of the complex valued sequences and keeping only the real part ($Re\{OPDG_x\}$). Likewise, one can ignore the real part of the sequence and keep only the imaginary part ($Im\{OPDG_x\}$). One can also add the real part to the imaginary part ($Re\{OPDG_x\} + Im\{OPDG_x\}$). It is also possible to apply a sign function to any of the previous sequences. A sign function ($Sgn(x)$) returns -1 to negative inputs, and 1 to positive ones. Another possibility is to make a cyclic shift of the imaginary part of each code, prior to the sum, thus generating $L - 1$ new complex valued sequences.

It is also possible to decode the original input value A , from (9), back from the OPDG codes. A recursive decoding method can be used as follows

$$\begin{aligned} a_{n-1}[k] &= q \cdot W_{2^n}^{-k \cdot 2^{n-1}} \cdot \{a_n[k] + b_n[k]\} \\ b_{n-1}[k] &= a_n[k] - b_n[k], \end{aligned} \quad (10)$$

where $1 \leq n \leq N$, a_n and b_n are the $OPDG_1$ and $OPDG_2$ that resulted from (9), and, as previously, $W_L = \exp(-j2\pi/L)$. Notice that in (10), n varies from N down to 1. From a_0 and b_0 , a vector A' can be created by

$$A'[k] = a_0[k] + b_0[k] \quad (11)$$

The resulting A' is an interesting vector because it presents two different method decoding processes:

$$\operatorname{Re}\{DFT(A')\} = A[q]^N 2^{2N+1} \delta[k - 2^N + 1] \quad (12)$$

and

$$|A'|^2 = A^2 2^{2N+2}. \quad (13)$$

As seen in (12), the real part of a *DFT* applied to A' is proportional to a Dirac pulse delayed by $2^N - 1$. This property allows an enhanced detection process in spite of MPI.

C. Usage in the ZigBee communication system

The novel OPDG codes are derived from real orthogonal perfect DFT sequences. To be more precise, the first OPDG code is obtained by making the sum of the real and imaginary part of $OPDG_1$. The second OPDG code is built using the addition of the real and imaginary part of $OPDG_2$. These novel codes are real, orthogonal and perfect. As such, they should be optimum alternative codes for a ZigBee communication system, which uses PN codes defined in [13] and [15].

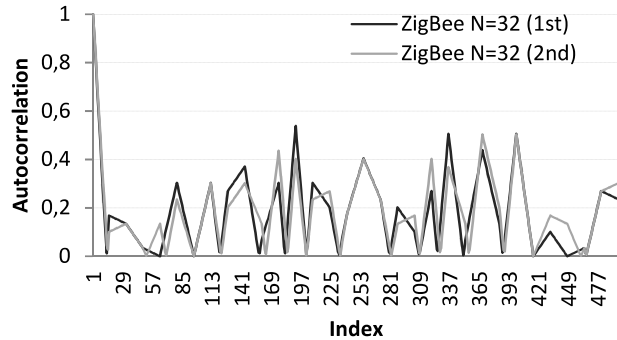
An autocorrelation crest factor can be used as a parameter of autocorrelation efficiency. The autocorrelation crest factor ACCF is defined as a ratio of the maximum peak A_{peak} and the root mean square of the autocorrelation function A_{rms} as:

$$ACCF = \frac{A_{peak}}{A_{rms}}. \quad (14)$$

When the autocorrelation is perfect, like a Dirac pulse, the ACCF of a periodic sequence of length L is equal to \sqrt{L} .

A comparison between these two codes follows. Figure 1 shows the normalized periodic autocorrelation properties of the standard ZigBee codes with the code length of 32. The ACCF average is 7.77. Figure 2 shows the normalized periodic autocorrelation properties of the OPDG codes with the length of 32. The ACCF average is 9.48. Furthermore, by increasing the code length, autocorrelation properties (or ACCF) increase greatly. Increasing the code length of the OPDG codes results in a reduction of fluctuation in the normalized periodic autocorrelation function, as can be seen in Fig. 3. This last ACCF average - 18.62 - is much higher.

As it may be observed, the novel OPDG codes have better correlation properties despite using a simple 16-bit resolution.



D. Indoor Positioning System

Building an IPS system that would enable us to accurately determine the position of an entity in a closed space, with a lot of MPI, is a difficult problem in positioning systems. We believe that the use of the OPDG codes can greatly enhance the accuracy of low cost IPS systems that use CDMA.

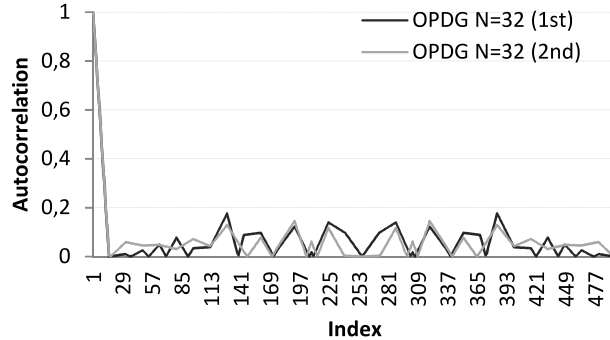


Fig. 1. Normalized absolute periodic autocorrelation – OPDG codes, with resolution of 16 bits.

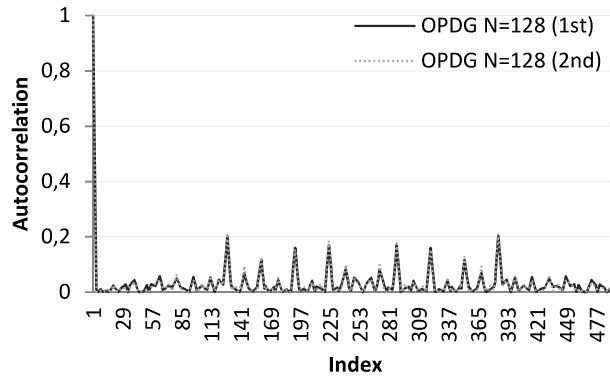


Fig. 2. Normalized absolute periodic autocorrelation - OPDG codes with the code length of 128, with a resolution of 16 bits.

We propose a system that can use the communication of FM transmitters and receivers with OPDG codes to determine the indoor location of a device. The computing device we use to receive and process the codes is a small, low-powered single-board computer Raspberry Pi [15]. A second Raspberry Pi is also used to control the transmissions of all emitter pairs.

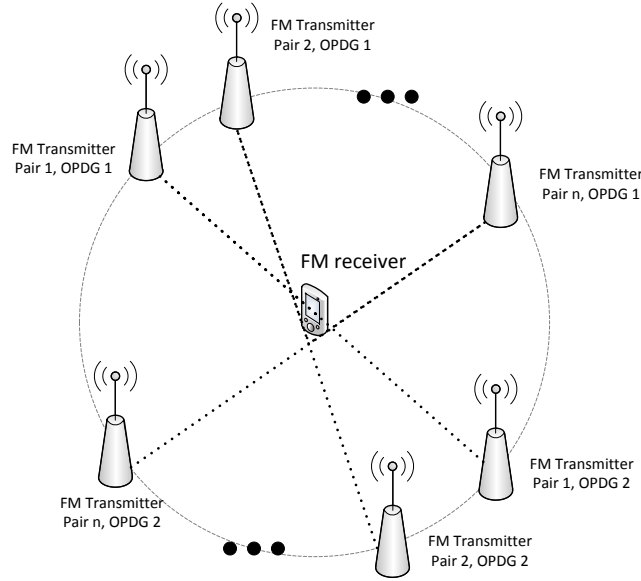


Fig. 3. IPS network topology

Our system is depicted by Fig. 4, where each pair transmits its code in TDM. Inside the indoor scenario, FM transmitters are placed in optimum positions to cover the room with as much signal as possible. The Raspberry Pi is mounted on an object that allows its location discovery. As the different FM transmitters emit different OPDG codes, Raspberry Pi uses those codes to approximate the distance to each individual transmitter using the following formula:

$$\hat{d}_{ij} = d_0 10^{\frac{P_{0i}-10\log(ACCF \times A_{rms})}{10\beta}}. \quad (15)$$

Equation (15) was derived from the distance estimation equation introduced in [6], and represents the distance between nodes i and j . P_{0i} denotes the power in dB at the distance d_0 , β is a path-loss exponent that is usually between 2 and 6 [16], ACCF is the autocorrelation crest factor and A_{rms} is the root mean square of the autocorrelation function.

E. Use case scenario

We have implemented an IPS scenario using a pair of FM transmitters. Each emitter was broadcasting one different real OPDG code of the set $\{\text{Re}[OPDG_1] + \text{Im}[OPDG_1] \cup \text{Re}[OPDG_2] + \text{Im}[OPDG_2]\}$. Both FM emitters transmitted 128-length OPDG codes with a total-length of 128×4 chips, at 106.9 MHz (mono), with a sample rate of 8000 sample/sec and a hardware resolution of 16 bits. The broadcast was continuous during 30 seconds. FM transmitters were located 7 m away from each other.

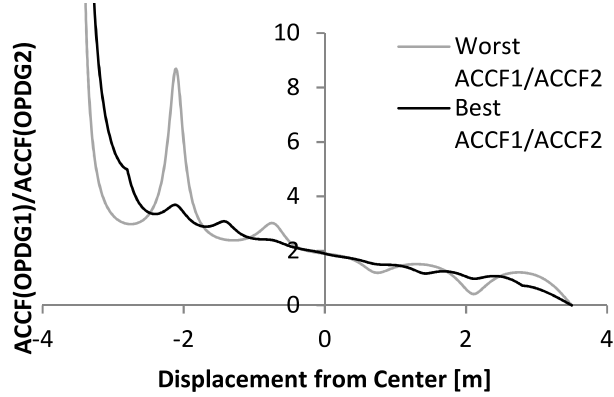


Fig. 4. Theoretical ACCF1/ACCF2 ratios.

Figure 5 shows two theoretical ratios of ACCF values of a pair of OPDG codes. Using this ratio, we can approximate a linear function for the displacement estimation, and reduce the error of the IPS. The theoretical worst case ratio of Fig. 5 was calculated using all phases of the two FM signals.

On the other hand, the theoretical best case ratio was achieved considering 2 constructive multipath interferences. These interferences were created by placing a RF (Radio Frequency) reflector 35 cm behind each emitter. Using this scenario, a stationary wave average has less fluctuation, and represents the best theoretical case.

This theoretical model shows the possibility of finding a linear function based on the interval around -1.75 m and 3 m.

3. Results and Discussion

We have implemented the first stage of our low cost IPS testbed and in this section we will present some results. Normalized autocorrelation functions and ACCF parameters are presented in the next figures.

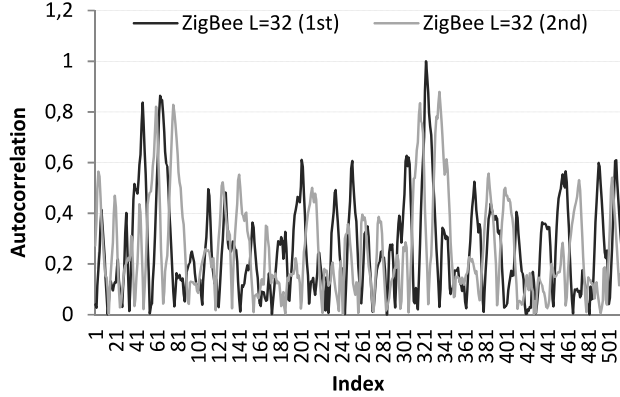


Fig. 5. Normalized autocorrelation of ZigBee codes, 32-length

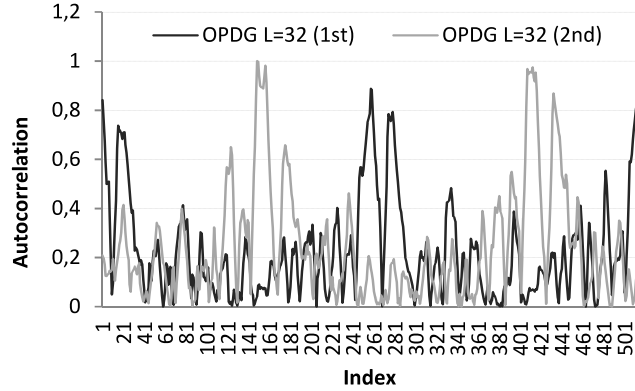


Fig. 6. Normalized autocorrelation of OPDG codes, 32-length

Figures 6 and 7 show the correlation between the received and reference codes within the Raspberry FM receiver. When compared to the ZigBee codes, OPDG codes with the length of 32 can reveal an *ACCF* 40% higher and therefore substantially better. Figure 8 shows the correlation of 128-length OPDG codes. Peaks are distinguishable and the fluctuation is significantly lower. Its better autocorrelation properties enable better approximation of the crest factor using (14).

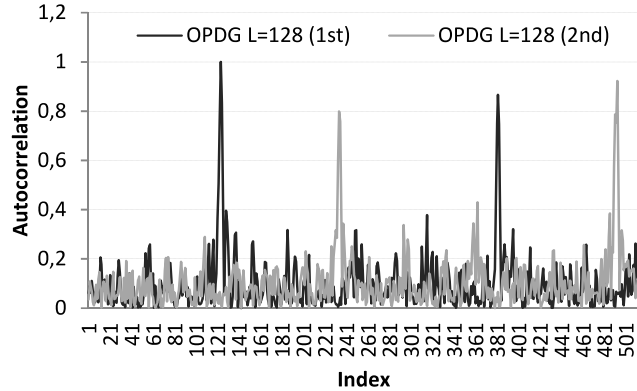


Fig. 7. Normalized periodic autocorrelation of OPDG codes, 128-length

Our IPS measurements of the ACCF are shown in Fig. 9. OPDG codes with the same code length as ZigBee codes give an average of 8% better ACCF, while increasing the code length of the OPDG codes to 128 highly improves the ACCF to an average of 7.1. These measurements were made during 30 seconds.

In the last scenario, a pair of real OPDG codes $\{\text{Re}[\text{OPDG}_1] + \text{Im}[\text{OPDG}_1]\}$ and $\{\text{Re}[\text{OPDG}_2] + \text{Im}[\text{OPDG}_2]\}$ has been used. The first FM emitter of the pair, with the code $\{\text{Re}[\text{OPDG}_1] + \text{Im}[\text{OPDG}_1]\}$, was located at -3.5 meters of the central point zero. The second FM emitter of the pair, with the code $\{\text{Re}[\text{OPDG}_2] + \text{Im}[\text{OPDG}_2]\}$, was located at +3.5 meters. Both emitters were in LOS, with some walls around them, creating a real indoor environment with some MPI.

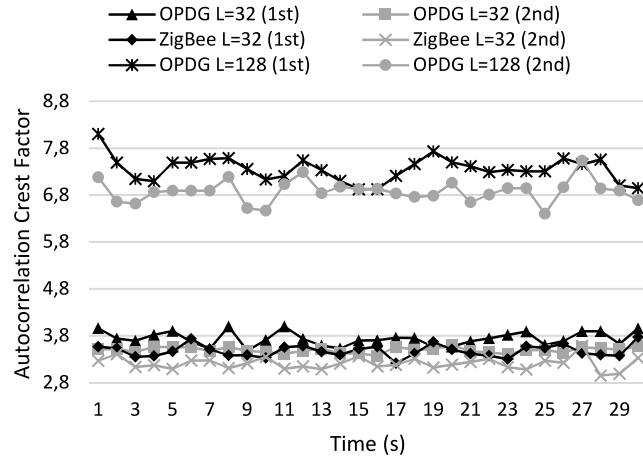


Fig. 8. ACCF measurements of different codes

We have tested the theoretical model of the ACCF ratios in a real scenario, and have come to the following results. By emitting 2 pairs of 128-length OPDG codes, a decreasing line trend from one FM emitter to the other is visible, as can be seen in Fig. 10. Two linear equations are also shown in the figure, along with reliability R.

Reliability can be further increased by calculating the average of the functions in Fig. 10, as seen in Fig. 11.

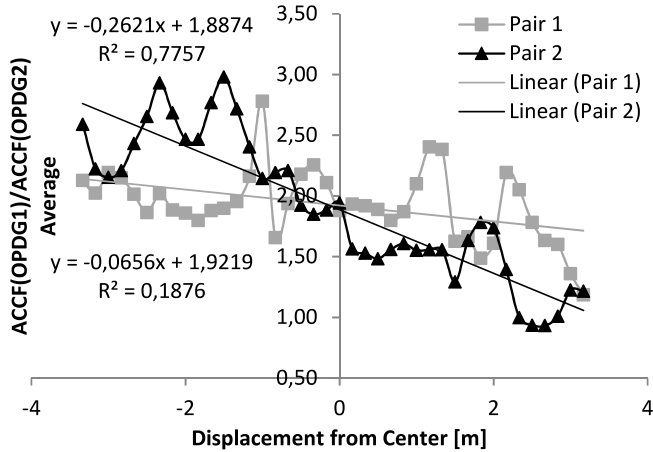


Fig. 9. ACCF ratios of 2 pairs of OPDG codes with FM modulation at a distance of 7 m

With two pairs of FM OPDG emitters, we obtain an average IPS error of 0.86 meters, with a maximum error of 2 meters. However, it is possible to predict a lower error if more pairs of emitters can be used around the FM receiver. The correct emitter locations are an open issue that should be solved shortly.

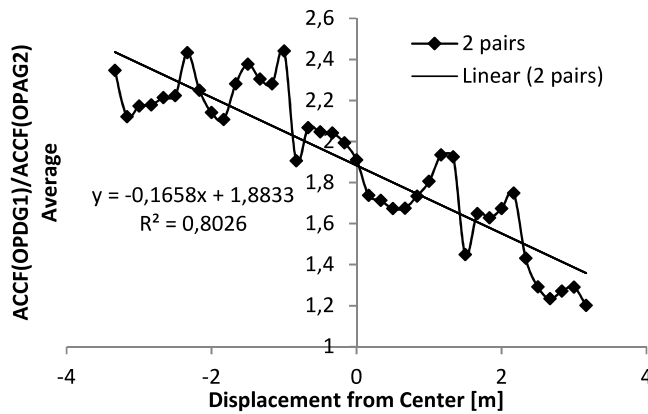


Fig. 10. The average of 2 ACCF ratios of 2 pairs of 128-length OPDG codes with FM modulation at a distance of 7 m

4. Positioning the sensors using Genetic Algorithms

The indoor location, as seen in the previous section, is estimated using the Received Signal Strength (RSS) of multiple emitters. The placement of these emitters can have a large influence on the location estimation error of the receiver sensor. In this section, we will show a metaheuristic approach to this signal emitter placement problem, namely using Genetic Algorithms.

A. Positioning of the sensors

The emitter placement presents two different problems to solve: how many emitters are needed to cover an area (such as a building or a room), and where to place them so that their signal is best used. The first problem is a standard coverage problem and can be stated as follows: given a site plant, including all possible emitter locations, how many emitters are needed so that every position in that location receives n different signals? This is a minimization problem where the variable to minimize is the number of required emitters.

The second problem is more complex. When a receiver detects n signals it will start the triangulation calculations to estimate its location. However, the resulting precision of that estimation will vary greatly with the source of those signals. Figures 12 and 13 exemplify this problem. These figures represent a simple 4 m x 4 m square room with 3 emitters (represented by triangles in the figures) and 1 receiver (represented by an x). The plus sign (symbol +) represents the location estimation of the receiver considering the RSS of the emitters. The 3 emitted signals cover all the room, so the signal coverage is the same for both figures. In figure 1, the emitters are close to each other, which makes having 3 signals almost as good as having only 1, resulting in a large location estimation error (above 1 meter). Dispersing the location of the emitters, as shown in figure 13, result in better conditions to estimate the receiver location. In this example, the theoretical location estimation error is reduced from around 1 meter in figure 12 to mere 4 cm in figure 13. Taking this into account, the second problem consists in finding the best location of n signal emitters so that the location estimation error of a receiver is minimized for all possible receiver locations.

Both of the previously described problems can be seen as combinatorial optimization problems. The number of possible combinations is, however, extremely large, and would take too long for a computer to calculate and evaluate all of the possible combinations. Since the finding of the optimal solution is very hard, in these classes of problems one generally accepts a near optimal solution. Metaheuristic algorithms deliver this near optimal solution and have been successfully applied to combinatorial optimization problems. One such algorithm is the Genetic Algorithm.

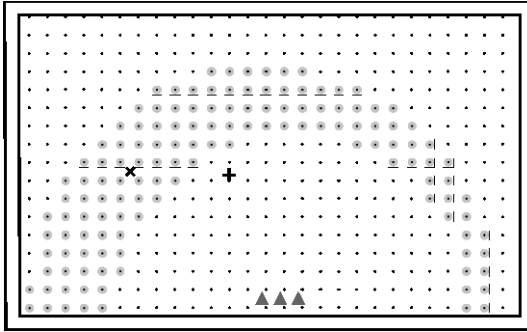


Fig. 11. Low precision of the location estimation when the signal sources are too near to each other. The estimation is approximately 1 m away from the true location of the receiver.

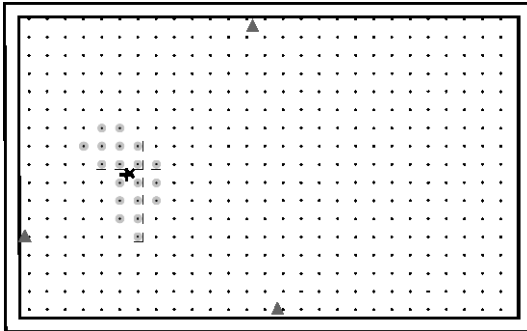


Fig. 12. High precision of the location estimation when the emitters are scattered around the target location. In here, the estimated location is only 4 cm away from the true receiver location.

B. Genetic Algorithms

A Genetic Algorithm (GA) is a population based metaheuristic search algorithm [17][18]. Its basic operation is depicted in Algorithm 1. A GA starts by creating an initial population P_0 and evaluating it. Then, a new population P_0' is created by selecting parents from the original population P_0 and applying several different operators to them. These operators are usually crossover and mutation operators. The execution of the GA proceeds to the evaluation of P_0' and then combine P_0 with P_0' , replacing the previous generation of the population (P_0) with a new population generation (P_1). Since the population size is usually immutable during the algorithm execution, this combination is basically a selection of a few members from the old population P_0 with the remaining slots being filled with elements of the new population P_0' . Selection, modification, evaluation and replacement operations repeat for many generations until a stopping condition is reached.

```

n=0
P0 = generateInitialPopulation()
evaluate(P0)
while not stoppingCondition() do
    Pn' = selectParents(Pn)
    Pn' = applyVariationOperators(Pn')
    evaluate(Pn')
    Pn+1 = selectNewPopulation(Pn, Pn')
    n = n + 1
end while
return the best found solution

```

Alg. 1. Pseudocode of a Genetic Algorithm

With GA being a metaheuristic algorithm, all these operations must be tuned to the problem it will solve. The adaptations that need to be made consist in the definition of the solution representation for the GA, the evaluation and scoring of a solution (also called the fitness calculation), the initial population creation method, the mutation and crossover operators, the parent selection and the population replacement method.

C. Solution representation

In both emitter placement problems, a solution consists simply in the location of a set of signal emitters. These locations are chosen from a larger set of all possible locations. Visually, this set can be represented as in figure 14, which shows a small part of a site plant. In this figure, 12 possible locations for signal emitters are presented, with a signal emitter being placed in the 6th location (from left to right). A solution like the one presented can be encoded in a binary string of length n , where n is the number of possible emitter locations. In this bit string, 0 indicates an unused possible location while 1 indicates a used location. The solution in figure 14 would then be encoded as ‘000001000000’.



Fig. 13. Possible signal emitter locations near a wall. Light gray triangles are the possible locations for the placement of signal emitters, while the dark triangle is a placed signal emitter.

Encoding a solution as a string of bits present a few advantages: they are easy to encode and decode, they don't require large amounts of memory and they have a fixed size, independently of the number of signal emitters placed. This encoding also facilitates the mutation and crossover operations. Also, this encoding makes it easy to calculate the number of possible emitter placement combinations: 2^n different combinations. This exponential growth of the number of combinations is what makes it impossible to find the optimal solution using classic search techniques, such as brute-force searching.

D. Solution fitness calculation for the coverage problem

The evaluation of a solution regarding the coverage problem is based on a few input parameters: the area and shape to cover, the minimum signal strength detected by a receiver, the power of the signal emitter and the properties of the transmission media. We define the area and shape as a set of rectangular areas. While this does not allow all possible shapes (circular shapes are impossible with this setup), it does allow a good approximation of them while simplifying the calculations.

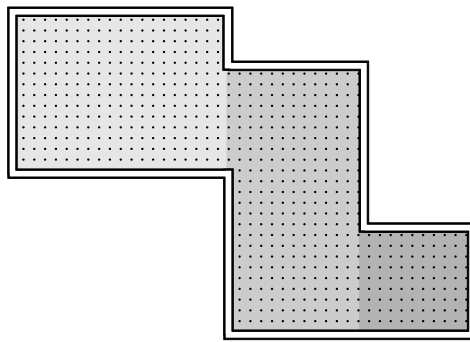


Fig. 14. An irregular shaped area approximated by 3 rectangular areas.

For the calculation of the area covered by a single signal emitter, we model the power decay, in dB, of the transmitter with

$$P_{ij} = P_{0i} - 10\beta \log\left(\frac{d(X_i, X_j)}{d_0}\right) + \eta_{ij} \quad (16)$$

where P_{0i} is the power at distance d_0 , $d(x_i, x_j)$ is the Euclidean distance between x_i and x_j , b is a path-loss exponent, x_i and x_j are the location of the emitter and the signal power measurement location respectively, and η_{ij} is a zero mean Gaussian random variable with variance σ_{ij}^2 . We ignored the noise and assumed always zero for η_{ij} while calculating the coverage of a signal emitter. We also reduce the signal power whenever it crosses a wall by 2 dB per 15 cm of wall. We considered all walls to be brick walls and this value was found experimentally.

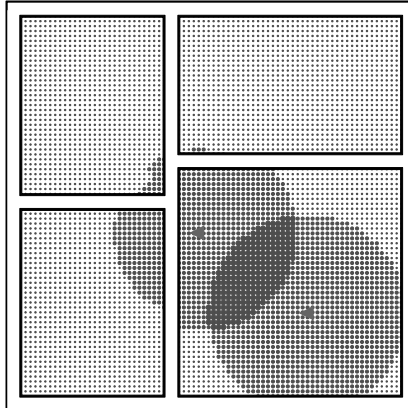


Fig. 15. Graphical representation of the coverage of 2 signal emitters. Small dots indicate that no signal reaches it, larger dots indicate that the area is covered by at least one signal (larger dots means more signal coverage).

Figure 16 shows a graphical representation of the coverage of 2 signal emitters. In this figure, it is easy to see the effects of walls in the signal power, as well as the overlap of two different signals. After determining the area covered by each and every signal emitter, we calculate the average number of signals in every location in the area (each location is represented by a dot in figures 15 and 16), as well as the minimum coverage and the standard deviation. The fitness value can then be calculated by:

$$f = \text{map}(\text{avg}, \text{curve}) + \text{stddev} + \max(\text{ideal}-\text{min}, 0) \quad (17)$$

where avg is the average number of signals at every location, curve is the fitness curve shown in figure 17, $\text{map}(a,b)$ is a function that maps the value a to the corresponding value in the curve b , stddev is the standard deviation of the coverage, $\max(a,b)$ is the mathematical maximum between a and b , ideal is the ideal coverage, and min is the minimum coverage found at all possible locations. The fitness curve shown in figure 17 allows the guidance of the Genetic Algorithm by having a clear preference for more signals than ideal over less signals than ideal. Also, the stddev and the $\max(\text{ideal}-\text{min})$ are penalties applied to the fitness. The first one will guide the GA to solutions where there is no deviation (all locations have exactly the same number of signals covering the location), while the second one heavily penalizes the solution if there are still locations where the ideal number of signals is not reached.

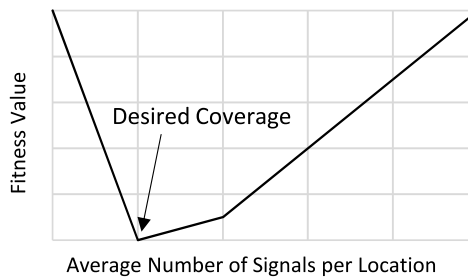


Fig. 16. Fitness curve for the average of the coverage. The horizontal axis is the average number of signals in each location, while the vertical axis is the fitness value.

E. Solution fitness calculation for the error minimization problem

When considering the minimization of the location estimation error, a different evaluation of possible solutions must be used. Firstly, let us define how the location is estimated. Given a received signal strength s sent from a specific emitter i , according to (16) the distance d of the receiver from the emitter is

$$d = d_0 10^{\frac{P_{0i} - s + \eta}{10\beta}} \quad (18)$$

where P_{0i} is the power measured at d_0 from emitter i , η is a zero mean Gaussian random variable with variance σ_{ij}^2 and d is the distance of the receiver to the emitter i , given a signal strength of s . Since this distance d depends on the unknown value of η , and the signal strength read by the receiver may contain oscillations, one can assume that the receiver is located somewhere in an area defined by an inner circle of radius $d - \varepsilon$ and an outer circle of radius $d + \varepsilon$, both centered around the emitter, with ε being a configurable reading precision error. If another signal is read by the receiver, then the receiver location can be restricted to the intersection of the calculated circular areas of both emitters. As the number of signals increase, so does the intersected area decreases. After all the intersections are made, the estimated location is calculated to be the geometrical center of the resulting area. Figure 18 illustrates this process by showing the inner and outer circles of two received signals, as well as their intersection and estimation of the receiver's location. After estimating the location, its error can be easily calculated as the Euclidean distance between the receiver's real location and the receiver's estimated location. For calculus simplification, we discretize the space into square cells and consider only the center of each cell. This discretization can also be seen in figure 18, with each dot corresponding to the center of each cell.

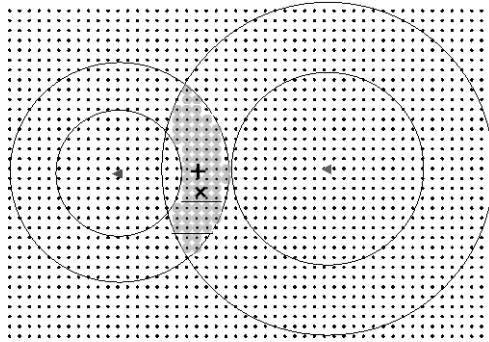


Fig. 17. Estimation of the location (+) of a receiver (x) using the signal strength of 2 different emitters.

With the estimated location error calculated for each cell, the solution fitness is simply the average of all the errors. Since the error is a Euclidean distance, there will be no negative errors, so an ideal solution would have a fitness of 0, meaning no error at all in any location.

F. Mutation operators

As described in algorithm 1, the new generation of a population is obtained by applying different operators to selected parents of the current generation. One of those operators is the mutation operator.

During the mutation, each gene can, according to a given probability, maintain its value, flip it or swap it with another gene. Figure 19 shows an example of a gene's value flip, with the third gene flipping its value from 1 to 0. A gene flip will either increase or decrease the solution's number of emitters. Figure 20 shows an example of a gene swap, where the first gene is swapped with the third gene. A gene swap always maintains the number of emitters, but changes their location. The gene swaps always occur between a gene with value 1 and a gene with value 0. This condition guarantees that no unnecessary work is done by the genetic algorithm in the reevaluation of an identical solution.

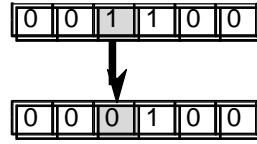


Fig. 18. Example of a gene value flip. On top is the original solution, on bottom is the mutated solution.

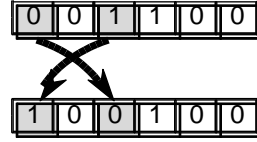


Fig. 19. Example of a gene swap. On top is the original solution, on bottom is the mutated solution.

In the coverage problem, the number of emitters varies and must be able to grow or shrink as necessary, thus we use the bit flip mutation. In the error minimization problem, however, the number of emitters is fixed, so the gene swap mutation is applied.

G. Crossover operators

A crossover operator is responsible for recombining the chromosomes of parent solutions into offspring solutions. This process will hopefully combine the best parts of the parents into fitter offspring for the problem.

As with the mutation operators, we must consider crossover operators that may change the number of emitters for the coverage problem and operators that do not change the number of emitters for the error minimization problem. We use a one-point crossover operator in the coverage problem. This operator will randomly select one point on two different parent solutions, split them at that point and then recombine them into two other offspring solutions. Since the point of crossover is selected blindly, the crossover may increase or decrease the number of emitters in the solution. Figure 21 exemplifies a one-point recombination where the top offspring has less emitters and the bottom offspring has more emitters than the parent solutions

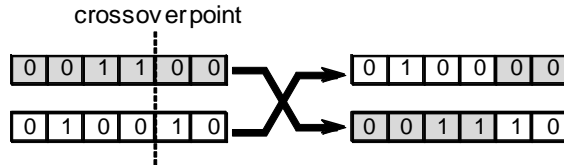


Fig. 20. One-point crossover. On the left are the parent solutions while at the right are the offspring generated by crossing over the parents.

For the error minimization problem, the number of emitters is constant, so a different approach has to be used for the crossover. For this problem, the crossover creates offspring solutions where each emitter is placed from a location of one of the parents. This maintains the number of emitters, while still hopefully use the best parts of each parent solution. Figure 22 shows an example of the application of this crossover to solutions with 2 emitters.



Fig. 21. Error minimization problem crossover. This crossover maintains the number of ones in the offspring by selecting ones from any of the parents

In both problems we select the parents to crossover using a Binary Tournament selection. In a binary tournament selection two solutions are randomly selected from the population and the best of them (according to their fitness value) is chosen as a parent for the crossover. Doing the selection twice, we get both parents needed for a crossover.

5. Experiments and Results

To evaluate the proposed Genetic Algorithms, we created two different test scenarios. The first test scenario is a long L-shaped corridor of 15 m by 10 m, 3 m wide. In this scenario, the emitters can be placed near the walls with a 25 cm minimum distance between them. Figure 23 shows a map of this corridor along with all the possible emitter locations. The second test scenario is based on the plant of the Telecommunications Institute office at the Polytechnic Institute of Leiria and, as such, represents a real building. In this last scenario we allow the emitters to be near the walls with a 25 cm minimum distance between them as in the last scenario, but we also allow them to be in the ceiling through the middle of each room. Figure 24 shows the map used in this scenario.

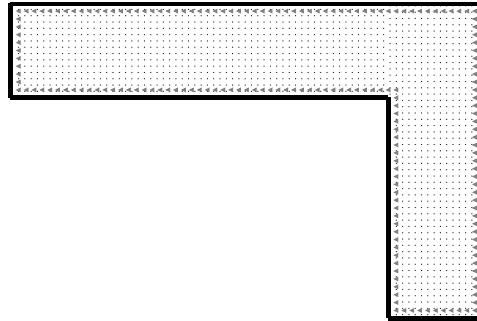


Fig. 22. Test scenario 1: a L-shaped corridor.

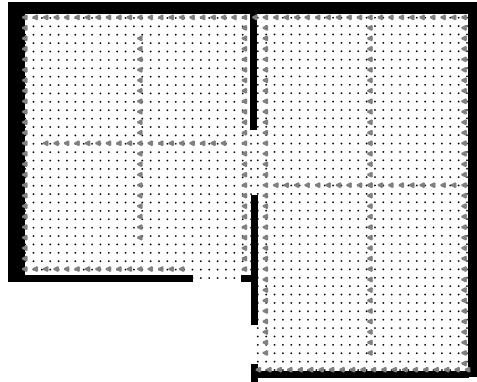


Fig. 23. Test scenario 2: the TI office at Polytechnic Institute of Leiria.

We used the genetic algorithms we described for both placement problems and for the two test scenarios. The parameters we used for the genetic algorithm in each problem is detailed in table I. The values of these parameters were chosen using some well-known values, and fine-tuned while experimenting [19]. The large population size was chosen to have some diversity in the population and it proved to be enough according to our results. We found the stopping criteria of 20000 evaluations to be sufficient to converge the results, as shown by Fig. 27. The selection operator (Binary Tournament) puts pressure on the convergence, while not falling into premature convergence in our experiments, thus being employed. Mutation and crossover operators used were the ones explained in previous sections and were specifically tailored to this problem. The mutation probability was chosen so that, on average, only one bit is mutated per individual, thus not making large changes to each individual. Further studies are required to determine if and how these parameters can be improved. We believe that the convergence speed may be improved, although the rest of the results are technology dependent. Also, we have discretized the space for the measurements into 50 cm by 50 cm cells. Each measurement was simulated in the center of each cell. Because of the stochastic nature of the genetic algorithm, we ran each experiment 50 times to get statistically valid results.

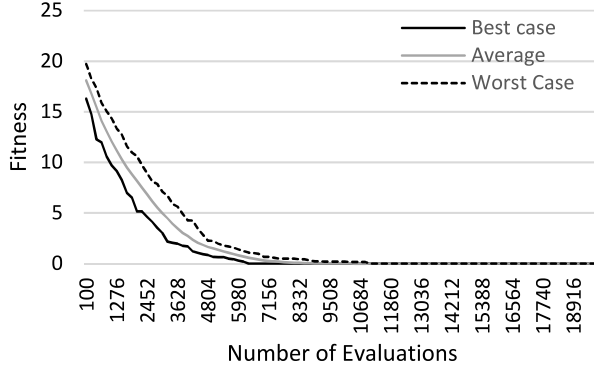


Fig. 24. Convergence of the coverage problem genetic algorithm in the first test scenario.

TABLE I - PARAMETERS USED IN THE GENETIC ALGORITHMS

Parameter	Coverage	Error Minimization
Population size	100	100
Stopping Criteria	20000 Evaluations	20000 Evaluations
Selection Operator	Binary Tournament	Binary Tournament
Mutation Operator	Bit flip	Bit swap
Mutation Probability	1/number of possible emitter locations	1/number of emitters
Crossover Operator	One-point crossover	Random emitters from parents
Crossover probability	0.5	0.5

Regarding the coverage problem, the experiment consisted in trying to find the minimum number of emitters to get coverage of 16 signals in each cell. In the first scenario, the GA converged to an ideal solution in every execution after around 12000 solution evaluations. Figure 25 shows the best, worst and average solution fitness of the 50 runs.

In the minimization of the location estimation error, we instructed the algorithm to place 16 emitters. Figure 26 shows how the average estimation error improved as more solutions were tried by the genetic algorithm. The figure shows that, on average, the location estimation improves in an order of 20%. For the location estimation we set a power reading error of $\pm 5\text{dB}$ and even with this large error, the algorithm placed the emitters to reduce the estimation error to an average of 15cm and a maximum estimation error of 43cm.

In the second scenario, the results are about the same. Figure 27 shows that, again, the GA finds optimum solutions in the coverage problem, although it took more evaluations (and thus, more generations) to reach those solutions.

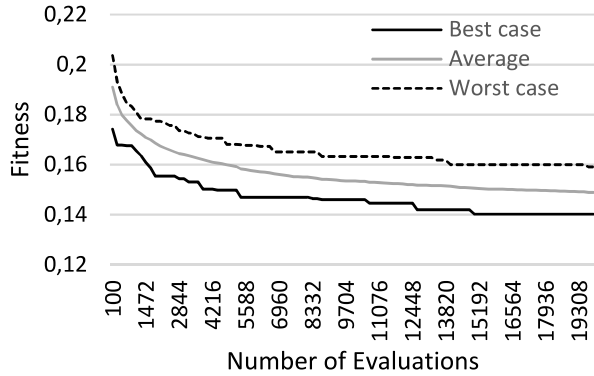


Fig. 25. Evolution of the solutions in the minimization of the estimation error.

Even though the optimum solution for the minimization of the estimation error with 16 emitters is unknown to us, the GA still shows that it will find good solutions. Figure 28 shows the improvement of the solutions as generations pass.

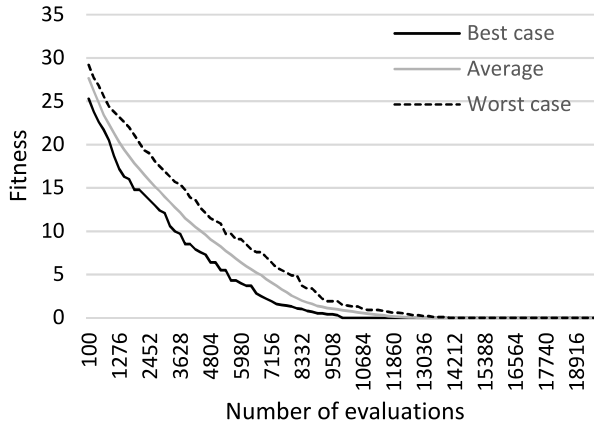


Fig. 26. Convergence of the coverage problem genetic algorithm in the second test scenario.

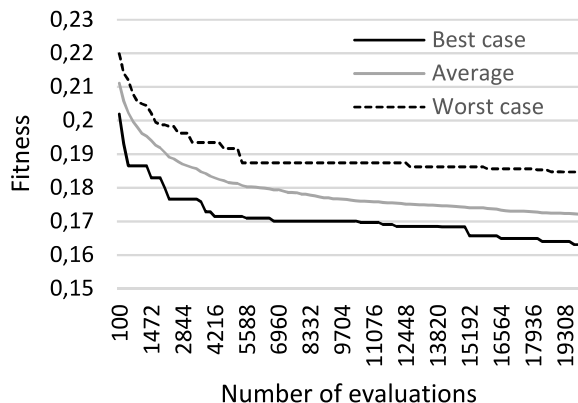


Fig. 27. Fitness of the solutions found during the minimization of the estimation error for the second test scenario.

Although the genetic algorithms appear to give good results, they can be further improved. One such improvement is to join both of the search objectives into a single algorithm, creating a multi-objective algorithm. Such an algorithm

will show how the number of emitters affects the precision of the location estimation and also if and when the law of diminishing returns affects that precision.

6. Conclusions

By creating a testbed for a new low cost Indoor Positioning System based on distributed sensor networks, we have to come to encouraging results.

We have shown that the OPDG codes, used in a TDM-CDMA network with a FM modulation, provide better results in an IPS scenario than the ZigBee system, due to its natural immunity to multipath interference.

The new approach with the Autocorrelation Crest Factor shows a way to find a linear function of the distance between the FM receiver and a pair of transmitters, which lowers the error of the IPS. Likewise, the introduction of the genetic algorithm to find the optimum FM transmitter positioning helps in lowering the error and the cost of the IPS.

Results shown in this paper suggest that our IPS system can be further developed to prove itself a viable alternative to existing solutions based on other distributed sensor network technologies.

7. Acknowledgements

This work was partially funded within the framework of the FCT/MEC (Fundação para a Ciência e a Tecnologia / Ministério da Educação e Ciência) project, entitled “Low-cost Indoor Positioning System (Linposys)”, nationally funded by the program PEst-OE/EEI/LA008/2013 of IT (Instituto de Telecomunicações).

References

- [1] David Schneider, “New Indoor Navigation Technologies Work Where GPS can’t” [Online] Available: <http://spectrum.ieee.org/telecom/wireless/new-indoor-navigation-technologies-work-where-gps-can't>
- [2] Skyhook Wireless, SkyHook [Online] Available: <http://www.skyhookwireless.com/>
- [3] Jay Donovan, Wifarer Brings Indoor Navigation To The Royal BC Museum [Online] Available: <http://techcrunch.com/2012/08/01/wifarer-brings-indoor-navigation-to-the-royal-bc-museum/>
- [4] Q-Track-Accurate Real Time Location Systems [Online] Available: <http://q-track.com/>
- [5] DecaWave, “Precise Indoor Location and RTLS” [Online] Available: <http://www.decawave.com/>
- [6] Mohammad Reza Gholami, “Positioning Algorithms for Wireless Sensor Networks”, Department of Signals and Systems, Chalmers University of Technology, Gothenburg, Sweden 2011.
- [7] L. Song and J. Shen, Evolved Cellular Network Planning and Optimization for UMTS and LTE. Taylor & Francis, 2010.
- [8] A. Ndili, “Gps pseudolite signal design,” in Proceedings of the 7th International Technical Meeting of the Satellite Division of The Institute of Navigation (ION GPS 1994), Sep. 1994, pp. 1375–1382.
- [9] A. Alejos, D. Muhammad, and H. Mohammed, “Ground penetration radar using golay sequences,” in 2007 IEEE Region 5 Technical Conference, Apr. 2007, pp. 318–321.
- [10] P. Fan, M. Darnell, and B. Honary, “Crosscorrelations of frank sequences and chu sequences,” Electronics Letters, vol. 30, no. 6, pp. 477–478, Mar. 1994.

- [11] J. S. Pereira, H. A. da Silva, FCTUC, IT, and IPL, “Codificador e descodificador eletrônico de sinais ortogonais e perfeitos,” Portugal Pending-Patent 106755, Jul., 2014.
- [12] S. Budisin, “Efficient pulse compressor for golay complementary sequences,” Electronics Letters, vol. 27, no. 3, pp. 219–220, Jan. 1991.
- [13] Homepage of IEEE 802.15 WPAN Task Group 4 (TG4). [Online]. Available: <http://grouper.ieee.org/groups/802/15/pub/TG4.html>
- [14] K. Shuaib, M. Alnuaimi, M. Boulmalf, I. Jawhar, F. Sallabi and A. Lakas, “Performance Evaluation of IEEE 802.15.4: Experimental and Simulation Results,” *Journal of Communications*, vol. 2, No. 4, June 2007.
- [15] The Raspberry Pi Foundation, “Raspberry Pi – Model B+” [Online]. Available: <http://www.raspberrypi.org/products/model-b-plus/>
- [16] N. Patwari, “Location estimation in sensor networks,” Ph.D. dissertation, University of Michigan, Ann Arbor, 2005.
- [17] J. H. Holland, “Genetic algorithms,” Scientific American, vol. 267, no. 1, pp. 66–72, 1992.
- [18] F. Glover and G. A. Kochenberger, Handbook of metaheuristics. Springer, 2003.
- [19] A. Aleti, “An Adaptive Approach to Controlling Parameters of Evolutionary Algorithms”, Swinburne University of Technology, 2012

Appendix 2 – Scientific Paper

ConfTele 2015
 Conference on Telecommunications
 Aveiro, Portugal
 18 September 2015, 4 pages

On estimating indoor location using wireless communication between sensors

J. Bagarić^{1,3}, M. Ferreira^{1,2}, J. S. Pereira^{1,2,3}, S. Priem-Mendes^{1,2}

¹Polytechnic Institute of Leiria, School of Technology and Management, Leiria, Portugal

² Center for research in Informatics and Communications, Polytechnic Institute of Leiria, Portugal

³Instituto de Telecomunicações, Leiria Branch, Portugal

Abstract – The use of wireless communication in determining the location of a sensor within a sensor network enables a number of added conveniences. Mobile sensors can use information such as time-of-arrival and wireless signal strength of the received signal to determine its location relative to the stationary sensors. Using such information within indoor scenarios, as opposed to outdoor scenarios, becomes more problematic due to the added accuracy requirements. Coding sequences used in the wireless communication can greatly affect the estimation of location. This paper deals with comparing the use of perfect sequences to the use of mainstream coding sequences for the purpose of indoor location estimation of wireless sensors. A new approach has been used to show that the use of perfect sequences delivers accuracy improvement over mainstream solutions.

1. Introduction

As opposed to outdoor scenarios, determining the location of sensors in indoor scenarios require much higher accuracy due to the added number of obstacles. While solutions like the GPS (Global Positioning System) work well for outdoor scenarios, where location accuracy is not as delicate, restrictions like line-of-sight (LOS) and an error of 3 meters render them unusable in indoor scenarios.

A different approach is needed in order to meet the requirements of the indoor scenario. Different types of positioning methods have been considered [36] to solve the positioning problem. Choosing the correct model for measurements is of utmost importance in order to achieve the highest accuracy. The positioning method used in this paper uses an approach based on the received signal strength (RSS) method. Furthermore, the performance of communication systems using Code Division Multiple Access (CDMA) [54] and Orthogonal Frequency Division Multiple Access (OFDMA) is directly related to the coding sequence used, especially in noisy environments, where perfect autocorrelation and cross-correlation properties of the sequences are essential for code detection and synchronization. The importance of these properties is pronounced even more in indoor scenarios, where multipath interferences become an issue.

In this paper we will compare and test the behavior of novel OPDG (Orthogonal Perfect DFT Golay) [55] coding sequences to the widely used ZigBee sequences (Pseudo Noise code used in wireless sensor networks [56]) as well as other coding sequences such as Golay [57] and Chu [58].

A small TDM-CDMA (Time Division Multiplexing - Code Division Multiple Access) wireless sensor network (WSN) will be created using low cost FM (Frequency Modulation) transmitters and receivers inside an indoor scenario. Then, wireless communication and RSS estimation method will be used to test and compare coding sequences, using

the same code length and testing environment. RSS estimation method will be extended using a novel approach with the autocorrelation crest factor (ACCF) ratio as described in [6].

2. Indoor Positioning System Model

A major issue in wireless communication is multipath interference (MPI). Radio waves can bounce off certain objects, thus taking multiple paths to reach their destination. These multiple paths can create delays on the receiver side, and thus cause interference in communication. The problem of multipath interference is even more pronounced in indoor scenarios, where large amount of objects and the lack of line-of-sight greatly increase the chances of having interference in communication.

To reduce the problem of MPI, perfect sequences can be used in the transmission. Furthermore, if these sequences are orthogonal for any delay between them, other common interferences can also be reduced such as multicarrier interference, inter-symbol interference, and the multiple access interference.

This section will cover the methods used to determine the position of a wireless receiver inside an indoor positioning system (IPS) scenario. Firstly, autocorrelation, cross-correlation, perfect sequences and the autocorrelation crest factor will be explained. Afterwards, an indoor scenario will be defined, set up and explained.

A. Autocorrelation and cross-correlation

A sequence x is a periodic sequence with a period M when, where $x(n) = x(\text{mod}(n, M))$ where $\text{mod}(a, b)$ is the remainder of a divided by b .

Let $x[n]$ with $n = 0, 1, 2, \dots, M - 1$, be one of the M values of a periodic sequence x . The DFT (Discrete Fourier Transform) of $x[n]$ is defined as

$$X[k] = DFT\{x[n]\} = \sum_{n=0}^{M-1} x[n] W_M^{kn}, \quad (1)$$

where $W_M = \exp(-j2\pi/M)$, $k = 0, 1, 2, \dots, M - 1$, with $j = \sqrt{-1}$ for convenience of notation. The IDFT (Inverse Discrete Fourier Transform) of $X[k]$ is then given by

$$IDFT\{X[n]\} = x[n] = \frac{1}{M} \sum_{k=0}^{M-1} X[k] W_M^{-kn}. \quad (2)$$

Using (1) and (2), the periodic cross-correlation between two different sequences $x^{(r)}$ and $x^{(s)}$ is defined as

$$\begin{aligned} R_{x^{(s)}x^{(r)}}[n] &= \sum_{k=0}^{M-1} x^{(r)}[k] x^{*(s)}[\text{mod}(k+n, M)] \\ &= \sum_{k=0}^{M-1} x_k^{(r)} x_{k+n}^{*(s)}. \end{aligned} \quad (3)$$

Alternatively, it can be defined as

$$R_{x^{(s)}x^{(r)}}[n] = IDFT\{X^{(r)} X^{*(s)}\}, \quad (4)$$

where the superscript * denotes the complex conjugate.

The autocorrelation of a periodic sequence can also be calculated using (4), when $r = s$.

When a periodic sequence has an autocorrelation of zero for any non-zero delay, the sequence is said to be a perfect sequence. Additionally, the two different sequences are called orthogonal if the cross-correlation between them is zero for a null delay. Because of these correlation properties, orthogonal perfect sequences are ideal to be used in several applications, such as radar systems, sonar systems, communication synchronization systems, etc.

B. OPDG code

The OPDG coding sequences are an essential part of our IPS system. Its perfect autocorrelation properties make them a good candidate to be used in asynchronous communication systems, such as DS-CDMA (Direct-Sequence Code-Division Multiple Access), or any other system where the signal reception may be contaminated by the multi-path problem. The properties of the OPDG coding sequences allow for enhanced detection of codes in spite of MPI, as described in detail in [6]. In this new work, we present more measurements in a real two-dimensional scenario with different code families and using low cost hardware.

C. Autocorrelation Crest Factor

In calculating the efficiency of autocorrelation, an autocorrelation crest factor can be used as a parameter. The autocorrelation crest factor (ACCF) is defined as a ratio of the maximum peak A_{peak} and the root mean square of the autocorrelation function A_{rms} as:

$$ACCF = \frac{A_{peak}}{A_{rms}}. \quad (5)$$

When the autocorrelation is perfect the ACCF of a periodic sequence of length L is equal to \sqrt{L} .

D. Indoor Positioning System

In order to accurately determine the indoor position of an entity in closed space, a number of problems need to be solved. One of the problems is the MPI, which we believe can be mitigated using the OPDG codes.

To test out our theory we set up a number of indoor scenarios, starting with a simple scenario with two emitters, and then moving to the 2D scenario with four emitters.

For the first scenario we placed two FM emitters at a distance of 13 meters away, as shown in Fig. 1. Each transmitter was transmitting one code from a code pair on the frequency of 106.9 MHz, which has been chosen to minimize the problem of MPI due to the absence of commercial FM radio emitters in the measurement zone. The receiver, a Raspberry Pi with a FM receiver module, was moved from one emitter to the other, and measurements were taken every 0.625 meters (~1/4 wavelength). Measurements were done by simultaneously calculating the ACCF for both codes in the pair, after which a ratio was made between the two obtained values. The dots in between the emitters denote the positions of the measurements taken. Encouraging values were obtained and the scenario was fit into a two-dimensional area.

To setup the two-dimensional scenario, we used 4 emitters, which were placed in the corners of a large classroom filled with tables and chairs with metallic legs. The codes were transmitting in pairs, as depicted in Fig. 2 and all emitters were put on corner tables.

The emitters were placed 6.8 and 11.5 meters apart, and the pairs were transmitting the signals interchangeably. The receiver, in this case, was moved around a number of points in the middle of the scenario. Positions closer to the emitters (less than a 1.25 m) were avoided in order to minimize the near-field effect of the emitters which is a well-known issue [59]. Measurements were taken in these points in a similar fashion as the ones in the scenario with two emitters. For each point, two ACCF ratios were measured. The first ratio was a ratio of the first and second code of the first pair. The

second was the ratio of the first and second code of the second pair. Each of the ratios were measured and calculated 30 times, and average values were taken in account for further calculations in order to decrease the error of measurement.

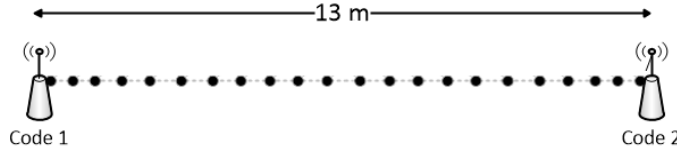


Figure 1: Two antenna position estimation scenario

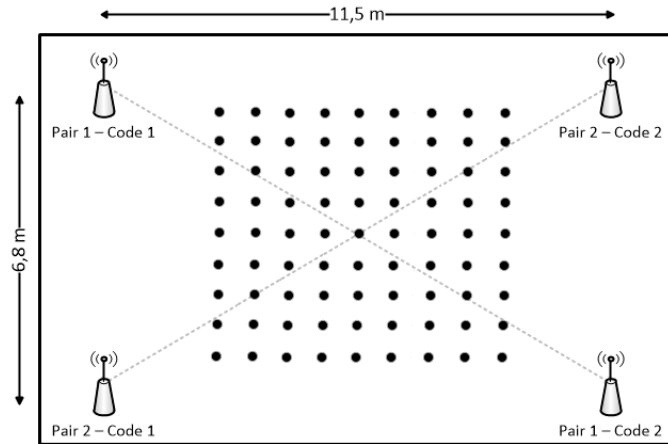


Figure 2: Indoor positioning scenario with 4 emitters

3. Results and Discussion

The results obtained in testing the scenario in Fig. 1 reveal some good OPDG properties, as can be seen in Fig. 3. The results show that, using the linear trend line of the ACCF1/ACCF2 ratios, we are able estimate the position of the receiver between the two emitters and calculate the error. OPDG codes have shown better properties in this scenario by trend line with a higher absolute slope, which can be used to approximate the position between the two emitters.

To estimate the position of the receiver between the two emitters the trend line equation y has been used. By doing that, the x value in the equation would provide us with the estimated location. A few measurements that are close to the emitters were discarded in order to avoid the near-field effect.

By calculating the average estimation error using the trend line equation and the ACCF1/ACCF2 ratio for each of the code family, we can determine the efficiency of the code family. For the measurements displayed in Fig. 3, average indoor location estimation errors can be seen in Table 1.

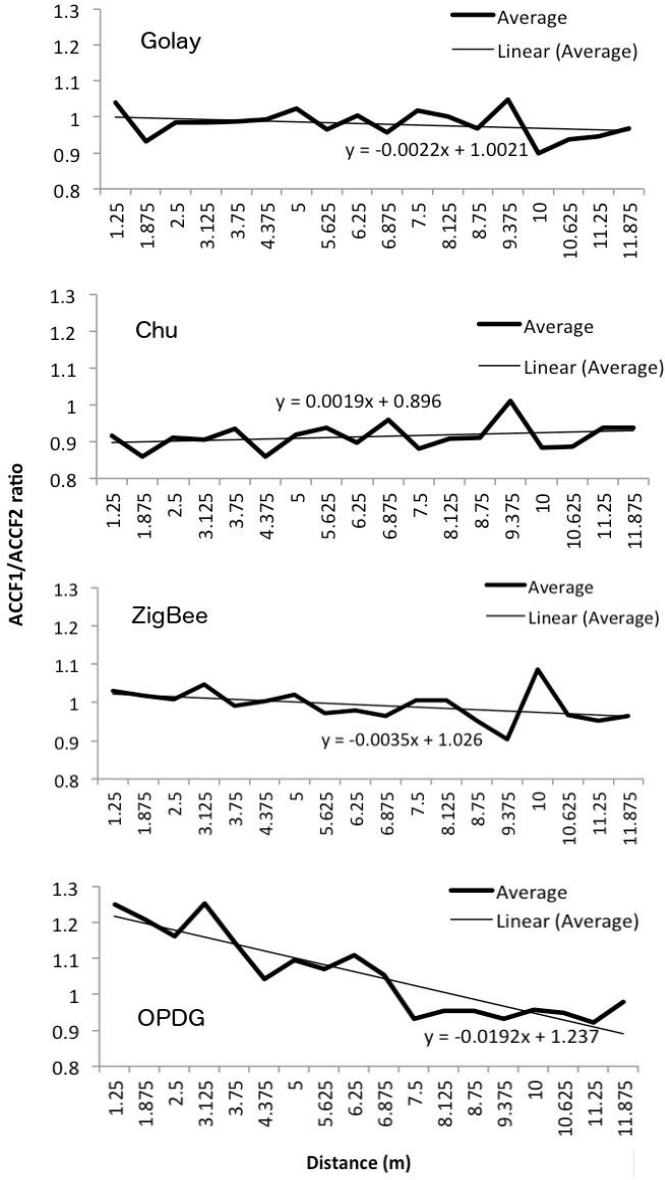


Figure 3: Two emitter scenario results for Golay, ZigBee, OPDG and Chu

All codes used are real orthogonal codes and they have been selected with the same length of 128 chips. The 128-length ZigBee codes have been constructed using a Hadamard transform based on 32-length ZigBee codes. All codes have been transmitted with the same power in our TDM-CDMA system with a mono FM transmission at 106.9 MHz. The transmission rate for all different codes was 4000 samples/sec.

Results show that using the OPDG codes we were able to estimate the position of the receivers between two emitters with an error near 3.5 meters (almost the same error as the commercial GPS). This shows better estimation properties than ZigBee, Golay and Chu codes, which had an error higher than 7, 13 and 14 meters respectively. The error averages were calculated without discarding the estimated distances that were higher than our real scenario (classroom distances).

The same method can be used to estimate positions inside a 2D scenario with 4 emitters, as displayed in Fig. 2. Since we are using 4 emitters, the transmitters emit the codes in pairs in order to cover the whole scenario.

In order to estimate the location of the receiver, we used the average ACCF ratios for each one of the pairs to estimate the power coverage area to that specific location. The location process was calculated using a representation of emitter influence radii. An example of the triangulation process for the influence radii can be seen in Fig. 4. Shaded areas represent the influence radius of each of the emitters on the two-dimensional scenario. In our calculation we have assumed that the influence radius of the second emitter in the pair reaches half way to the other emitter. By setting those influence radii to fixed values, we can use the ACCF1/ACCF2 ratio of that pair to estimate influence radius of the other emitter in the pair. If we define the distance between the two emitters in the pair as d , then the influence radius (IR) of the second emitter in each of the pairs would be half the distance between those emitters, as can be seen in Fig. 4.

TABLE 1: AVERAGE INDOOR LOCATION ESTIMATION ERROR BETWEEN TWO EMITTERS - DIFFERENT CODE FAMILIES

Code Family	Average estimation error
Golay	13.48 m
Chu	14.28 m
ZigBee	7.99 m
OPDG	3.67 m

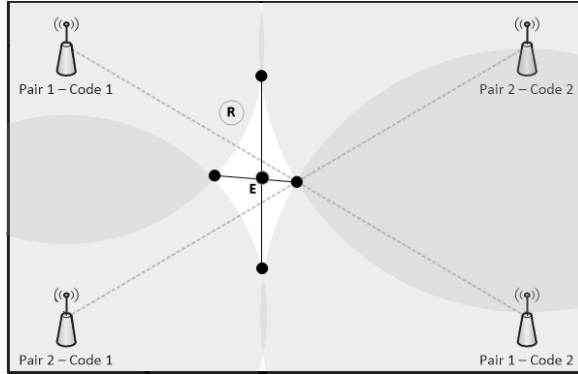


Figure 4: Approximate emitter influences and estimation calculation representation

TABLE 2: INFLUENCE RADII OF EMITTERS

Emitter	Influence radius
Pair 1 – Code 1	$IR_{e_{11}} = IR_{e_{12}} + \frac{ACCF - 1}{ACPM_{e_{11}e_{12}}}$
Pair 1 – Code 2	$IR_{e_{12}} = \frac{1}{2}d_{e_{11}e_{12}}$
Pair 2 – Code 1	$IR_{e_{21}} = IR_{e_{22}} + \frac{ACCF - 1}{ACPM_{e_{21}e_{22}}}$
Pair 2 – Code 2	$IR_{e_{22}} = \frac{1}{2}d_{e_{21}e_{22}}$

The IR distance used in Table 2 is in function of e_{xy} , where x indicates the number of the pair and y indicates the emitter number inside the pair. $ACCF$ represents the calculated $ACCF1/ACCF2$ ratio of the pair in the measuring position, and $ACPM$ represents the change of $ACCF1/ACCF2$ ratio values per meter when moving from one emitter in the pair to the other (calculated from the linear equation of the trend line).

After calculating the influence radii of all the emitters, we use the intersection points of the radii to estimate the position of the receiver. The position is estimated using a method similar to the triangulation process [60], by calculating the intersection of the lines that pass through the intersection points, as shown in Fig. 4. E marks the estimated position and R marks the real position of the receiver.

By testing this scenario, we were able to calculate the error estimation for each of the code families using the calculation methods above. The results have shown that OPDG codes display better ratio of average localization estimation errors (2.78 m) and the number of successful estimations (25.9%), as presented in Table 3. Unsuccessful estimations occur when emitter influence radii do not intersect. In spite of presenting a lower error (2.27 m), the Chu sequences reveal the lowest successful estimation (7.4%) inside the classroom.

4. Conclusions

Results of testing the indoor position estimation properties of the new OPDG codes have led to encouraging results. We have shown that the OPDG coding sequences, used in a TDM-CDMA network with FM modulation, have shown superior location estimation properties when compared to other well-known coding sequences such as ZigBee, Golay, due to their natural immunity to multipath interference.

TABLE 3: AVERAGE INDOOR LOCATION ESTIMATION ERROR IN A SCENARIO WITH FOUR EMITTERS - DIFFERENT CODE FAMILIES

Code Family	Average estimation error	Successful estimations (inside the classroom of Fig. 2)
Golay	4.29 m	19/81 (23.5%)
Chu	2.27 m	6/81 (7.4%)
ZigBee	2.90 m	23/81 (28.4%)
OPDG	2.78 m	21/81 (25.9%)

Besides the location estimation accuracy, OPDG codes have shown to be good candidates for usage in this scenario by displaying one of the highest successful estimation rates within the test area (even higher than Chu codes).

We have also shown that improving our IPS scenario could give way to a viable low cost alternative to existing indoor positioning systems based on the signal strength of a FM signal. Future work will show how to improve the location precision and success rate by deploying additional pairs of emitters, by mitigating the negative effects of the standing wave, as well as introducing a more realistic indoor scenario with some walls between each emitter pair.

5. Acknowledgements

This work was partially funded within the framework of the FCT/MEC (Fundação para a Ciência e a Tecnologia / Ministério da Educação e Ciência) project, entitled “Low-cost Indoor Positioning System (Linposys)”, nationally funded by the program PEst-OE/EEI/LA008/2013 of IT (Instituto de Telecomunicações).

References

- [1] W. H. Dutton, E. M. Rogers, and S.-H. Jun, “Diffusion and social impacts of personal computers,” *Commun. Res.*, vol. 14, no. 2, pp. 219–250, 1987.
- [2] F. Cristian, “Understanding fault-tolerant distributed systems,” *Commun. ACM*, vol. 34, pp. 56–78, 1991.
- [3] G. H. Forman and J. Zahorjan, “The challenges of mobile computing,” *Computer (Long. Beach. Calif.)*, vol. 27, no. 4, pp. 38–47, 1994.
- [4] M. Satyanarayanan, “Pervasive computing: Vision and challenges,” *IEEE Personal Communications*, vol. 8, no. 4, pp. 10–17, 2001.
- [5] H. Liu, H. Darabi, P. Banerjee, and J. Liu, “Survey of wireless indoor positioning techniques and systems,” *IEEE Transactions on Systems, Man and Cybernetics Part C: Applications and Reviews*, vol. 37, no. 6, pp. 1067–1080, 2007.
- [6] M. Ferreira, J. Bagaric, J. M. Lanza-Gutierrez, J. S. Pereira, J. A. Gomez-Pulido, and S. Priem-Mendes, “On the Use of Perfect Sequences and Genetic Algorithms for Estimating the Indoor Location of Wireless Sensors,” *Int. J. Distrib. Sens. Networks*, vol. 2015, pp. 2–5, 2015.
- [7] J. Bagaric, M. Ferreira, J. da S. Pereira, and S. P. Mendes, “On estimating indoor location using wireless communication between sensors,” *Proc 10th Conference on Telecommunications Conftele*, 2015. .
- [8] J. Bagaric, J. da S. Pereira, and S. Priem-Mendes, “Standing wave cancellation - Wireless transmitter, receiver, system and respective method,” 109137, 2016.
- [9] P. K. Enge, “The Global Positioning System: Signals, measurements, and performance,” *Int. J. Wirel. Inf. Networks*, vol. 1, no. 2, pp. 83–105, 1994.
- [10] J. Hallberg, M. Nilsson, and K. Synnes, “BLUETOOTH POSITIONING,” *10th Int. Conf. Telecommun. 2003 ICT 2003*, vol. 2, pp. 954–958, 2003.
- [11] B. Srivastava, “Radio frequency ID technology: The next revolution in SCM,” *Bus. Horiz.*, vol. 47, no. 6, pp. 60–68, 2004.
- [12] D. Porcino and W. Hirt, “Ultra-wideband radio technology: Potential and challenges ahead,” *IEEE Communications Magazine*, vol. 41, no. 7, pp. 66–74, 2003.
- [13] V. Filonenko, C. Cullen, and J. Carswell, “Indoor Positioning for Smartphones Using Asynchronous Ultrasound Trilateration,” *ISPRS Int. J. Geo-Information*, vol. 2, no. 3, pp. 598–620, 2013.
- [14] S. Phillips, M. Katchabaw, and H. Lutfiyya, “WLocator: An indoor positioning system,” in *3rd IEEE International Conference on Wireless and Mobile Computing, Networking and Communications, WiMob 2007*, 2007.
- [15] N. Lemieux and H. Lutfiyya, “WHLocator: hybrid indoor positioning system,” *Proc. 2009 Int. Conf. Pervasive Serv.*, pp. 55–63, 2009.
- [16] C. Yang and H. R. Shao, “WiFi-based indoor positioning,” *IEEE Commun. Mag.*, vol. 53, no. 3, pp. 150–157, 2015.
- [17] D. Vasisht, S. Kumar, and D. Katabi, “Decimeter-Level Localization with a Single WiFi Access Point,” *Proc. 13th USENIX Symp. Networked Syst. Des. Implement.*, pp. 165–178, 2016.
- [18] H. S. Kim, D. R. Kim, S. H. Yang, Y. H. Son, and S. K. Han, “An indoor visible light communication positioning system using a RF carrier allocation technique,” *J. Light. Technol.*, vol. 31, no. 1, pp. 134–144, 2013.
- [19] M. Yasir, S.-W. Ho, and B. N. Vellambi, “Indoor Positioning System Using Visible Light and Accelerometer,” *J. Light. Technol.*, vol. 32, no. 19, pp. 3306–3316, 2014.
- [20] S. S. Saad and Z. S. Nakad, “A standalone RFID indoor positioning system using passive tags,” *IEEE Trans.*

Ind. Electron., vol. 58, no. 5, pp. 1961–1970, 2011.

- [21] B. Ozdenizci, K. Ok, V. Coskun, and M. N. Aydin, “Development of an indoor navigation system using NFC technology,” in *Proceedings - 4th International Conference on Information and Computing, ICIC 2011*, 2011, pp. 11–14.
- [22] R. Want, E. Engineering, B. Bilginer, P. Ljunggren, S. M. Sadik, J. Nilsson, E. T. Jansson, M. Technology, I. Electrical, S. Ericsson, and M. Communications, “Near field communication,” *IEEE Pervasive Comput.*, vol. 10, no. 3, pp. 4–7, 2011.
- [23] S. E. Kim, Y. Kim, J. Yoon, and E. S. Kim, “Indoor positioning system using geomagnetic anomalies for smartphones,” in *2012 International Conference on Indoor Positioning and Indoor Navigation, IPIN 2012 - Conference Proceedings*, 2012.
- [24] A. Baniukevic, C. S. Jensen, and H. Lu, “Hybrid indoor positioning with Wi-Fi and Bluetooth: Architecture and performance,” in *Proceedings - IEEE International Conference on Mobile Data Management*, 2013, vol. 1, pp. 207–216.
- [25] P. Bolliger, “Redpin-adaptive, zero-configuration indoor localization through user collaboration,” ... *Work. Mob. entity localization Track*. ..., p. 55, 2008.
- [26] W. Inc., “Wifarer.” [Online]. Available: <http://www.wifarer.com/>. [Accessed: 12-Aug-2016].
- [27] W. Inc., “Wifarer - Image.” .
- [28] IndoorAtlas USA Inc., “IndoorAtlas.” [Online]. Available: <https://www.indooratlas.com/>. [Accessed: 13-Aug-2016].
- [29] IndoorAtlas USA Inc., “IndoorAtlas - Image.” .
- [30] Pozyx Labs, “Pozyx.” [Online]. Available: <http://pozyx.io/>.
- [31] Acuity Brands, “ByteLight.” [Online]. Available: <http://www.acuitybrands.com/solutions/services/bytelight-services-indoor-positioning>. [Accessed: 14-Aug-2016].
- [32] nextome SRL, “Nexttome.” [Online]. Available: <https://www.nextome.net/en/indoor-positioning-technology.php>.
- [33] ibeacon.com, “WHAT ISIBEACON? A GUIDE TO BEACONS,” *ibeaconinsider*, 2016. .
- [34] Ludovic Privat, “Nextome: Bluetooth Indoor Location Made in Italy.” [Online]. Available: http://www.gpsbusinessnews.com/Nextome-Bluetooth-Indoor-Location-Made-in-Italy_a5322.html. [Accessed: 14-Aug-2016].
- [35] A. Doucet, N. de Freitas, and N. Gordon, “An Introduction to Sequential Monte Carlo Methods,” *Seq. Monte Carlo Methods Pract.*, pp. 3–14, 2001.
- [36] M. R. Gholami, “Positioning Algorithms for Wireless Sensor Networks,” Chalmers University of Technology, Gothenburg, Sweden, 2011.
- [37] R. Dalce, “Comparison of Indoor Localization Systems Based on Wireless Communications,” *Wirel. Eng. Technol.*, vol. 2, no. 4, pp. 240–256, 2011.
- [38] “Perfect and almost perfect sequences.” [Online]. Available: http://qh.eng.ua.edu/e_paper/phd_research/pinhole_image/perfect_almost_perfect_Jungnickel_1999.pdf. [Accessed: 14-Feb-2016].
- [39] Wikipedia, “Autocorrelation vs. Cross-correlation - Image.” .
- [40] J. da S. Pereira, *Sequências perfeitas para sistemas de comunicação*. 2015.
- [41] Z. Zhou and X. Tang, “Generalized modified Gold sequences,” *Des. Codes, Cryptogr.*, vol. 60, no. 3, pp. 241–253, 2011.

- [42] J. S. Pereira and H. J. A. Da Silva, "M-ary mutually orthogonal complementary gold codes," in *European Signal Processing Conference*, 2009, pp. 1636–1640.
- [43] S. Kounias, C. Koukouvinos, and K. Sotirakoglou, "On Golay sequences," *Discrete Math.*, vol. 92, no. 1–3, pp. 177–185, 1991.
- [44] S. Z. Budisin, "Efficient pulse compressor for Golay complementary sequences," *Electron. Lett.*, vol. 27, no. 3, pp. 219–220, 1991.
- [45] H. Dieter Like, "Sequences and Arrays with Perfect Periodic Correlation," *IEEE Trans. Aerosp. Electron. Syst.*, vol. 24, no. 3, pp. 287–294, 1988.
- [46] J. S. Pereira and H. J. A. Da Silva, "Alternative Zigbee codes derived from orthogonal perfect DFT sequences," in *Proceedings of 6th International Conference on Wireless Communication and Sensor Networks, WCSN-2010*, 2010.
- [47] C. M. Ramya, M. Shanmugaraj, and R. Prabakaran, "Study on ZigBee technology," in *ICECT 2011 - 2011 3rd International Conference on Electronics Computer Technology*, 2011, vol. 6, pp. 297–301.
- [48] R. P. Feynman, R. B. Leighton, and M. L. Sands, *The Feynman Lectures on Physics*, vol. 1. 1963.
- [49] Raspberry Pi Foundation, "Raspberry Pi - Teach, Learn, and Make with Raspberry Pi," *Www.Raspberrypi.Org*, 2012..
- [50] I. Silicon Laboratories, "Si4702/03-C19," 2009.
- [51] C. C. PiHack, "Turning the Raspberry Pi Into an FM Transmitter." [Online]. Available: http://www.icrobotics.co.uk/wiki/index.php/Turning_the_Raspberry_Pi_Into_an_FM_Transmitter. [Accessed: 01-Sep-2015].
- [52] C. Girard, C. Joachim, and S. Gauthier, "The physics of the near-field," *Reports Prog. Phys.*, vol. 63, no. 6, pp. 893–938, 2000.
- [53] W. K. Pratt, J. Kane, and H. C. Andrews, "Hadamard transform image coding," *Proc. IEEE*, vol. 57, no. 1, pp. 58–67, 1969.
- [54] S. Hara, "Overview of Multicarrier CDMA," *IEEE Communications Magazine*, vol. December, pp. 126–130, 1997.
- [55] J. S. Pereira and H. A. Silva, "Codificador e descodificador eletrônico de sinais ortogonais e perfeitos," 106755, 2015.
- [56] P. Kinney, "ZigBee Technology : Wireless Control that Simply Works," *Communications Design Conference*, no. October, pp. 1–20, 2003.
- [57] A. V. Alejos, D. Muhammad, and H. U. R. Mohammed, "Design and implementation of Ground Penetration Radar system using coded Sequences and improved target detection using Golay codes," in *2008 IEEE Region 5 Conference*, 2008, pp. 318–321.
- [58] B. M. Popovic, "Generalized Chirp-Like Polyphase Sequences with Optimum Correlation Properties," *IEEE Trans. Inf. Theory*, vol. 38, no. 4, 1992.
- [59] A. Yaghjian, "An overview of near-field antenna measurements," *IEEE Transactions on Antennas and Propagation*, vol. 34, no. 1. pp. 30–45, 1986.
- [60] J. Hightower and G. Borriello, "Location Sensing Techniques," *Computer (Long. Beach. Calif.)*, no. August, pp. 1–4, 2001.

Appendix 3 – Patent

ABSTRACT

STANDING WAVE CANCELLATION WIRELESS TRANSMITTER, RECEIVER, SYSTEM AND RESPECTIVE METHOD

The present invention is enclosed in the area of wireless communication systems, generally directed towards the problem of multipath interference, and specifically towards mitigating the effect of the standing wave in indoor positioning systems.

The present invention includes a standing wave cancellation wireless transmitter which is configured to, for each signal with wavelength λ to be transmitted, transmit a first wave with wavelength λ and transmit a second wave with wavelength λ and a shift equal to half the wavelength λ .

It is also an object of present invention a standing wave cancellation wireless receiver which it is configured to perform the average of a first wave with wavelength λ and a second wave with wavelength λ and a shift equal to half the wavelength λ , creating a single received signal.

It is yet part of the present invention a system which comprises at least one of said wireless transmitters and at least one of said wireless receivers, as well as a method implemented by said transmitter and receiver.

DESCRIPTION

STANDING WAVE CANCELLATION WIRELESS TRANSMITTER, RECEIVER, SYSTEM AND RESPECTIVE METHOD

FIELD OF THE INVENTION

This invention is enclosed in the area of wireless communication systems, generally directed towards the problem of multipath interference, and specifically towards mitigating the effect of the standing wave in indoor positioning systems. It relates to the impact of standing waves in wireless communication and proposes a solution to reduce the negative impact of standing waves when wireless communication is used in indoor positioning systems (IPS).

PRIOR ART

A common occurrence in the field of wireless communication is the standing wave. In environments that contain many obstacles, such as closed spaces, the wave that is being sent from the transmitter to the receiver propagates through space and gets reflected from different kinds of surfaces. These reflections cause the receiving end to receive multiple instances of the same wave, some of them arriving directly, while others arriving after being reflected from a certain object. This occurrence is commonly called multipath interference (MPI), and represents a common issue in indoor positioning systems that use wireless technology.

The MPI has another side-effect, which is called the standing wave. When a wave gets reflected from a surface, it generates another wave that propagates back in the opposite direction. If one puts a receiver somewhere between the transmitter and the reflective surface, detecting the strength of the signal would vary on the position in which the receiver is placed because of the standing wave effect. Certain positions, particularly those that are half wave length apart, would show no oscillations in the signal strength when measured multiple times. These points along the medium are called nodes (N). Some other points along the medium would yield different results, showing high oscillations in signal strength. The points that contain the highest amount of oscillations are called the antinodes (AN).

In order to achieve accurate and consistent indoor positioning estimation using signal strength, inside closed spaces, mitigating the effect of the standing wave is one of the problems that needs to be addressed. Currently, a technical solution to this problem does not exist, and this patent introduces a way to solve the problem of the standing wave when wireless communication is used in indoor positioning systems.

The Portuguese patent number 106755 (J. Pereira , H. A. Silva , Codificador e descodificador eletrónico de sinais ortogonais e perfeitos) has been presented to cancel multipath interferences through a CODEC of orthogonal perfect DFT of Golay codes (OPDG). However this CODEC does not address the standing wave issue. The OPDG autocorrelation peak follows the standing wave fluctuation.

SOLVED TECHNICAL PROBLEMS

As detailed above, the present invention is directed into the problem of multipath interference, more specifically to standing wave cancellation.

Another problem is the displacement speed of the standing wave. When too slow, real-time measurements cannot be achieved, and as a result such a system is not usable in a real-world application.

The present invention proposes to correct the slow motion standing wave problem. This is achieved by devices and methods that swiftly alternate a primary standing wave with a second one that is generated in opposite phase.

Therefore, this invention provides a solution to a well-known problem in wireless communication indoor scenarios, where multipath interferences may generate standing waves between reflective obstacles. These are a common issue in indoor scenarios that in turn makes

such an approach unfeasible when considering indoor positioning system accuracy. Until now this problem remains unsolved as no solution has ever been presented.

SUMMARY OF THE INVENTION

It is an object of the present invention a standing wave cancellation wireless transmitter configured to, for each signal with wavelength λ to be transmitted, transmit a first wave with wavelength λ and transmit a second wave with wavelength λ and a shift equal to half the wavelength λ .

Referring to Figure 1, it depicts a graph displaying the effect of the standing wave on the indoor positioning system estimation. The graph also displays the standing wave effect mitigation used in the standing wave cancellation wireless transmitter, standing wave cancellation wireless receiver and methods of the present invention. The standing wave effect has a major impact on the accuracy of location estimation in the radio wave mechanism, due to the constant change in amplitude of the wave that affects signal strength readings, and thus, location accuracy. To mitigate the effect of the standing waves, hardware-based techniques are implemented to generate two different standing waves.

The first standing wave is a wave with a full wavelength of λ . The second standing wave also has a wavelength of λ , but starts with a shift of $\lambda/2$. The curve gained from summing up the two waves proves to be better for usage, for example, in location estimation scenarios when considering that the X-axis is the distance and the Y-axis is the power of the signal received. It may be used both in radio frequency waves and ultrasonic waves.

It is also object of the present invention a standing wave cancellation wireless receiver which is configured to perform the average of a first wave with wavelength λ and a second wave with wavelength λ and a shift equal to half the wavelength λ , creating a single received signal.

Also as said for the standing wave cancellation wireless transmitter, this receiver enables the mitigation of the effect of the standing waves, as seen in the graph of Figure 1, by combining said two received waves.

Also, the present invention includes a standing wave cancellation wireless system which comprises at least a standing wave cancellation wireless transmitter as previously defined and at least a standing wave cancellation wireless receiver as previously defined.

Additionally, it is also an object of the present invention a method for the cancellation of standing wave in wireless communications implemented by said system, which comprises a transmission stage and a receiving stage, wherein:

- In the transmission stage a standing wave cancellation wireless transmitter, based in a single signal, transmits a first wave with wavelength λ and a second wave with wavelength λ and a shift equal to half the wavelength λ and
- In the receiving stage, a standing wave cancellation wireless receiver, for a received first wave with wavelength λ and a received second wave with wavelength λ and a shift equal to half the wavelength λ , calculates their average on power or amplitude, obtaining a single signal.

DESCRIPTION OF DRAWINGS

The features of the invention believed to be innovative are set forth with particularity in the claims. The invention itself, however, may be best understood by reference to the following detailed description of the invention, which describes exemplary embodiments of the invention, taken in conjunction with the accompanying drawings, in which:

Figure 1 – a graph displaying the effect of the standing wave on the indoor positioning system estimation, along with the effect of the mitigation used within the system;

Figure 2 – a schematic view of the electric circuit used to mitigate the standing wave effect in the radio wave transmission.

Figure 3 – a schematic view of the electric circuit used to mitigate the standing wave effect in ultrasound transmission.

Figure 4 – a graph displaying linear estimations of signal strength trend lines gained from measuring signals from different pairs of transmitters after the standing wave cancelation process, in a range of approximately 12 meters. It is gained from measuring signals from different pairs of transmitters. This graph contains a number of lines equal to the number of emitter pairs inside an example scenario (not limited to three pairs).

DETAILED DESCRIPTION OF THE INVENTION

The most general configurations of the present invention are defined in the Summary of the invention. These configurations may be further detailed.

The standing wave cancellation wireless transmitter may further comprise a signal generator suitable for creating a signal with wavelength λ , an output and a relay switch, so connected that the double pole double throw (DPDT) relay switch alternatively connects the signal generator through a first path generating a first wave and to a second path to the output, wherein the second path contains a coaxial cable suitable for shifting the signal in half the wavelength λ , creating the second wave. It consists in a possible implementation of the previously defined transmitter, delivering two waves, in which the second wave is shifted in half the wavelength.

When the relay switch is in the initial position, the signal generator transmits a first wave directly to the output using the shortest path possible. The signal generator may also control the relay switch, so when it switches the relay switch to the alternate position, the signal passes through a coaxial cable of a certain length, and then to the output. This causes the half wavelength delay generated by the correct length of the coaxial cable and generates the second wave. The dashed line surrounding all of the elements besides the antenna represents a metallic enclosure that serves as a reflector and isolator of the radio signal contained inside the electric circuit.

The transmitter of the present invention may implement radio or ultrasound communications.

Specifically for radio communications, said signal generator is a radio signal generator, the relay switch is a DPDT relay switch and the output an antenna. The half wavelength delay generated by the correct length of the coaxial cable (the "Coax" displayed in Fig. 2) generates the second radio wave. A radio wireless transmitter according to the present invention uses the relay switch to emit two radio waves in time-division multiplexing, thus mitigating the effect of the standing wave by summing up the two waves before processing them. The dashed line in Fig. 2 surrounding all of the elements besides the antenna represents a metallic enclosure that serves as a reflector and isolator of the radio signal contained inside the electric circuit.

Therefore, in a preferred embodiment relative to radio communication, the wireless transmitter of the present invention is further configured to implement time division multiplexing which, as said, mitigates the effect of the standing wave by summing up the two waves before processing them.

Specifically for ultrasound communications, said signal generator is an ultrasonic signal generator and the relay switch is a single pole double throw (SPDT) relay switch and the output a speaker. Similarly to what was referred to radio communications and considering Fig. 3, which

displays a hardware-based solution that implements the standing wave mitigation for ultrasound waves, the ultrasound transmitter is connected to a Single Pole Double Throw (SPDT) relay switch, which enables the signal generator to switch between two audio outputs. One of the outputs is a regular λ wavelength ultrasound wave. The other audio output outputs the same ultrasound wave, but with a shift for $\lambda/2$.

Considering the wireless receiver of the present invention, said average performed to the first and second received waves, it is the average of the amplitude or power of said first and second waves.

Also, the wireless receiver of the present invention may implement radio or ultrasound communications.

Specifically for radio communications, it comprises an antenna and radio wave transducer means.

Specifically for ultrasound communications, it comprises a microphone and ultrasound transducer means.

The system defined in Summary of the invention may include a wireless transmitter and a wireless receiver as defined in any of previously defined embodiments.

Also, the method defined in Summary of the invention may also be implemented by this system, including its previously referred embodiment. This method may still be further detailed in that it comprises the following steps:

- a signal with wavelength λ is generated in a wave generator;
- said signal is inserted into a first path and into a second path by means of a relay switch;

- in said second path, the signal is passed through a coaxial cable which shifts it in half the wavelength λ ;
- both the signal from the first path and the signal from the second path are wirelessly transmitted through the output.

Also, in any of the embodiments of said method, the signal may be a radio signal or an ultrasound signal.

The present invention also includes the use of the previously referred system, in any of its embodiments, in positioning systems, preferably indoor positioning systems.

CLAIMS

1. Standing wave cancellation wireless transmitter **characterized in that** it is configured to, for each signal with wavelength λ to be transmitted, transmit a first wave with wavelength λ and transmit a second wave with wavelength λ and a shift equal to half the wavelength λ .

2. Standing wave cancellation wireless transmitter according to the previous claim **characterized in that** it comprises a signal generator suitable for creating a signal with wavelength λ , an output and a relay switch, so connected that the DPDT relay switch alternatively connects the signal generator through a first path generating a first wave and to a second path to the output, wherein the second path contains a coaxial cable suitable for shifting the signal in half the wavelength λ , creating the second wave.

3. Standing wave cancellation wireless transmitter according to claim 1 **characterized in that** the signal generator is an ultrasonic signal generator and the relay switch is a single pole double throw (SPDT) relay switch and the output a speaker.

4. Standing wave cancellation wireless transmitter according to claim 1 **characterized in that** the signal generator is a radio signal generator, the relay switch is a double pole double throw (DPDT) relay switch and the output an antenna.

5. Standing wave cancellation wireless transmitter according to the previous claim **characterized in that** it is further configured to implement time division multiplexing.

6. Standing wave cancellation wireless receiver **characterized in that** it is configured to perform the average of a first wave with wavelength λ and a second wave with wavelength λ and a shift equal to half the wavelength λ , creating a single received signal.

7. Standing wave cancellation wireless receiver according to the previous claim **characterized in that** said average is the average of the amplitude or power of said first and second waves.

8. Standing wave cancellation receiver according to any of the claims 6-7 **characterized in that** it comprises an antenna and radio wave transducer means **or in that** it comprises a microphone and ultrasound transducer means.

9. Standing wave cancellation wireless system **characterized in that** it comprises at least a standing wave cancellation wireless transmitter as defined by any of the claims 1-5 and at least a standing wave cancellation wireless receiver as defined by any of the claims 6-8.

10. Method for the cancellation of standing wave in wireless communications implemented by the system of claim 9 **characterized in that** it comprises a transmission stage and a receiving stage, wherein:

- In the transmission stage a standing wave cancellation wireless transmitter, based in a single signal, transmits a first wave with wavelength λ and a second wave with wavelength λ and a shift equal to half the wavelength λ , and
 - In the receiving stage, a standing wave cancellation wireless receiver, for a received first wave with wavelength λ and a received second wave with wavelength λ and a shift equal to half the wavelength λ , calculates their average on power or amplitude, obtaining a single signal.

11. Method according to the previous claim **characterized in that** the transmission stage further comprises the following steps:

- a signal with wavelength λ is generated in a wave generator;
- said signal is inserted into a first path and into a second path by means of a relay switch;
- in said second path, the signal is passed through a coaxial cable which shifts it in half the wavelength λ ;
- both the signal from the first path and the signal from the second path are wirelessly transmitted through the output.

12. Method according to any of the claims 10-11 **characterized in that** the signal is a radio signal or an ultrasound signal.

13. Use of the system of claim 9 in positioning systems, preferably indoor positioning systems.

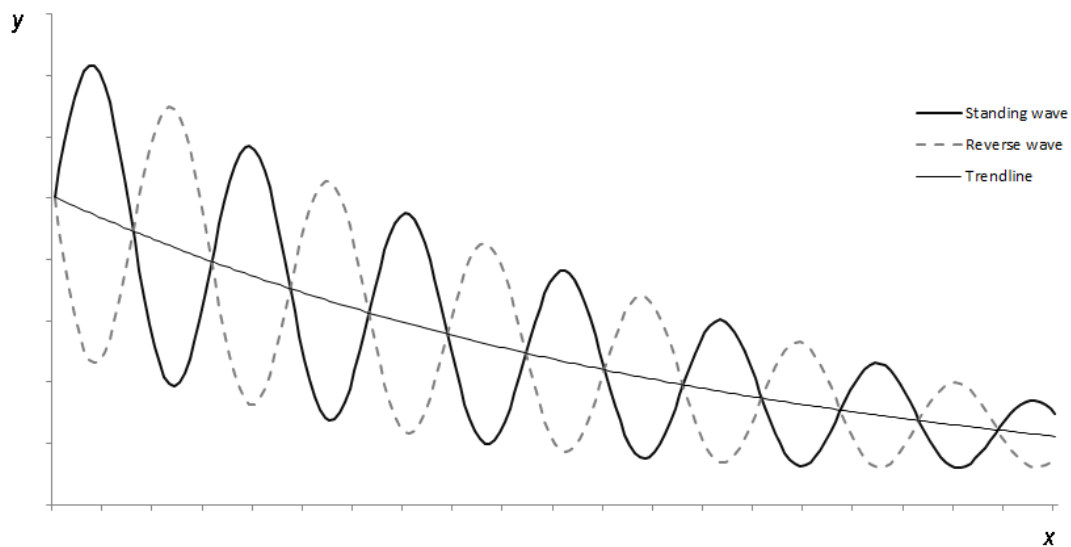


Figure 42

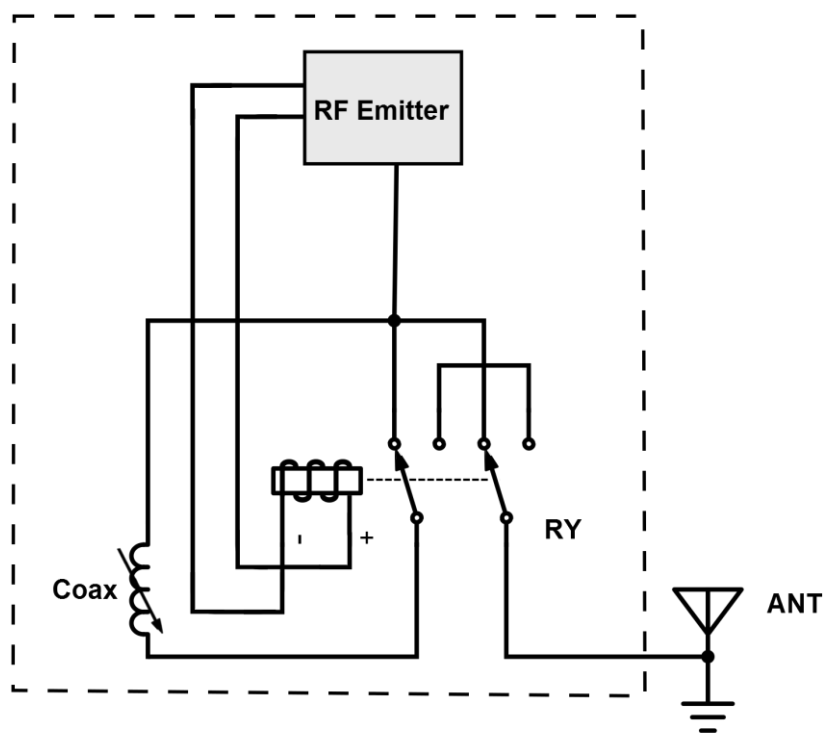


Figure 43

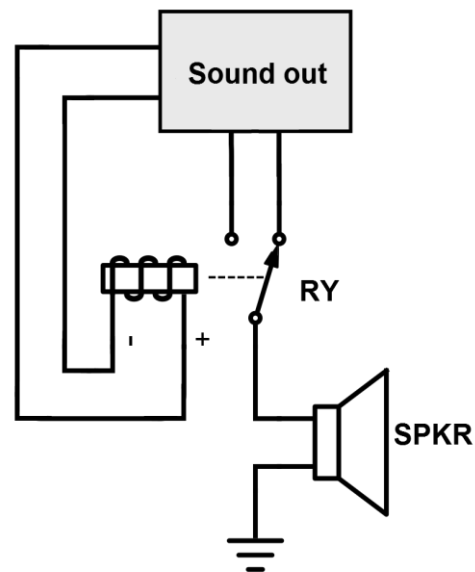


Figure 44

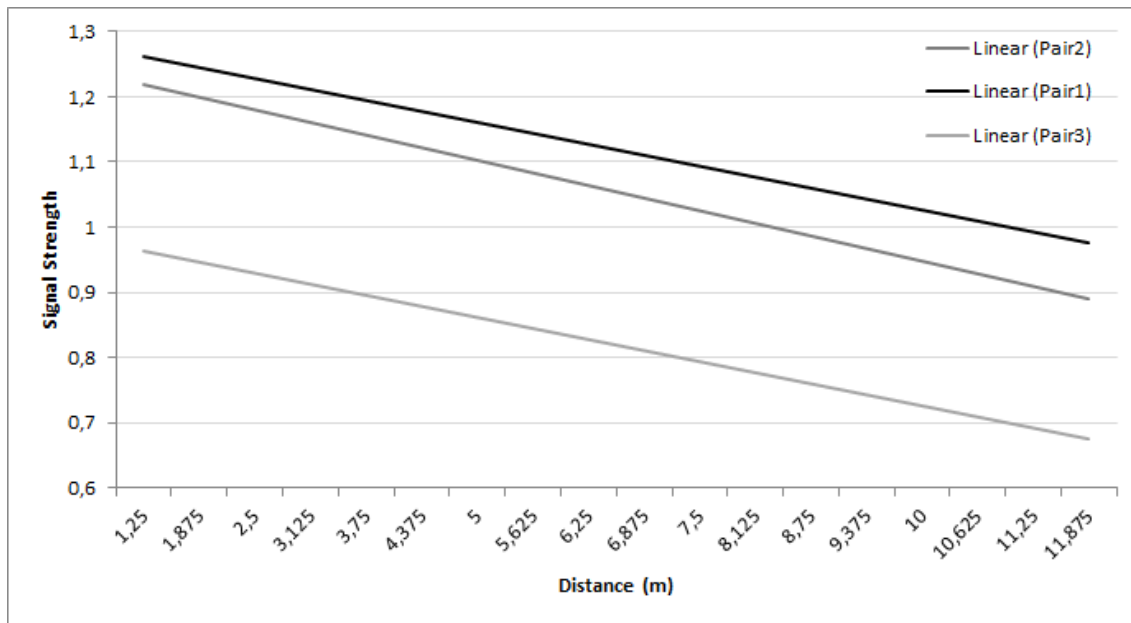


Figure 45